PRINCIPLES OF NEUTRONICS PHYSICS

Dr. Usman Pasha
Amit Kumar Sharma

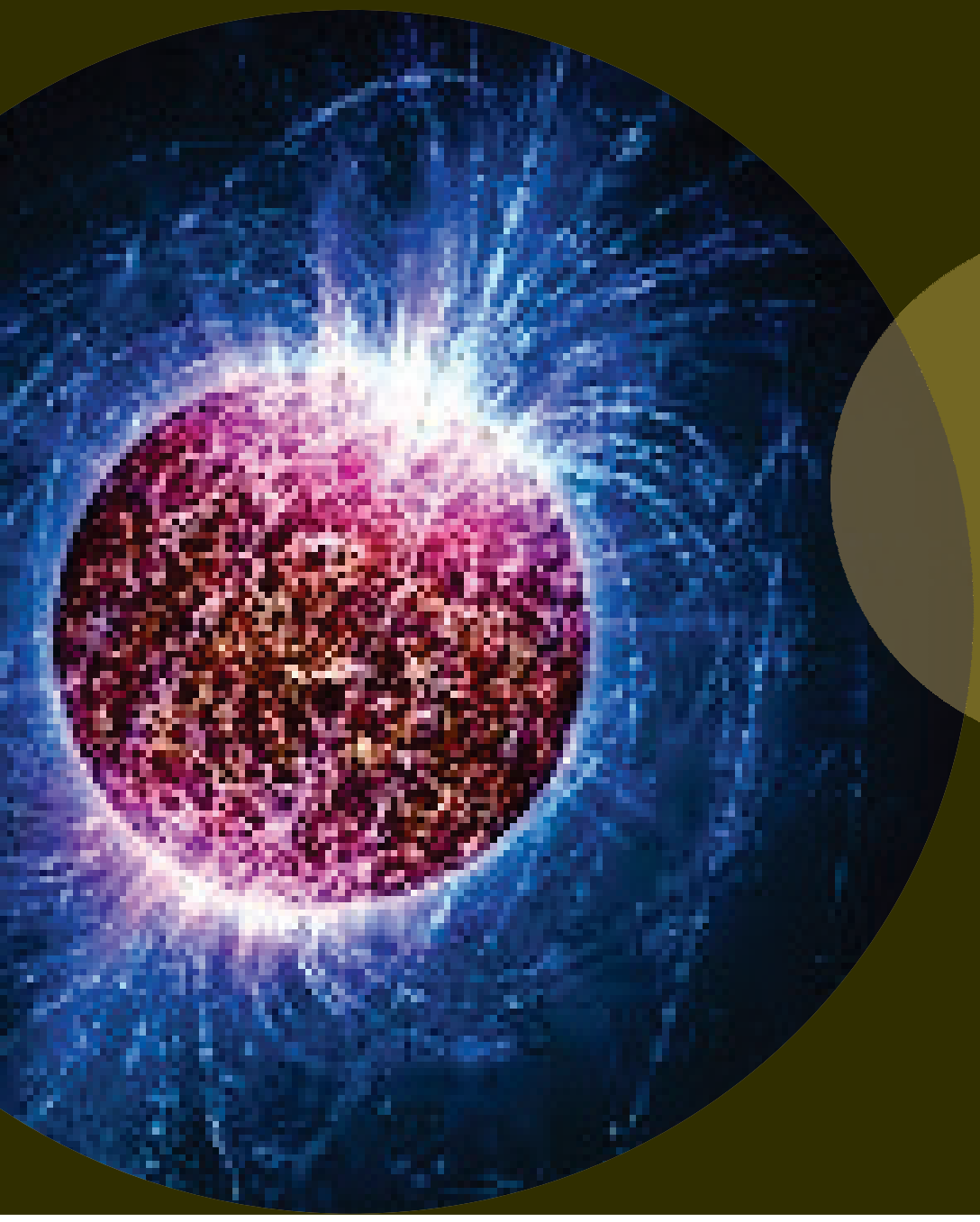

ALEXIS PRESS
JERSEY CITY, USA

PRINCIPLES OF
NEUTRONICS PHYSICS

PRINCIPLES OF NEUTRONICS PHYSICS

Dr. Usman Pasha

Amit Kumar Sharma

ALEXIS PRESS

ALEXIS PRESS

Published by: Alexis Press, LLC, Jersey City, USA
www.alexispress.us

First Published 2022

A catalogue record for this publication is available from the British Library

Library of Congress Cataloguing in Publication Data

Includes bibliographical references and index.

Principles of Neutronics Physics by *Dr. Usman Pasha, Amit Kumar Sharma*

ISBN 978-1-64532-371-6

CONTENTS

CHAPTER 1

INTRODUCTION TO NEUTRONICS

Dr. Usman Pasha, Associate Professor,
Department of Physics, Presidency University, Bangalore, India,
Email Id-mahaboobpasha@presidencyuniversity.in

ABSTRACT:

A key area of research in nuclear reactors is neutronics, which is concerned with how neutrons behave and interact within a reactor core. For nuclear power facilities to operate safely and effectively, this sector is essential. The study of neutron transport, nuclear reactions, and their impacts on reactor efficiency are all included in the field of neutronics. Neutronics aids in reactor design, fuel optimization, and safety analysis by precisely forecasting neutron flux, criticality, and radiation levels. The difficult equations regulating neutron behavior are solved by computational approaches, such as Monte Carlo simulations and deterministic methods.

KEYWORDS:

Neutronics, Nuclear reactors, Neutron transport, Reactor core, nuclear fuel, Radiation shielding.

INTRODUCTION

The proton and the neutron, two particles thought to make up the atomic nucleus, were initially discovered by the British physicist James Chadwick in 1932. He used a radioactive emitter to blast a beryllium target in order to study the radiation of the neutrons emitted during the nuclear reaction.These particles are likely to experience scattering in certain particular materials, which causes them to slow down until they are absorbed. Because neutrons are electrically neutral, as implied by their name, they can only interact with atomic nuclei that are ten to one hundred thousand times smaller than individual atoms and may travel as a result nearly in vacuum. Their routes are around one centimeter long, passing through 100 million atoms, and in materials where they can disperse effectively, like water, heavy water, or graphite, they can even stretch over decimeters in a straight line. This is why the study of neutrons moving through matter is known as neutron physics, often known as neutronics, and was founded with Chadwick's experiment[1], [2].

A few years later, in 1938, German scientists Otto Hahn, Fritz Strassmann, and Lise Meitner discovered fission caused by a neutron. Frédéric Joliot-Curie in France noticed the production of two to three secondary neutrons during fission in 1939.The nuclear chain reaction that would result from neutrons => fissions => neutrons => fissions => etc. was quickly recognized by physicists. If the reaction can be maintained, it will release 200 MeV per fission, or about one million times more energy than a chemical reaction. Thus, the following definition has to be

added to the preceding one includes the investigation of the factors that lead to a chain reaction, particularly the multiplication factor, which is the proportion of neutrons to all other particles in a generation[3].

To maintain a steady neutron population in a nuclear reactor, the nuclear chain reaction is regulated using the appropriate mechanisms. The reactor is referred to as being "critical*" in this instance since the neutron multiplication factor is equal to 1. The reactor is referred to be "supercritical" if this factor is more than 1, which causes the neutron population to increase exponentially over time. Last but not least, if it falls below 1, the reactor is referred to be "subcritical*" since the neutron population vanishes[4].

The proton and the neutron, two particles thought to make up the atomic nucleus, were initially discovered by the British physicist James Chadwick in 1932. He used a radioactive emitter to blast a beryllium target in order to study the radiation of the neutrons emitted during the nuclear reaction.These particles are likely to experience scattering* in certain particular materials, which causes them to slow down until they are absorbed. Because neutrons are electrically neutral, as implied by their name, they can only interact with atomic nuclei that are ten to one hundred thousand times smaller than individual atoms and may travel as a result nearly in vacuum. Their routes are around one centimeter long, passing through 100 million atoms, and in materials where they can disperse effectively, like water, heavy water, or graphite, they can even stretch over decimeters in a straight line. This is why the study of neutrons moving through matter is known as neutron physics, often known as "neutronics*", and was founded with Chadwick's experiment[5], [6].

The Case for Fusion

Bread alone cannot sustain human life. We are little, weak animals with little power, yet we have limitless aspirations. We want to move a mountain when we see one in order to make a way for ourselves.

When we see a river, we want to control it. that it watered our farms with. To ensure a future for our offspring, we spot a star and desire to go to its planets. We need a genie to solve all of these problems at the touch of a finger. A genie like energy exists. For a comfortable existence, modern people need a lot of energy. In reality, there is a clear relationship between the per capita energy usage and the quality of living in various parts of the globe.

In this regard, the amount of per capita electricity consumption directly affects the human development index of various countries based on various reports by the United Nations Development Program, which is a parameter measuring the quality of life in a given part of the world. The majority of the developing world is slowly advancing down the UN curve of HDI against per capita power consumption, from pitifully low values now to the average of the whole globe, and ultimately towards the average of the developed world. This causes the whole world to have a tremendous energy need. In a high development scenario, it has been predicted that by 2050, the world's power consumption would increase by a factor of up to 3. Beyond 2050, the needs increase much further.

DISCUSSION

How will humanity generate the enormous quantity of energy it requires? In the absence of any fresh innovations, fossil fuels are probably going to remain the workhorse. On the other side, the use of fossil fuels as the primary energy source throughout the last century has significantly contributed to global warming by releasing greenhouse gases. Additionally, the fossil fuel stocks have begun to run out, with just coalthe main source of CO2possibly remaining for a few hundred years[7]–[9].

According to different estimations, oil and gas reserves have already begun to deplete and will only be available for a few tens of years. Over the last 10 years, political and military battles over the control of oil and gas have dominated the global energy scene.Contrarily, widespread public resistance to the use of conventional fission-based nuclear power has been strong owing to worries about proliferation, radioactive hazardous wastes, the possibility of catastrophic Chernobyl-like events, etc.

Despite being politically and technically solvable, challenges continue to be an issue. Alternative clean energy sources like solar and wind have the potential to be a significant source of energy, but before they can replace traditional energy sources, they must significantly address issues with energy density, efficiency, and cost of production. The human species is thus at a crucial crossroads right now, where we must act rapidly to produce a workable alternative source of clean energy that is easily accessible everywhere and can promote sustainable growth.

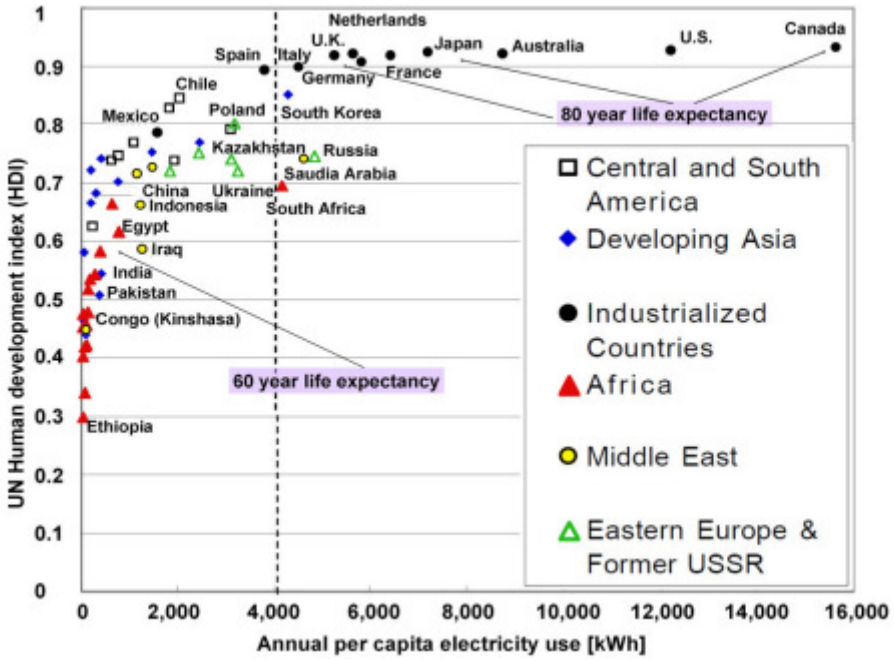

Figure 1: Represents the United Nations human development.

It takes time to create new energy technologies, and it takes much longer for them to become established as an affordable, secure, and environmentally acceptable alternative energy source.

So starting now is not too early. In this chapter, we'll argue for the quick advancement and use of nuclear fusion energy, a cutting-edge nuclear technology with less radioactive wastes and none of the proliferation or accident risks of traditional fission reactors. Since it began in earnest some 50 years ago, nuclear fusion research has made impressive strides, which have culminated in the commencement of building of the first experimental fusion reactor, known as ITER.

It takes time to create new energy technologies, and it takes much longer for them to become established as an affordable, secure, and environmentally acceptable alternative energy source. So starting now is not too early. In this chapter, we'll argue for the quick advancement and use of nuclear fusion energy, a cutting-edge nuclear technology with less radioactive wastes and none of the proliferation or accident risks of traditional fission reactors. Since it began to take off in a significant manner some 50 years ago, nuclear fusion research has made impressive strides, which have culminated in the beginning of the building of the first experimental fusion reactor, known as ITER, for all of mankind. This is especially encouraging since the globe is now realising that national differences must be set aside in order to collaborate and discover creative solutions to complex issues. In today's closely linked globe, one region's industrial progress is fueled by investments from another, and one region's economic woes and stagnation have a direct impact on another region's success. Therefore, this collaboration in nuclear fusion research might serve as a template for future technological solutions to other global issues.

the developing and developed worlds to clearly state the magnitudes of energy needs in the short term and in the long term , the techniques that are likely to be used in the absence of any new technologies, the effects on our environment, and how we might benefit in the long run by using non-fossil fuel sources of energy. We also contend that it will be required to encourage the expansion of CO2 free nuclear energy sources to provide roughly 40% of the total demand in order to satisfy the needs of centralised industrial and metropolitan hubs. Nuclear fusion holds a special place among advanced nuclear technologies due to its benefits, including easy, universal, and nearly limitless access to the basic fuel, decreased and more benign wastes, better safety features, and the promise suggested by recent technological advancements in the area. The following sections go into further depth about several of these aspects.

Energy Scenarios

The total resource base's resource lives, which take into account non-conventional oil resources like oil shale, tar sand, and heavy oil, as well as gas resources like Devonian-era shale gas, tar sand gas, ground aquifers, coal bed methane, methane hydrate, and deep layer gas, may be a few hundred years. Fossil fuel resources might thus support humanity for around 100 years if we so choose. However, it is important to note that in roughly 300 years of modern human civilization, the wealth of fossil fuels that has been created by millions of years of geological evolution on Earth and that our grandchildren and their descendants may need for various reasons will have been wasted.

Furthermore, throughout the last century, the widespread usage of fossil fuels for energy production has been gravely harming our ecosystem. The globe is significantly warming as a result of greenhouse gases, with all the related effects. Our main metropolitan areas now often

experience pollution and acid rain as a result of the extensive usage of coal. The effects on the environment will probably be horrifying if we triple the amount of fossil fuels we use. Given the aforementioned debate, it seems doubtful that, despite the necessity, the usage of fossil fuels for energy generation will continue to rise unchecked.However, although playing a significant supporting role, modern fission-based nuclear energy has problems with safety, radioactive waste management, and proliferation. Similar to fossil fuel-based power plants, renewable energy sources like wind and solar will continue to play a supporting role due to their low energy density and unsuitability for supplying electricity to urban industrial complexes despite their rapid growth.

So, even while we may be able to meet our short-term energy demands in some way, how will we address our long-term energy needs, and who will step up to the plate? Fortunately, governments all over the globe are starting to realize more recently how important it is to encourage the development of new energy technologies and the potentially terrible effects of unchecked global warming. A objective of not permitting a temperature increase of more than 2o C has been established by several nations. Over the next 50 years, carbon emissions would need to be reduced by around 80%. It's critical to recognize that the demands on the energy chain are in sharp contrast, with the ever-increasing global demand on the one hand and social and environmental concerns on the other. Additionally, in order for the whole human race to thrive sustainably, energy systems must meet current requirements without sacrificing those of coming generations.Alternative energy sources that don't further damage the ecology or completely deplete the finite fuel supplies, preventing future generations from using them for diverse purposes. The following factors must be taken into consideration while the new energy resources are developed. They must be built on effective, clean energy conversion techniques that have broad public support[3], [10].

CONCLUSION

A key area in the research and development of nuclear reactors is neutronics. Neutron transport, interactions with nuclear fuel, and radiation shielding are all covered, with the main emphasis being on comprehending and simulating the behaviour of neutrons in a reactor core. Neutronics is essential for guaranteeing the safe and effective operation of nuclear power facilities by precisely forecasting neutron flux and criticality. To solve the difficult equations regulating neutron behaviour, computational approaches are often used, including Monte Carlo simulations and deterministic methods. Advancements in reactor design, fuel optimisation, and safety analysis are made possible by neutronics research and analysis. For analysing radiation levels, evaluating reactor operation, and creating plans to prevent accidents, the field's results and methodology are crucial. We can improve the dependability, safety, and sustainability of nuclear energy as a key element of the world's energy mix by consistently improving our knowledge of neutronics.

REFERENCES

[1] Y. Wu, Neutronics of advanced nuclear systems. 2019. doi: 10.1007/978-981-13-6520-1.

[2] Y. Wu, Fusion neutronics. 2017. doi: 10.1007/978-981-10-5469-3.

[3] V. Gopalakrishnan, “Nuclear data,” in Physics of Nuclear Reactors, 2021. doi: 10.1016/B978-0-12-822441-0.00002-9.

[4] W. Li, H. Lu, J. Li, Z. Dang, X. Zhang, Y. Wu, and X. Fan, “Development of a new flux map processing code for moveable detector system in PWR,” 2013.

[5] P. V Subhash, C. V Suresh, S. Jakhar, C. V. S. Rao, and T. K. Basu, “B2S: A Program to Reconstruct Geometrical Information from Computer Aided Design Models (CAD) and Converting into Primitive Mathematical Form,” Adv. Energy Eng., 2013.

[6] F. M. Mann, D. E. Lessor, and J. S. Pintler, “REAC nuclear data libraries,” Radiat. Eff., 1986, doi: 10.1080/00337578608208323.

[7] D. M. Pérez, L. H. Pardo, D. M. Pérez, L. P. R. Garcia, D. E. M. Lorenzo, and C. A. B. de Oliveira Lira, “Reactivity Effects in a Very-High-Temperature Pebble-Bed Reactor,” Atom Indones., 2021, doi: 10.17146/AIJ.2021.1075.

[8] H. Nifenecker, S. David, J. M. Loiseaux, and O. Meplan, “Basics of accelerator driven subcritical reactors,” Nuclear Instruments and Methods in Physics Research, Section A: Accelerators, Spectrometers, Detectors and Associated Equipment. 2001. doi: 10.1016/S0168-9002(01)00160-7.

[9] Y. Wu, “Neutron Transport Theory and Simulation,” in Fusion Neutronics, 2017. doi: 10.1007/978-981-10-5469-3_2.

[10] N. Mitsuboshi and H. Sagara, “Effects of U3Si2 fuel and minor actinide doping on fundamental neutronics, nuclear safety, and security of small and medium PWRs in comparison to conventional UO2 fuel,” Ann. Nucl. Energy, 2021, doi: 10.1016/j.anucene.2020.108078.

CHAPTER 2

NEUTRONICS CHARACTERISTICS, SHIELDING SYSTEM,ACTIVATION

Dr. Veerabhadrappa Jagadeesha, Assistant Professor,
Department of Physics, Presidency University, Bangalore, India
Email Id-jagadeeshaangadi@presidencyuniversity.in

ABSTRACT:

Awareness and analyzing the behavior of neutrons in nuclear reactors requires an awareness of many fundamental aspects of neutronics. The neutron flow, neutron energy spectrum, neutron interaction cross-sections, and neutron multiplication are some of these features. The density or quantity of neutrons per unit volume in a reactor core is referred to as neutron flux, and it is a key factor in determining the overall performance of the reactor. The distribution of neutron energies within the reactor is referred to as the neutron energy spectrum, and it may change based on the kind of reactor and its operating circumstances. The possibility of neutrons interacting with different materials, including as fuel, coolant, and structural materials, is described by neutron interaction cross-sections.

KEYWORDS:

Neutronics, Neutron flux, Neutron energy spectrum, Neutron interaction cross-sections, Neutron multiplication

INTRODUCTION

Four power plants constructed using a variety of aggressive and conservative tokamaks have been created by the ARIES team. The four ARIES-ACT designs went forward interactively as the systems code established the reference parameters by usingadjusting the physics and engineering factors to get the most cost-effective design for each situation:

1. SiC-based blanket for aggressive physics
2. Conservative physics with blanket based on ferritic steel.
3. Conservative physics with a SiC-based blanket and aggressive physics with a ferritic steel-based blanket[1].

The extensive use of 3-D analyses to ensure the accuracy of the overall TBR with high fidelity, the evaluation of the neutron wall loading distribution, the definition of the radial/vertical builds that satisfy the shielding, breeding, and other design requirements, the determination of the radiation damage profile in particular behind assembly gaps, and the assessment of nuclear heat loads to all components are some of the main goals of the nuclear assessment. The nuclear

environment for ARIES-ACT-2, the last power plant design in the ARIES series, must be described using these nuclear parameters [2].To provide the best design, an integrated plan that took into account the entire configuration, design specifications, choice of low-activation materials, nuclear evaluations, structural integrity of all components, and safety concerns was deemed important. Extensive 3-D evaluations were used to specify the size of the inboard and outboard blankets that fulfil the breeding requirement before the nuclear assessments were included into the design. Next, the NWL for the real 3-D arrangement of the FW and divertor is discovered. These peak values at the inboard midplane, divertor dome, and outboard midplane give the data necessary to determine the radial and vertical builds. The next step in the shielding design is to size and optimize the shielding components while taking into account the performance of the desired shielding materials, their activation properties, and the influence on safety. After other design inputs are used to define the radial/vertical constructs, the integration process utilizing the CAD system starts, allowing for the addition of further geometric complexity. Detailed analyses of the economy and safety are then conducted, closely followed by neutronics interactions [3].

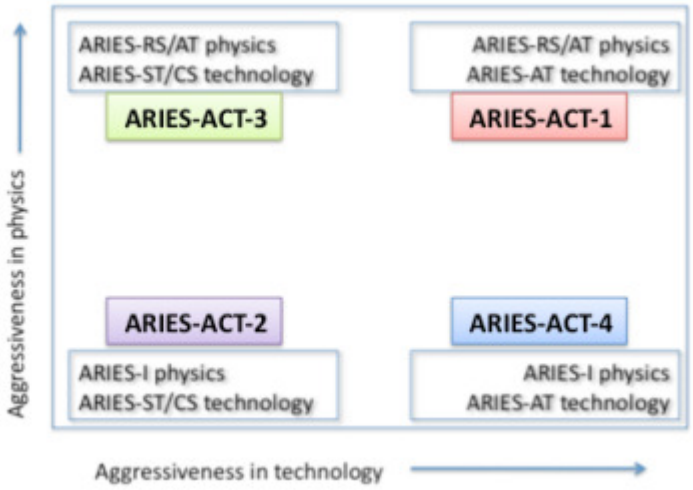

Figure 1: Represents the Four-corner designs of ARIES-ACT power plants.

Similar to the ARIES-ST and ARIES-CS systems, ARIES-ACT-2 makes use of a dual cooled LiPb blanket with a helium-cooled reduced activation ferritic/martensitic steel framework, a LiPb breeder, and SiC flow channel inserts. Similar to ARIES-ST, the LiPb enables both breeding and blanket self-cooling. The blanket is protected from heat and neutron fluxes from the plasma by the He-cooled F82H RAFM steel first wall. The structural ring acts as the high-temperature shield and is cooled with helium in the ARIES-ACT-2 design, which is seen in Figure 1 [4]. Additionally, helium is used to cool the W-based divertor. A thin water-cooled low-temperature shield and a vacuum vessel are the two distinct parts found outside the SR. It should be noted that, unlike all prior ARIES tokamaks, the ARIES-ACT-2 main radius and total machine size are determined by the peak heat flux at the divertor[5]. This change in design concept eliminated the need for inboard shielding components with WC filler that were small and very effective. In other words, the economics and size of the machine as a whole are not significantly

impacted by the ARIES-ACT-2 inboard standoff.The nuclear specifications given here are for the final design, which has a major radius of 9.75 meters, a minor radius of 2.44 meters, a plasma surface area of 1440.5 meters, a fusion power of 2637.5 megawatts, and a net electric output of 1000 megawatts. Neutronics, shielding, and activation are three closely linked processes that fall under the nuclear analysis. Following is a breakdown of each subtask[6]:

Neutronics:

1. Distribution of neutron wall loading: maximum and average values
2. Radial and poloidal nuclear heating distribution and the tritium breeding ratio for T-self sufficiency
3. Multiplication of nuclear energy
4. Radiation damage to building materials;
5. Energy shared between He and LiPb coolants.

DISCUSSION

3-D Model and Codes

The neutronic analysis for ARIES-ACT-2 was carried out using a collection of computer programs and a nuclear data library, including CUBIT, MCNP5, DAGMC, and the FENDL-3 data library. When dealing with complicated geometries, CUBIT constructs the 3-D model that DAGMC will utilise to execute the Monte Carlo radiation transfer right onto the CAD model. The Computational Nuclear Engineering Research Group at the University of Wisconsin–Madison created the DAGMC code as a software tool to perform Monte Carlo radiation transport on intricate 3-D geometries produced by solid modelling software. The radiation transport algorithm MCNP5 and its FENDL-2.1 continuous pointwise cross section data library are coupled with DAGMC, which transforms any complicated three-dimensional geometry into a faceted geometry of tetrahedrons. ARIES-ACT-2 consists of 16 toroidal modules spaced 2 cm apart from one another[6].

The 16 modules each cover a 22.5o toroidal angle. For the 3-D TBR and nuclear heating assessments, the top half of an 11.25o wedge of the tokamakrepresenting one fourth of the module or 1/64th of the total tokamakwas modelled. Three reflecting boundaries that were positioned at the midplane, both sides of the 11.25o wedge, and the midpoint were used to convert the 1/64 neutronics model to the entire toroidal geometry.The neutron source distribution is represented by three nested zones with intensities of 63.0%, 32.5%, and 4.5% within the plasma border. The magnetic axis is located around 30 cm outside of the primary radius[7]. When we evaluated the actual neutron source distribution on the R-Z grid from PPPL's plasma physics simulations, the three-region neutron source presentation demonstrated to capture almost all of the impacts of the real source and produced results for the NWL and TBR that were similar.Acceptable statistical errors are present in the 3-D data shown here.

Tritium Breeding Assessment

The DCLL blanket's capacity to supply tritium self-sufficiency is one of the most crucial topics

that we have examined for ARIES-ACT-2 in order to identify the design components that influence the breeding. The major objective of this study is to pinpoint the precise circumstances that the internal blanket components and exterior, vital tokamak components create to harm or enhance the TBR. We propose running all LiPb utilising designs with 6 Li enrichment 90% and changing the Li enrichment online during operation to reduce concerns about shortage or excess of tritium in order to address the difficulties of dealing with tritium-related uncertainties in multiple subsystems[8].

The numbers in brackets show how much each category is predicted to contribute to the breeding margin of ARIES-ACT-2, translating to an estimated TBR of 1.05 for the LiPb breeder. The most recent ENEA experiment to confirm the nuclear data for the LiPb breeder provided the 3% of the first margin. Even with measurement errors, the C/E is 15%. An informed estimation places the shortfall in the LiPb nuclear data at 3% or less. For ARIES-ACT-2, this parameter is not as important since breeding must be adjusted online by design. By modifying the 6 Li enrichment online, as will be addressed later in Section III.B, a few percent up or down in breeding may be regained during operation[9].

The ARIES-ACT-2 3-D TBR model incorporates all the blanket's technical specifics, as specifically mentioned in Section III.C. The additional 1% margin covers any neglected design component. Given that our 3-D model has all structural information supplied by blanket designers, the associated third margin has been wiped out. If unanticipated design changes have a negative effect on the TBR as the design develops into a mature engineering design, the online adjustment of the 6 Li enrichment will make up for the breeding losses. The T bred in excess of T used in the plasma is accounted for by the last 1% margin. The 5% sum of the three margins gives the minimum TBR required for reliable breeding in ARIES-ACT-2. Such an excess T is required to provide the startup inventory for a new fusion power plant, to account for the decay of the total T inventory, and to account for the T lost to the environment. The Net TBR during plant operation might be as low as 1.01 due to the LiPb nuclear data and modelling limitations, both of which have the tendency to lower breeding. In fusion systems using cutting-edge physics and technology, where the T fractional burnup surpasses 10%, the T inventory is limited, and the T extraction and reprocessing system are very dependable, such a low Net TBR of 1.01 is realistically feasible. It should be noted that when the nuclear data assessment improves with a concerted R&D program, the little percent gap between the estimated TBR and Net TBR will eventually disappear[10].

Need for Online Adjustment of TBR

After the DEMO operation with fully integrated blanket, T extraction, and T processing systems, the Net TBR of 1.01 won't be validated. While a surplus of T creates licensing and storage issues, a scarcity of T affects the plant's operating schedule and necessitates buying T from outside sources at unreliable prices, and/or the accessibility of T recovered from the detritylation system. Fusion designs shouldn't create more T than necessary for plasma fueling, which is crucial for licencing purposes. All of these problems provide credence to the claim that DEMO and power plants must have an online breeding adjustment.

By addressing each topic separately, previous research has made many efforts to provide answers to various concerns. The degree of trust in the single-effect analysis and the interdependence and synergistic effects of the many design features on TBR remain some of the remaining questions, however. We created a step-by-step process to pinpoint the precise reason for the decline in TBR and almost all queries were looked at integrally to address these concerns as a group. It should be noted that this new method was originally used on an intermediate ARIES-ACT-2 design to solve the issues raised above. To confirm that the most recent alterations to the top/bottom ends of the OB blanket and the addition of manifolds behind the divertor system comply with the ARIES breeding requirements, we once again applied the stepwise approach to the final ARIES-ACT-2 design[11].

The decline in TBR is caused by ten distinct design components. These components are the FW, side/back/top/bottom walls, cooling channels, SiC FCIs, W stabilizing shells, assembly gaps, and penetrations and are part of the internals and externals of the ARIES-ACT-2 DCLL blanket. Every feature has been meticulously modelled to perfectly match the blanket's design requirements. The progressive addition of the individual components to the blanket envelope and recording of the corresponding incremental change to the TBR were made possible by the stepwise technique. The individual blanket pieces were initially modelled using the CAD system for an accurate representation, and then connected with the MCNP code by DAGMC. According to Section II, the 3-D TBR model represents 1/64th of ARIES-ACT-1. For the real LiPb breeding channels, complete heterogeneity was employed. As in ARIESAT, the initial 6 Li enrichment is 90%. The variance in TBR as a result of 6 Li enrichment was next looked at.

The final outcome for the reference LiPb eutectic with 15.7 at% Li and 84.3 at% Pb. This bar chart displays the computed TBR from ten successive 3-D runs in which breeding performance was degraded gradually by different blanket internals and environmental factors. The 10 distinct processes are covered in full below, along with any changes that were specifically made to the 3-D model at each step.

Neutron Wall Loading Distribution

Designers may specify radial and vertical structures using the NWL, ensuring that peripheral components are properly shielded from intense neutrons. For the shielding and radiation damage assessments in Section V, peak NWL values must be evaluated together with additional information, such as average values for the activation analysis in Section VIII. By definition, the NWL is the first solid wall encircling the plasma that has a normalized neutron current density based on fusion power. By observing the neutron current that travels between the divertor and first wall plates' three-dimensional surfaces, it is assessed. Neutronic simulations were carried out to determine the NWL distribution over the FW and divertor surfaces of ARIES-ACT-2 using CUBIT , DAGMC , and a 3-D model of the FW and divertor that was constructed and prepared. The three-region neutron source description inside the plasma boundary is used to create the 3-D model for this specific investigation in Figure 9. The final ARIES-ACT-2 design's NWL distribution along the IB and OB FWs yielded the results shown in Fig. 10. At the midplane of the OB FW, the NWL reached its maximum value of 2.2 MW/m2.The NWL diminishes as the vertical distance from the midplane increases, as predicted. The distribution of NWL along each

divertor plate. The tokamak's centerline serves as the reference point for calculating the dome's radial distance. Be aware that the divertor surface's orientation affects the NWL, with a surface facing the plasma experiencing a greater NWL than a surface that is vertical[12].

CONCLUSION

Understanding and analyzing the behavior of neutrons in nuclear reactors depends heavily on neutronics features. Key elements that affect reactor performance and safety include neutron flux, neutron energy spectrum, neutron interaction cross-sections, and neutron multiplication. While the neutron energy spectrum reflects the range of neutron energies, the neutron flux indicates the density of neutrons inside the reactor core. The probability of neutron interactions with various materials is indicated by their neutron interaction cross-sections, and neutron multiplication has an impact on the reactor's criticality and power production.

REFERENCES

[1] L. El-Guebaly and L. Mynsberge, “Neutronics characteristics and shielding system for ARIES-ACT1 power plant,” Fusion Sci. Technol., 2015, doi: 10.13182/FST14-791.

[2] G. Stankunas and A. Tidikas, “Neutronic analysis of IFMIF-DONES test cell cooling system,” Appl. Radiat. Isot., 2020, doi: 10.1016/j.apradiso.2020.109207.

[3] X. Yuan and L. Cao, “Analysis of neutronics characteristics of small modular Pb-Bi cooled reactor core with nitride fuel,” Hedongli Gongcheng/Nuclear Power Eng., 2014, doi: 10.13832/j.jnpe.2014.S2.0038.

[4] W. Tan, P. Long, G. Sun, J. Zou, and L. Hao, “Neutronics analysis of JSI TRIGA Mark II reactor benchmark experiments with SuperMC3.3,” Nucl. Eng. Technol., 2019, doi: 10.1016/j.net.2019.05.014.

[5] I. A. Larionov, A. V. Lopatkin, I. B. Lukasevich, V. I. Moroko, and V. E. Popov, “Homogenous Transmutation of 237Np, 241Am, 243Am in a Lead-Cooled Fast Reactor,” At. Energy, 2021, doi: 10.1007/s10512-021-00756-1.

[6] Y. Alzaben, V. H. Sanchez-Espinoza, and R. Stieglitz, “Core neutronics and safety characteristics of a boron-free core for Small Modular Reactors,” Ann. Nucl. Energy, 2019, doi: 10.1016/j.anucene.2019.04.017.

[7] K. Tsujimoto, T. Sasa, K. Nishihara, H. Oigawa, and H. Takano, “Neutronics design for lead-bismuth cooled accelerator-driven system for transmutation of minor actinide,” J. Nucl. Sci. Technol., 2004, doi: 10.1080/18811248.2004.9715454.

[8] I. K. Baidoo, B. Li, Q. Yang, J. Song, and L. Q. Hu, “Verification of SuperMC for MNSRs core analysis: The case of Ghana Research Reactor-I,” Ann. Nucl. Energy, 2018, doi: 10.1016/j.anucene.2017.10.046.

[9] A. V. Sobolev, A. S. Gazetdinov, and D. S. Samokhin, “Genetic algorithms for nuclear reactor fuel load and reload optimization problems,” Nucl. Energy Technol., 2017, doi: 10.1016/j.nucet.2017.07.002.

[10] T. Sasa, K. Tsujimoto, T. Takizuka, and H. Takano, "Code development for the design study of the OMEGA Program accelerator-driven transmutation systems," Nucl. Instruments Methods Phys. Res. Sect. A Accel. Spectrometers, Detect. Assoc. Equip., 2001, doi: 10.1016/S0168-9002(01)00166-8.

[11] U. Fischer and A. Möslang, "The gas dynamic trap as neutron source for material irradiations," Fusion Technol., 1999, doi: 10.13182/fst99-a11963843.

[12] M. Z. Youssef and R. Feder, "3D assessment of nuclear heating, dose rate, and structural damage in the generic ITER diagnostics upper port plugs and adjacent magnet coils," 2010. doi: 10.1016/j.fusengdes.2010.02.034.

CHAPTER 3

NEAR TERM ENERGY SCENARIO

Dr. Usman Pasha, Associate Professor
Department of Physics, Presidency University, Bangalore, India
Email Id-mahaboobpasha@presidencyuniversity.in

ABSTRACT:

The next few years to a decade are often included in the near-term energy scenario, which describes the present and expected energy situation. This research focuses on elements including energy sources, technology, regulations, and market dynamics as it analyses the major trends, obstacles, and possibilities in the energy industry. Numerous variables, such as changing global energy consumption, worries about climate change, technology breakthroughs, regulatory frameworks, and geopolitical considerations, have an impact on the near-term energy landscape. This research sheds light on the existing and anticipated mix of energy sources, including nuclear, renewable energy sources, fossil fuels, and upcoming technologies. It also looks at the effects on economic development, sustainability, and energy security.

KEYWORDS:

Near-term, Energy scenario Energy landscape, Energy sources, TechnologiesPolicies.

INTRODUCTION

Several of the currently available non-fossil energy sources, which are constantly being improved for better efficiency, wider availability, and reduced pollution are likely to be increasingly used to supplement the fossil fuel energy sources in the near future in order to satisfy the world's energy demand and possibly address environmental concerns.Two such resources came to mind right away. Nuclear energy and solar energy are the two options.Being renewable, solar energy is a natural contender for sustainable development. Solar energy may be used in a variety of ways, including solar photovoltaic (solar cells), solar thermal (hot water for homes, businesses, or power generation), and biofuel production. The main issue in each of these situations is the Earth's surface's low solar energy flow, which makes it challenging to design for large, energy-hungry industrialised cities that operate on solar energy. However, with the introduction of nanotechnology, solar energy technologies have recently seen tremendous growth[1]–[3].

The infrared spectrum of solar energy, which is invisible, may be converted into electrical energy by new plastic materials consisting of polymer nanoparticles called quantum dots. Conventional solar panels, especially those made of plastic, utilize the visible portion of the light, although the Sun really emits around 50% of its energy in the infrared spectrum.Recently, researchers from the Boeing subsidiary Spectro lab disclosed the creation of multijunction solar cells with an efficiency of over 40%, setting a new world record for solar photovoltaic cells.

This is much superior than the greatest solar cells currently on the market, which have efficiencies of 22%, and the current industry average of 12–18%. Theoretical efficiencies for concentrator solar cells are over 58% in cells with more than three connections, according to the Spectro lab experts, who also anticipate that these cells might eventually attain efficiencies of more than 45% or even 50%.

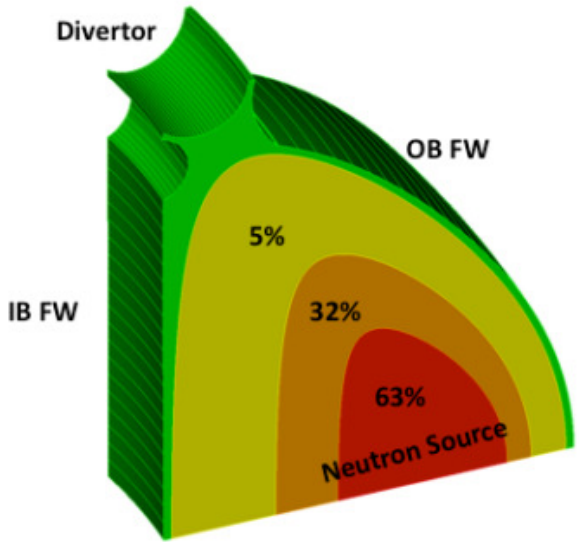

Figure 1: Represents the 3-D ARIES-ACT-2 model used for NWL analysis.

Radial/Vertical Build Definition

As soon as the blanket dimension and enrichment were established, the defining of radial and vertical constructions followed, with a strong connection between the desired shielding materials' efficacy and their activation properties. The MF82H ferritic steel-based SR with He cooling

supports the divertor and blanket. Similar to ARIES-ACT-1 , ARIESACT-2's thin VV (10 cm) is manufactured of 3Cr-3WV bainitic steel cooled by helium, and operates hot at 300oC to prevent tritium accumulation-related problems. Outside of the thin VV is where the main shielding element (LT shield) is placed. To aid in the dissipation of decay heat after loss of coolant/flow mishaps, this shield functions at room temperature. To assist manage the decomposition heat of the IB side during such events, the very effective WC filler was omitted.

Many requirements are met by the ARIES-ACT-2 radial/vertical constructions. Magnets and the VV are lifetime components. The total dimensions of the blanket and SR required to protect the VV for the 40 FPY plant life are determined by the design criteria in Table II. In order to improve the power balance, it was also mandated to maximize the amount of nuclear heating that could be recovered from the blanket and SR (about 99% of the thermal power) and to reduce the amount of low-grade heat that might seep into the VV and LT shields (about 1% of the thermal power). This specific criterion requires SR to be at least 30 cm thick. The protection of the 16 maintenance ports on the OB side is another unique need. The sides of the TF magnets are shielded by a 45 cm thick He-cooled shielding plug positioned at the inner radius of the maintenance ports.

All specialized parts (blanket, SR, and VV) share the objective of performing a shielding function to fulfil the radiation protection needs of the superconducting (S/C) magnets. With the least amount of radial standoff, this aids in defining the machine's most compact operating area, which frees up ex-vessel space for structural connections, cooling pipes, coil leads, etc. The ideal composition of IB, OB, and top/bottom LT shields with FS structure was determined by 1-D tradeoff analyses of water and B-FS filler using the PARTISN algorithm and FENDL-2.1 data library. In accordance with the ARIES-ACT-2 standards, the ideal radial and vertical constructions, and Table III provides the component composition.

The radial/vertical construction described thus far has been presumptively devoid of penetrations, it should be emphasized. As expected, all OB components have several penetrations for plasma heating and current driving that surround the OB midplane. These holes, combined with the 16 assembly gaps, enable neutrons to seep through, jeopardising the effectiveness of the shield. Only the impact of assembly gaps has been addressed for IB and OB components due to the study's constrained scope, and the 3-D findings will be presented in a separate paper[4]–[6].

DISCUSSION

Nuclear Heating Profile

LiPb with 40% 6 Li enrichment and fusion power of 2637.5 MW has been utilized to assess nuclear heating and total energy multiplication using the 3-D TBR model For a 1/16th module that generates 35.1 MWth in IB, 102.6 MWth in OB, and 8.1 MWth in the upper or lower divertor zone, Table IV shows the breakdown of heating by component. The gadget must be heated in order to learn more about the thermal hydraulic analysis and ultimately the thermomechanical stresses it experiences while in use. The entire quantity of nuclear heating that can be recovered is 2462.1 MW. The visual distribution of nuclear heating over all locations is shown in Figure 13. IB, OB, and divertor areas provide 23%, 67%, and 10% of the heating, respectively, as shown in Table V. The FW/blanket, stabilising shells, and SR absorb 9% of the warmth, while the divertor and its support structure deposit around 91% of it. By dividing the total heating (2637.5 MW x 0.8) by the neutron power, a total energy multiplication of 1.167 is achieved.

the nuclear heating is divided between He and LiPb high temperature coolants, producing 3119 MW of useable thermal energy, including surface heating.For the purpose of pricing the He and LiPb heat transfer/transport system, this split between the He and LiPb loads is a crucial parameter for the power conversion system as well as the ARIES Systems Code. The He and LiPb coolants recover the majority (about 90%) of the divertor and blanket He and LiPb pumping powers as thermal power. The final value for the He: LiPb thermal power ratio is 49:51.

Since then, a number of medium-sized solar photovoltaic power plants have been erected, especially in Europe and the USA. Initially, solar photovoltaic technologies were largely used to power tiny individual equipment like calculators or isolated dwellings not linked to grids. For instance, there are various power plants in Spain that produce tens of megawatts; the greatest is the Parque Photovoltaic Medalla de Alarcón, which has a capacity of 60 MW (85 GWh), but the Nellice Airforce base solar station in the USA has a capacity of 14 MW (30 GWh).Additionally,

a number of sizable photovoltaic power plants are being built, the biggest of which being the 550 MW Topaz Solar Farm in California. In order to expand its domestic electric energy consumption from solar to 50% by 2030 from the current level of a fraction of one percent Japan, one of the leading markets for solar energy, has set this goal. By 2030, it is hoped that the USA would have reached 10% of its peak generating capability, which would equate to 180 million barrels of oil's worth of energy.

Consequently, even while solar photovoltaic is steadily establishing itself as an alternative energy source, it is expected to only serve as a supplementary source of energy for a number of generations. It still needs to address the following matters: It cannot be installed in big urban industrial complexes since it lacks the energy density of other traditional large power plants, such as nuclear reactors (it requires large-scale installation). The stability of a grid with a substantial solar contribution, particularly in the winter when there is less sunshine or at night, has not been well explored. There are still concerns to be overcome about the high investment cost, maintainability, creation of hazardous waste during solar panel manufacture, and final disposal[7]–[9].

On the other hand, biofuel technologies, such the manufacture of ethanol or biodiesel from flora rich in sugar or starch or from biological wastes, have also seen tremendous growth over the years. In many nations nowadays, biofuels are combined with traditional fuels like petrol or diesel and utilised as the main source of fuel for cars. Growing in importance are also newer generation biofuels like algal oils or oilgae the conversion of vegetable oils or biodiesel into petrol, or genetically modified plants that absorb more carbon than is emitted during the burning of the biofuels they create.

Although crop cultivation has been shifted away from food production towards the development of biofuels, biofuels have been beset by problems such as shifting food prices and dramatically increasing greenhouse gas emissions, soil erosion, deforestation, and desertification. The usage of biofuels has caused parched environments, the growth of deserts, a general loss of biodiversity, and volatility in food prices in several emerging nations. Therefore, it is very improbable that biofuels would replace fossil fuels as the principal energy source for producing power.

On the other hand, the nuclear energy alternative based on nuclear fission is a useful one that is already being used at an average level of 25% in the industrialized world. Even nations like France use a larger share of nuclear energy (78%). Fission may provide the world with energy for many thousand years when one masters the usage of fissile materials like 239Pu and 233U, which can be bred from fissile elements like 238U and 232Th. Naturally fissile resources like 235U may run out in a few hundred years.

Nuclear energy plants can easily meet the demands of centralized industrial areas, but their usage has been restricted due to safety concerns and worries about nuclear proliferation. Free access to nuclear technology has been hindered by this. Concerns exist on the necessity for extreme caution while managing nuclear waste, as well. Although the majority of these issues have technological answers, they may also have important economic, political, and societal

repercussions. As a result, it is unclear how much of the world's energy requirements can be met by nuclear fission. As a result, the global energy situation is anticipated to stay mostly unchanged over the next 20–30 years, with fossil fuels continuing to be the mainstay as oil and gas progressively become more costly and scarcer. While alternative energy sources like solar photovoltaic and biofuels are anticipated to play a more major supporting role, particularly in established nations, conventional nuclear reactors are likely to grow their proportion of energy sources, especially in rising economies like India. However, it takes a long time for new energy technology to mature, thus the potential for alternative energy sources to provide.

Long term energy scenario and the role of fusion

On a regional and global scale, there have been several thorough efforts to generate scenarios for power demand and supply.The studies being conducted by the International Institute for Applied Systems Analysis (IIASA) under the supervision of the World Energy Council (WEC)and the studies by the Intergovernmental Panel on Climate Change (IPCC) are some of the most recent comprehensive ones.These studies' major goal was to determine the maximum level of future energy supply that could be ensured by the current power producing capabilities as well as an estimate of new power supply capacities created by potential technologies. The determination of a region-by-region breakdown of potential power production system growth trajectories was another goal of these research, particularly in the context of rapidly dwindling fossil fuel stocks. Estimates of each technology or fuel type's contribution in total installed capacity and maximum power supply, including those for advanced energy technologies like thermonuclear fusion, are also included.

One of the issues with such studies is that they all inevitably have to make a number of underlying assumptions, such as those related to population growth, economic development, industrial growth, new technological advancements, the availability of primary energy sources, and a variety of other factors. As a consequence, depending on the underlying variables in a particular situation, the predictions from these models vary slightly. The IIASA-WEC research [1.32] on eleven distinct globe areas, for instance, offers three alternate possibilities of future economic growth and energy consumption patterns, further subdivides them into six separate scenarios, and assesses their ramifications.

Fusion Basics

The stars and the Sun, which have been blazing brightly for billions of years using this method, are the greatest examples of fusion in our environment. With nuclear fusion, one starts with light elements and brings them together so that they may fuse to generate heavier elements, as opposed to nuclear fission, where heavy nuclei, like uranium, are broken and release energy. Due to the tiny mass differential between the heavier, resultant components and the lighter, fusing elements, energy is released. As an example, when deuterium and tritium nuclei are brought together (these are the two heavier isotopes of hydrogen with masses of 2 and 3, respectively), they fuse to create helium and a neutron, and the energy associated with the mass difference is 17.6 MeV. The kinetic energies of the product nuclei are the energy that escapes and may be captured and utilized to generate electricity. In order for fusion to take place, positively charged

and naturally repellant protons or heavier reactant nuclei must be brought close enough to overcome electrostatic attraction. This allows the nuclear strong force, a very short-range force that holds the nucleons in a nucleus together, to aid in the fusion process through a quantum mechanical tunnelling process.

Because the binding energy that keeps the nucleons in a nucleus together is far bigger than the energy that binds atoms and molecules together via electronic links, the energy produced during a fusion process is significantly greater than that in chemical reactions. For instance, the energy needed to remove a hydrogen atom's single electron, or ionisation energy, is 13.6 eV, or less than one millionth of the 17.6 MeV generated during the D-T process. Even while individual fission processes involving extremely heavy nuclei are often far more energetic than individual fusion events, fusion reactions also have an energy density (energy generated per unit mass of the reactants) that is significantly higher than fission reactions. More energy per unit of mass than in fusion processes can only be released by direct conversion of mass into energy, such as through matter-antimatter collisions[10].

CONCLUSION

The existing and expected energy situation in the next years are included in the near-term energy scenario. It is influenced by a number of things, including market dynamics, energy sources, technology, and legislation. Shifting global energy consumption, worries about climate change, technological breakthroughs, regulatory frameworks, and geopolitical factors all have an impact on the near-term energy landscape. For all parties involved in the energy industry, including governments, companies, and people, understanding the near-term energy environment is essential. Making wise judgements about energy planning, investment, and environmental stewardship requires analysing and anticipating trends in energy sources including fossil fuels, renewable energy, nuclear energy, and developing technologies.

REFERENCES

[1] S. Summa, L. Tarabelli, G. Ulpiani, and C. Di Perna, “Impact of climate change on the energy and comfort performance of nzeb: A case study in Italy,” Climate, 2020, doi: 10.3390/cli8110125.

[2] S. Fujimori et al., “A framework for national scenarios with varying emission reductions,” Nature Climate Change. 2021. doi: 10.1038/s41558-021-01048-z.

[3] T. Magnusson, S. Anderberg, S. Dahlgren, and N. Svensson, “Socio-technical scenarios and local practice – Assessing the future use of fossil-free alternatives in a regional energy and transport system,” Transp. Res. Interdiscip. Perspect., 2020, doi: 10.1016/j.trip.2020.100128.

[4] K. Oshiro, K. Gi, S. Fujimori, H. L. van Soest, C. Bertram, J. Després, T. Masui, P. Rochedo, M. Roelfsema, and Z. Vrontisi, “Mid-century emission pathways in Japan associated with the global 2 °C goal: national and global models’ assessments based on carbon budgets,” Clim. Change, 2020, doi: 10.1007/s10584-019-02490-x.

[5] G. Godínez-Zamora, L. Victor-Gallardo, J. Angulo-Paniagua, E. Ramos, M. Howells, W. Usher, F. De León, A. Meza, and J. Quirós-Tortós, "Decarbonising the transport and energy sectors: Technical feasibility and socioeconomic impacts in Costa Rica," Energy Strateg. Rev., 2020, doi: 10.1016/j.esr.2020.100573.

[6] M. P. Tootkaboni, I. Ballarini, and V. Corrado, "Analysing the future energy performance of residential buildings in the most populated Italian climatic zone: A study of climate change impacts," Energy Reports, 2021, doi: 10.1016/j.egyr.2021.04.012.

[7] A. Gambhir, J. Rogelj, G. Luderer, S. Few, and T. Napp, "Energy system changes in 1.5□°C, well below 2□°C and 2□°C scenarios," Energy Strateg. Rev., 2019, doi: 10.1016/j.esr.2018.12.006.

[8] G. Lorenzi and P. Baptista, "Promotion of renewable energy sources in the Portuguese transport sector: A scenario analysis," J. Clean. Prod., 2018, doi: 10.1016/j.jclepro.2018.03.057.

[9] F. Lallana, G. Bravo, G. Le Treut, J. Lefèvre, G. Nadal, and N. Di Sbroiavacca, "Exploring deep decarbonization pathways for Argentina," Energy Strateg. Rev., 2021, doi: 10.1016/j.esr.2021.100670.

[10] S. Mittal, J. Y. Liu, S. Fujimori, and P. R. Shukla, "An assessment of near-to-mid-term economic impacts and energy transitions under '2°C' and '1.5°C' scenarios for India," Energies, 2018, doi: 10.3390/en11092213.

CHAPTER 4

DETERMINATION OF FUSION REACTIONS

Dr. Sivasankara Reddy Nanja Reddy, Assistant Professor
Department of Engineering Physics, Presidency University, Bangalore, India
Email Id- sivasankarareddy@presidencyuniversity.in

ABSTRACT:

Grasp and using nuclear fusion's potential as a source of energy in the future requires a grasp of how fusion processes work. This research focuses on the techniques and procedures used to recognize and describe fusion reactions, which involve the fusing of lighter atomic nuclei to create heavier nuclei and release enormous quantities of energy. The inquiry looks at theoretical and experimental methods for figuring out fusion processes, including as lab tests, computer simulations, and theoretical models. To comprehend the viability and effectiveness of fusion reactions, important factors like reaction cross-sections, reaction rates, and energy thresholds are analyzed.

KEYWORDS:

Fusion reactions, Nuclear fusion, Atomic nuclei, Energy release, Experimental methods.

INTRODUCTION

The reaction between deuterium (D) and tritium (T) two isotopes of hydrogen with one neutron and two neutrons in their respective nuclei (normal hydrogen has only one proton and no neutron in its nucleus), is the most practical, though not always the most effective, to carry out in modern magnetic fusion devices like tokamaks. Because the D-T fusion processes have the biggest collision cross-section and take place at the lowest temperature, it is the most practical to achieve[1]–[3]**.**

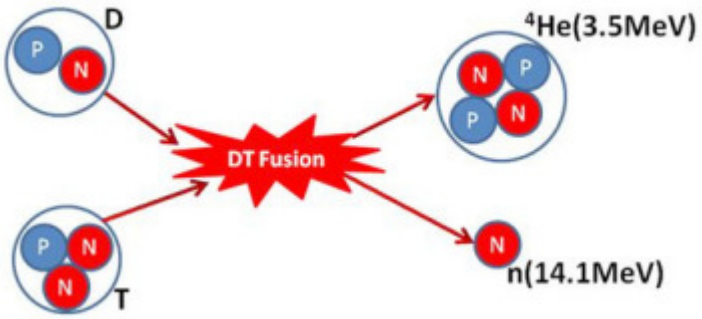

Figure 1: Represents the Schematic of a D-T fusion reaction.

The following illustration explains the causes of this. The nuclear strong force, which has a relatively small range and is responsible for the binding of the protons and neutrons in a nucleus, acts predominantly amongst nearby nucleons. Therefore, the nucleons that are entirely encircled by their nearby neighbors, such as those within a nucleus, are more tightly linked than those on the surface. Therefore, the energy needed to separate the nucleons is known as the nuclear binding energy. The Einstein formula 2 e m c, where m is the negligible mass difference between the nucleus and the entire mass of its component nucleons, and c is the speed of light, gives its magnitude.The binding energy per nucleon caused by the strong force is typically less for smaller nuclei than it is for larger nuclei because the ratio of their volume to surface area is smaller for smaller nuclei.

The electrostatic force between protons, on the other hand, is long-range and obeys the inverse square rule. As a result, in order to add a proton to a nucleus, one must get beyond the so-called Coulomb barrier that the approaching proton encounters owing to the electrical force that the other protons in the nucleus are exerting against it. The net resultant binding energy per nucleon normally rises with the size of the nucleus, up to the nuclei of the elements iron and nickel, since these two forces compete with one another in a nucleus. Beyond these nuclei, the binding energy per nucleon begins to decline for heavier nuclei, eventually becoming negative for really heavy ones that are therefore inherently unstable, fissile, and radioactive. Thus, with 26 protons and 30 neutrons, 56Fe, the most prevalent isotope of iron, is one of the most stable nuclei with a binding energy of 8.790 MeV/nucleon and is produced as the byproduct of the majority of fusion and fission chain processes. This explains why 56Fe, which is located in the centre of the Sun and stars, is the most common element in the universe.

The kinetic energy needed for the deuterium and tritium nuclei to have the best chance of fusion occurring is the lowest since they have the lowest nucleon binding energies. The collision cross-section curves for the D-T reaction and a few other typical fusion reactions are displayed in Figure 1 as an illustration of this. The vertical axis (measured in barns) in this diagram indicates the likelihood that a collision between two particles with the kinetic energy shown here would cause a fusion reaction. The kinetic energy of the interacting particles rises from left to right. Thus, the D-T reaction has the largest cross-section at about 100 keV, while the other reactions have much lower probabilities and peak temperatures at much higher temperatures. For instance, the p-11B reactions have the largest cross-section at 642 keV, at about 1.2 barns (roughly 5 times less than the peak D-T cross-section[4]–[6].

Fusion fuels

The creation of a 14.1 MeV neutron in each D-T reaction makes it less than the ideal fusion process, which is one of its key drawbacks. The neutrons are absorbed in the fusion chamber's surroundings for instance, in tokamaks, in the largely metallic blankets and vessels. Generally speaking, the effects of neutron activation on metals include hardening, brittleness, and radioactivity. This has two significant consequences: first, it necessitates the use of low activation materials within the vacuum chambers of fusion devices, and second, it severely reduces the lifetime of the machine parts that surround the fusion plasma. As a consequence, even though the initial generation of fusion devices will rely on D-T reactions because they are

simple to produce, more advanced devices may utilise processes that produce less neutron activation. Future fusion reactors for generating electricity might theoretically be built on any of the aforementioned processes. The degree of difficulty in obtaining them, however, depends on a number of variables. A mixture of D-T particles is contained in a magnetic trap and heated to high energies roughly 10–20 keV mean in the first-generation tokamak-based fusion reactors, such as ITER. At these energies, the particles have a distribution of kinetic energy known as a Maxwellian distribution, with a small portion of them reaching 40 keV and fusing.

The total energy of the fusion products fus E, the energy carried by the resulting charged particles Ech, and the atomic number Z of the non-hydrogenic reactant are all factors that must be taken into account in addition to the temperature and cross-section of the reactions. One intriguing example is the D-D reaction, which has two branches, each with a 50/50 chance of producing a T and a proton or a 3 He and a neutron. A D-T reaction may also be performed on the T, and a D-3 He reaction can be performed on the 3 He. The optimal temperature for D-3 He processes is substantially higher than that of D-D reactions, thus they are not anticipated to contribute to the total fusion energy, despite the fact that the T really burns up entirely in a deuterium plasma and provides its energy farther down the reaction chain. Thus, one may determine the total energy of D-D fusion.

The D-D reaction is special in that there is only one reactant, which is significant for determining the reaction rate. The reactants in any of these four reactions need also be combined in the right ratios. When each reactant ion plus its corresponding electrons makes up half of the pressure, this is the situation. This indicates that the density of the non-hydrogenic ion is 2/(Z+1) less than that of the hydrogenic ion, assuming that the total pressure is constant. In addition to the variations in the values of 2 v / e T, the rate for these reactions is thus decreased by the same amount. On the other hand, the rate of the D-D reaction is twice as high since there is only one reactant. As a result, the reaction rates for non-hydrogenic fuels are reduced by a factor of 2/(Z+1) because they need more electrons, which are responsible for roughly half the pressure but play no part in the fusion process. The electron temperature will often be close to the ion temperature, which is a fair assumption to make. However, it is possible that the electrons might be kept at a temperature that is far lower than the ions in certain operating modes, such as tokamaks. There is no charge number decrease in this situation, often known as the "hot ion mode." Due to the fact that every particle may interact with any other particle, there is a net gain of 2 for D-D reactions.

DISCUSSIONS

the values for reactivity are obtained by multiplying 1.24 10-24 by the sum of the products of the variables 2 v / e T and 2/(Z+1). The reactivity is an indication of the mechanism through which, given equivalent circumstances, other reactions proceed more slowly than the D-T process. The Lawson criteria values, which represent the reactivity weighted with Ech, demonstrate how much more challenging it is to ignite these reactions than the D-T reaction.The fusion power density attained in the various reactions is shown in the last column Thus, we can see that the D-T reaction, although having the maximum fusion power density and being the simplest to carry out, also has the most neutron city. As a result, D-T reactions need the greatest degree of neutron shielding, necessitate the use of low activation materials, and have concerns

with crucial machine component longevity[7], [8].The so-called advanced fuels, however, like D-3 He or p-11B, have the significant benefit of having extremely low neutron city. Small quantities of neutrons, gamma radiation, and X rays are produced via intermediary chains in the p-11B fusion as well as bremsstrahlung radiation in the p-11B processes, for instance. However, by reasonable quantities of shielding and careful design and fuel concentration selection, it would be feasible to reduce the total neutron energy to less than 0.2% and both neutron as well as X-ray and gamma doses to tolerable levels of occupational doses.

Similar to the D-3 He events, the D-D reactions that follow (half of them) generate a triton and a proton, whereas the other half make a 3 He and a 2.45 MeV neutron since the optimal temperature for these processes is above 50 keV. The 14.1 MeV neutrons are further created by the next D-T reactions. D-3 He processes cannot be classified as aneutronic since the entire neutron energy cannot be decreased to less than a certain percentage, even if the D-D reactions may be minimized by carefully choosing the D fuel concentration.

The main issue with advanced fuels is that in order to reach a high enough Lawson factor, one must heat the fusion plasma to significantly higher b (and thus higher n and T) values compared to the D-T plasmas, as well as much larger confinement durations. Unless new ideas and designs for stable configurations are developed, this might be the main obstacle for fusion reactors powered by improved fuels. Furthermore, the benefit of D-T fusion is that one may extract heat volumetrically from the reactor blankets since the majority of the energy is derived from neutrons that are caught in the surrounding blankets.

The surface heat that is transmitted to the divertor targets by the plasma particles must instead be extracted in extremely large quantities in order to build reactors based on low (or zero) neutron city fusion processes. It goes without saying that a significant portion of the plasma energy is also radiated out by synchrotron radiation in the microwave band at the high temperatures of these fusion events, and it should be feasible to develop technology to capture this microwave radiation and transform it into electricity. On the other hand, layers of metal foils may absorb the X rays produced by bremsstrahlung radiation. However, the divertor targets for the aneutronic reactions would have to withstand an unprecedented level of heat load, necessitating major advancements in the production of ultra-high heat flux materials and extremely considerable R&D in other related technologies. However, there hasn't been enough study done on these possibilities to completely rule out sophisticated fuel-based fusion technology in the future. Therefore, even though D-T fusion will be the basis of first fusion reactors since it is simple to create, future fusion devices may employ more novel fuels.

Direct conversion to electricity

Since charged particles get energy from multiple fusion processes, it is possible to transform fusion energy directly into electricity using a variety of techniques, such as induction effects or electrostatic effects that cause charged particles in an electric field to accelerate. It is true that the first generation of D-T reaction-based fusion reactors will have to generate the majority of their power using traditional steam turbines that use the heat produced by the neutron absorption since 80% of the fusion energy is converted into neutrons. However, it might be able to directly

convert roughly 80% of the charged particle energy in future fusion devices based mostly on aneutronic fusion, like p-11B. In addition to being released as X rays and microwave radiation via bremsstrahlung radiation and synchrotron radiation, a portion of the fusion energy that is contained in the charged particles is also released in these other forms. A appropriate technique may be developed to collect the microwave energy and transform it into electricity, or the microwaves can be utilized to generate a current in the plasma itself as necessary for tokamaks. In theory, it is also possible to turn X-ray energy into electricity via photoelectric processes by passing the rays through a system of conducting foils. However, because to the X-rays' great penetration, this may need several layers of metallic foils to absorb all the energy, which would necessitate inventive reactor designs.

Approaches To Fusion

In order to establish fusion on Earth, one must first produce a plasma of the fusion reactants with a high enough temperature and density and then contain it for a long enough period of time without any external material barriers. Inertial confinement and magnetic confinement are the two basic methods for doing this. The more advanced of the two methods, magnetic confinement fusion, is now the most promising way to create fusion reactors based on this idea since it can keep the plasma contained in a constant state for extended periods of time. On the other hand, the inertial confinement fusion (ICF) method predominantly employs pulsed operations, creating thermonuclear fusion by the micro explosions of reactant targets brought on by high intensity laser or particle beams at a high repetition rate.

The National Ignition Facility (NIF) at the Lawrence Livermore National Laboratory in the United States, which was inaugurated in March 2009, and the Laser Megajoule (LMJ) facility in France, whose development is expected to be finished in 2014, are currently the two biggest ICF experiments in the world. Both of these facilities are meant to create circumstances that lead to ignite. However, ICF facilities would need a fusion gain of about 100–200 for net power generation due to the fairly low driver conversion efficiency (10%) of the lasers and the conversion efficiency of 35–40% of fusion to electric power required for power production. ICF reactor technologies for power production thus seem to be more difficult.

Magnetic confinement fusion

In magnetic confinement fusion, charged plasma particles are trapped in a specially created magnetic field configuration known as a magnetic bottle to keep them away from material boundaries. This takes use of the magnetic field's capacity to allow for unfettered travel along the magnetic lines of force while drastically restricting the migration of charged particles in a plasma across those lines. There are many different confinement configuration ideas as a result of research and development in the field of magnetic confinement fusion.

The tokamak-based magnetic confinement fusion process has been the most effective in trapping plasma particles along magnetic field lines. A tokamak's magnetic field arrangement is specifically intended to create a torus- or doughnut-shaped plasma. A solenoidal arrangement of ring-shaped coils may be turned around to create a torus,to create a toroidal magnetic field, which can be used to create this configuration. However, a purely toroidal magnetic field is

unable to contain the plasma particles because the curvature of the field lines causes the ions and electrons to drift in different directions, causing a charge separation. The resulting electric field then causes the plasma to rapidly escape to the walls. One requires the poloidal magnetic field, an extra component of the magnetic field rotating on the minor cross-section of the torus, to avoid charge separation. A toroidal current is passed into the plasma itself to create the poloidal magnetic field in tokamaks.

Since inductive effects are by nature ephemeral, the tokamak plasma current drive is equally ephemeral. Tokamak discharges in a steady state may be produced by using a variety of non-inductive methods to drive plasma current. Currents in tokamak-like devices have so far been driven extremely successfully by the injection of high power energetic neutral particle beams and/or radiofrequency waves at distinctive resonance frequencies, imparting momentum selectively to the ions or electrons.

The self-generated bootstrap current, also known as a current produced by radial diffusion in the plasma itself in the presence of density gradients through momentum exchange between trapped and passing particles, has the potential to contribute significantly to the plasma current theoretically 100%. The bootstrap current is inevitably off-axis and zero at the center because the plasma pressure profile has maxima around the tokamak core and the bootstrap current is proportional to the radial gradient of pressure. Therefore, in mostly bootstrap current driven systems, some extra current drive is still needed to drive the current at the plasma core. The majority of the plasma current in sophisticated tokamaks in the future will be bootstrap-driven, reducing the energy needed for auxiliary current drive[9], [10].

CONCLUSION

knowledge and using nuclear fusion as a possible future energy source requires advancement in our knowledge of fusion processes. Scientists and researchers try to identify and categories fusion processes using a mix of experimental, computational, and theoretical techniques. To assess the viability and effectiveness of fusion reactions, important characteristics like reaction cross-sections, reaction rates, and energy thresholds are examined.

REFERENCES

[1] S. Akkoyun, “Estimation of fusion reaction cross-sections by artificial neural networks,” Nucl. Instruments Methods Phys. Res. Sect. B Beam Interact. with Mater. Atoms, 2020, doi: 10.1016/j.nimb.2019.11.014.

[2] Y. Taniguchi and M. Kimura, “C12+12C fusion S□-factor from a full-microscopic nuclear model,” Phys. Lett. Sect. B Nucl. Elem. Part. High-Energy Phys., 2021, doi: 10.1016/j.physletb.2021.136790.

[3] J. Rae et al., “A robust method for particulate detection of a genetic tag for 3D electron microscopy,” Elife, 2021, doi: 10.7554/ELIFE.64630.

[4] Z. Liu, “Review and prospect of thermal analysis technology applied to study thermal properties of energetic materials,” FirePhysChem, 2021, doi: 10.1016/j.fpc.2021.05.002.

[5] O. Tyshchuk, H. R. Völger, C. Ferrara, P. Bulau, H. Koll, and M. Mølhøj, "Detection of a phosphorylated glycine-serine linker in an IgG-based fusion protein," MAbs, 2017, doi: 10.1080/19420862.2016.1236165.

[6] M. Agostini et al., "Comprehensive measurement of pp-chain solar neutrinos," Nature, 2018, doi: 10.1038/s41586-018-0624-y.

[7] Y. Wang, T. Wan, Y. Zhong, X. Ma, Z. Chen, and X. Wang, "Environmental sustainability of renewable phosphogypsum by CaS: Characterization and process optimization," J. Therm. Anal. Calorim., 2020, doi: 10.1007/s10973-019-08718-3.

[8] W. H. Tan and S. Takeuchi, "Timing controllable electrofusion device for aqueous droplet-based microreactors," Lab Chip, 2006, doi: 10.1039/b517178d.

[9] M. Yiğit, "Theoretical study of cross sections of proton-induced reactions on cobalt," Nucl. Eng. Technol., 2018, doi: 10.1016/j.net.2018.01.008.

[10] M. Cerrone, M. Cantile, F. Collina, L. Marra, G. Liguori, R. Franco, A. De Chiara, and G. Botti, "Molecular strategies for detecting chromosomal translocations in soft tissue tumors (review)," International Journal of Molecular Medicine. 2014. doi: 10.3892/ijmm.2014.1726.

CHAPTER 5

DETERMINATION OF INERTIAL CONFINEMENT FUSION

Dr. Thimmapuram Reddy, Assistant Professor
Department of Engineering Physics, Presidency University, Bangalore, India
Email Id- ranjethkumar@presidencyuniversity.in

ABSTRACT:

A possible method for achieving controlled nuclear fusion is inertial confinement fusion (ICF), which involves compressing and heating a target that contains fusion fuel using high-energy laser or particle beams. The concepts, difficulties, and developments in the area of inertial confinement fusion are the main topics of this work. The inquiry looks on the several procedures and parts that go into ICF, such as target design, laser or particle beam systems, compression methods, and ignition circumstances.

KEYWORDS:

Inertial confinement fusion (ICF), Nuclear fusion, Fusion fuel, High-energy laser, Particle beams, Target design.

INTRODUCTION

A fusion reactor is constructed entirely differently for inertial fusion. It is conceivable to produce net fusion power before the solid fusion fuel pellet blows itself apart in a micro explosion if it is compressed to very high densities and a portion of it is heated to the temperatures needed for ignition. The heated fuel's inertia, which holds it together for a limited amount of time hence the term inertial confinement, is used in this method to accomplish confinement rather than external fields. The process of compression involves evenly heating the surface of a spherical hollow shell target from all sides. This high surface heating causes the fuel to implode inside as the top layer burns off and bursts outward. A massive laser pulse or a pulsed heavy ion beam from a particle accelerator may act as the compressor[1]–[3].

Here, let's first look at a few fundamental characteristics of inertial fusion; further information may be found in references. The normal fusion output energy must be about 100 MJ; if this is done at a frequency of a few Hz, we have a fusion reactor with many hundreds of MW of fusion power. This is necessary to repeatedly reuse the containment chamber of the micro-explosion. Calculating the size of a typical D-T fusion pellet that would completely burn and create this much fusion energy at cryogenic (solid) densities and fusion temperatures (10 keV), we arrive at a pellet radius of roughly 1 mm. The time it takes a rarefaction sound wave to travel from the surface of the pellet to its inside, which is the usual disintegration time of the pellet, is of the order of a fraction of a millisecond in a D-T plasma at fusion temperatures.

$$G = \eta_c \times f_b \times \left(\frac{E_f}{E_{in}} \right)$$

Relies on the coupling efficiency (c), the fractional burn ratio (bf), the maximal fusion energy output (f E), and the ratio of the input energy content (in E), and may be maximized by achieving the best values for each of these ratios. The situation of low circulating electric power (25%) in the reactor, which results in 10 d d G (or G = 70–200 for a 5–15% driver efficiency d d), determines its desired value. The ratio of fusion reaction time to disassembly time, which is given by, determines the fractional burn ratio of the pellet.

Fuel density is represented by, and sound speed is represented by s c, which is equal to 2 / s B f c k T m, and m f, which is the average mass of the fuel ions (2.5 m m f p for an equimolar D-T plasma, where mp is the proton mass). Therefore, the fractional burn ratio is determined by the pellet's factor R. In order to achieve the fundamental ignition condition for inertial fusion, a fuel with a R of about 4 kgm-2 must be heated to a minimum temperature of around 5 keV, or a fractional burn of approximately 3.5%. Inertial fusion, on the other hand, has to overcome a factor of 10 in the efficiency of the hydrodynamic coupling and a further factor of 10 in the efficiency of the driver in addition to ignition.

ICF capsule implosions will need a global fuel R of around 30 kgm-2, resulting in a fractional burn of about 30%, to overcome these inefficiencies. The Lawson criteria in magnetic fusion is analogous to this R criterion in inertial fusion. Having either a low density, big radius configuration or a high density, small radius configuration may definitely accomplish it. Simple calculations demonstrate that the needed driving energy roughly scales with the square root of the fuel density. Therefore, compression of the D-T fuel to very high densities (approximately 200-400 g.cm-3 of D-T density for a mm size pellet, which is around 1000-2000 times the usual solid density) will be necessary to reduce the driver size needed for inertial fusion. Additionally, it turns out that compressing the fuel to the necessary densitieswhere matter is degenerateрequires orders of magnitude less energy than heating the whole assembly to the point of fusion ignition. In order to achieve the requisite densities, the whole system is compressed, but only a tiny hot spot is heated to ignition temperatures. The size of the hot area is selected such that alpha particles created there may escape and heat nearby layers of fuel, which causes a burn wave to spread and ignite fusion reactions over the whole fuel.

The capsule is destroyed at energies in the order of a few keV, and the heated plasma bursts forth at a speed of around 100-1000 km/s. As a result, the remaining section of the spherical capsule accelerates towards the core at a speed of around 300–500 km/s, compressing and heating the thermonuclear fuel via mechanical effort. A high burnup will result from thermonuclear ignition at the center and subsequent propagation of a "thermonuclear burn wave" throughout the whole fuel if specified parameters related to the compressed fuel arrangement are met at the implosion's peak. The external driving pressure, which must reach 108 atm, the target matter's resistance to compression (low isentrope should be maintained), the development of hydrodynamic instabilities and asymmetry during the implosion process, and the final density attained by the fuel during a capsule implosion are all important factors. The ablated material and incident driver energy flow together determine the external pressure. Compression is energetically appealing

and minimizes the size of the driver needed for effective fuel burnup, but high gain also needs a high temperature zone (known as the hot spot) for ignition to take place.

If hydrodynamic instabilities do not mix the hot spots with the surrounding cool fuel, the hot spots occur during the latter phases of the inertial confinement fusion capsule implosion. The capsule for D-T fuel may be thought of as transparent to the 14.6 MeV neutrons generated during the fusion process, particularly when the reaction is just about to ignite. As a result, the alpha particles emitted during D-T reactions and the implosion's operation are mostly responsible for the hot spot's self-heating.

The areal density of the hot spot must be equivalent to the alpha particle range, which is determined to be 0.3 g cm-2 at a temperature of 10 keV, in order for self-heating to be successful. The fundamental scientific problem with inertial fusion is the development of a hot patch inside the cold main fuel. The high degree of symmetry of the spherical implosion, which necessitates uniform irradiation and management of certain hydrodynamic instabilities, is a fundamental condition for the creation of the center hot spot[4].

DISCUSSION

Environment, safety and non-proliferation

Emissions in normal operation

Major goals in the design of fusion power plants are the safe containment of fusion reactor inventory, the minimizing of emissions during normal operation, potential accidents, decommissioning and waste storage. The high stream of fusion neutrons that enter the material surrounding the plasma and activate it is the other source of radioactivity in the plant, in addition to tritium. Fusion power plants will have an extremely low fuel inventory density within the chamber containing the fusing plasma; as a result, their power output ends a short time after fueling is halted. Due to the disintegration of neutron activated elements in their structure after the burn is over, fusion reactors would have low levels of residual power density. Fusion reactors do not produce any greenhouse gases. These advantageous general characteristics result in significant safety and environmental benefits, but the full exploitation of these benefits will rely on the specifics of design and material choice.

Numerous research on reactors have been conducted, particularly in the EU, the USA, and Japan. Although thorough safety and environmental evaluations have been conducted for the majority of them, they typically vary significantly in their gross power, main radii, aspect ratio, and power density, among other factors. All safety and environmental effect evaluations were built on thorough and in-depth calculations of neutronics, activation, and derived quantities.Vacuum vessels, cryostats, and outside buildings are all possible confinement barriers. During routine operation, little portions of the radioactive elements are discharged. The quantities heavily rely on design elements like the cooling method, the choice of structural materials, and the blanket pattern. There have been several research on typical operation dosages for the general population.

Post comparison with other sources of energy

Fusion-based power generation methods fall under the category of low "external" costs, on par with solar and wind-based technologies. Several models have been created during the last ten years to calculate the cost of electricity generated by fusion-based technologies. A fusion power source would incur two different types of expenses, just like any other conventional energy source.

They used a conventional economic technique and computations that have been approved by non-fusion specialists and supported by several international organizations. On the other hand, non-fusion specialists have mostly assessed the external expenses. A computer model used by EFDA-SERF to calculate one such estimate divided the plant into around eighty independently costed units.

This pricing model was compared to the expenses of the planned ITER, a major fusion experiment, which were determined by separate, simultaneous work by the ITER Parties and highly thorough studies mostly carried out by industry. To determine the cost of power, the whole capital cost, including interest rates throughout construction, was added to expected replacement costs, additional running expenses, contributions into a decommissioning fund, and availability assumptions. The 'levelized cost' approach, which is used in studies by the OECD and the IAEA, was utilized in accordance with standards to complete this. The breakdown of the cost of energy arising from a typical set of assumptions is shown in Figure 1.20. A fair evaluation of the uncertainties is especially important for forecasting the absolute cost of fusion-generated power in more than fifty years. As a result, several simulations encompassing a wide variety of assumptions for the crucial physics and technological aspects determining the economic performance of a power plant were made[5]–[7].

External costs of fusion power production

The above-described method of calculating the direct costs of energy production excludes expenditures like those related to harm to the environment or negative effects on health. These "external" expenses are significant in the case of certain current power sources.In the framework of the "ExternE" project, which included more than 40 different European institutes from nine different countries, a methodology for standardizing the evaluation of the external costs of electricity generation using various fuel cycles had previously been developed for the European Commission.

The ExternE technique is a bottom-up approach with a site-specific approach that takes into account the implications of an extra fuel cycle situated in a particular location. It evaluates a power plant's full life, fuel cycle, and shutdown.This covers the production of materials, the building of the facility, its operation, deconstruction, site cleanup, and trash disposal. At each level, variables including dangerous chemical or radioactive emissions, traffic accidents, workplace accidents, plant mishaps putting the public at risk, and occupational exposure to dangers are taken into account. Even adverse consequences like the loss of visual amenity are considered. An estimate of the overall external costs is created by summing the negative consequences in monetary terms. This suggests that items that aren't often traded or valued must

be appraised. The technique creates debates over the economic pricing of adverse health impacts and mortality and entails, obviously, considerable uncertainty in areas like the influence of CO2 emissions on climate and dose-response relationships. It also raises the issue of how to estimate the cost of potential long-term health effects at the time of electricity production.

Public acceptance of fusion

Sociological research conducted by SERF also looked at "Fusion and the public opinion." Fusion energy generation and the related advantages and hazards are not now a topic of public discussion since large-scale commercial applications won't be available for another 50 years. Therefore, empirical sociological investigations were either limited to populations with above-average previous knowledge of fusion structured interviews with scientific journalists, environmental journalists, fusion and fission which received introductory briefings from both fusion proponents and detractors, or they were not allowed to be conducted at all.

Both techniques revealed varying expectations for the future energy mix with everyone hoping for a bigger role for renewables, but also a fair amount of consensus that the fusion option should continue to be researched.Being aware of the global environment is what industries will focus on the most in the future. Fusion waste management may be one of the most crucial elements in this situation in line with this trend. Recent research in this area has concentrated on minimizing radiotoxicity and reducing the number of radioactive components, trying to find a solution by introducing the idea of "clearance" and recycling under regulatory supervision and by increasing the purity of materials.

Spin-offs of fusion research

The importance of R&D spin-offs is one of the crucial components of investing in fusion research and technology. A key determining element in national R&D strategies and public financing is the role, correct analysis and forecast of spin-offs, and calculation of the rate of societal return involved in a specific R&D program. It is a common truth about R&D projects and the organizations running them that they cannot effectively account for the advancements in knowledge spin-off to other disciplines and their customers in order to appropriate the entire returns of their investment. As a result, the overall societal benefits of any R&D effort are often greater than the direct profits. This is particularly true for fundamental research. For instance, the Oak Ridge National Laboratory in the United States developed the pressurized light water based nuclear reactor concept originally for nuclear submarine propulsion, but it also had significant additional spin-offs in the areas of satellite communication, radiotherapy, etc., leading to significant social and economic benefits and returns. All other significant fields of science and technology R&D have had similar spin-offs, including high energy physics and space exploration. Fusion research has a variety of spin-offs related to it. The most important ones are those that assist fusion directly, such as vacuum, superconducting magnets, neutral beam systems, and cryogenics. A second group includes non-fusion plasma technologies and related diagnostics that are largely related to fusion plasma research, such as industrial plasma applications such as material processing and diagnostics. The synthesis of rare but valuable isotopes of various elements, the treatment of waste and other materials, and fusion-based space

propulsion systems are a few other types of spin-offs that are specifically reliant on fusion plasmas. There has been a significant spin-off in knowledge. Through the massive number of publications, patents, codes, and standards, highly skilled workforces, and social networks, ongoing basic science and technology R&D in the fields of plasma and fusion technology has produced and continues to produce a great deal of knowledge spin-off. With the development of massive experimental facilities like the ITER, IFMIF, and DEMO reactors, this enormous body of knowledge will serve as the foundation for the expansion of applied R&D operations in the future. The knowledge spin-off effects in fusion science and technology are highlighted by the funding for fusion R&D being primarily open and public, the unprecedented international collaborations among major R&D labs across all continents, the technological complexity, and the sizeable number of researchers and institutions involved[8]–[10].

CONCLUSION

Future energy sources like inertial confinement fusion (ICF) show considerable promise. ICF seeks to create controlled nuclear fusion by compressing and heating a fusion fuel target with high-energy laser or particle beams. The field of inertial confinement fusion has advanced thanks to improvements in target design, compression methods, and ignition circumstances. Fuel pellet compression is a crucial part of ICF because it establishes the high temperature and pressure requirements for fusion reactions to take place. Energy balance, when the energy generated by fusion reactions surpasses the energy intake, is difficult to achieve and sustain in ICF.

REFERENCES

[1] D. A. Shaughnessy, K. J. Moody, N. Gharibyan, P. M. Grant, J. M. Gostic, P. C. Torretto, P. T. Wooddy, B. B. Bandong, J. D. Despotopulos, C. J. Cerjan, C. A. Hagmann, J. A. Caggiano, C. B. Yeamans, L. A. Bernstein, D. H. G. Schneider, E. A. Henry, and R. J. Fortner, "Radiochemical determination of Inertial Confinement Fusion capsule compression at the National Ignition Facility," Rev. Sci. Instrum., 2014, doi: 10.1063/1.4883186.

[2] P. L. Volegov, S. H. Batha, V. Geppert-Kleinrath, C. R. Danly, F. E. Merrill, C. H. Wilde, D. C. Wilson, D. T. Casey, D. Fittinghoff, B. Appelbe, J. P. Chittenden, A. J. Crilly, and K. McGlinchey, "Density determination of the thermonuclear fuel region in inertial confinement fusion implosions," J. Appl. Phys., 2020, doi: 10.1063/1.5123751.

[3] S. Martellucci, C. Bellecci, M. Francucci, P. Gaudio, M. Richetta, D. Toscano, A. Rydzy, M. Gelfusa, and P. Ciuffa, "Soft x-ray generation by a tabletop Nd:YAG/glass laser system," J. Phys. Condens. Matter, 2006, doi: 10.1088/0953-8984/18/33/S19.

[4] Y. Kim et al., "Determination of the deuterium-tritium branching ratio based on inertial confinement fusion implosions," Phys. Rev. C - Nucl. Phys., 2012, doi: 10.1103/PhysRevC.85.061601.

[5] Z. Chen, X. Zhang, Y. Pu, J. Yan, T. Huang, W. Jiang, B. Yu, B. Chen, Q. Tang, Z. Song, J. Chen, X. Zhan, Z. Liu, X. Xie, S. Jiang, and S. Liu, "Ion temperature measurements of indirect-drive implosions with the neutron time-of-flight detector on SG-III laser facility," Rev. Sci. Instrum., 2018, doi: 10.1063/1.5022767.

[6] Y. Aglitskiy, C. Zulick, J. Oh, A. L. Velikovich, A. J. Schmitt, S. P. Obenschain, M. Karasik, and J. L. Weaver, "Plasma hydrodynamic experiments on NRL Nike KrF laser," High Energy Density Phys., 2020, doi: 10.1016/j.hedp.2020.100866.

[7] R. Prasad and M. Pandey, "Rice husk ash as a renewable source for the production of value added silica gel and its application: An overview," Bulletin of Chemical Reaction Engineering and Catalysis. 2012. doi: 10.9767/bcrec.7.1.1216.1-25.

[8] S. Y. Gus'Kov, D. V. Il'In, J. M. Perlado, V. B. Rozanov, V. E. Sherman, and N. V. Zmitrenko, "Spectral composition of thermonuclear particle and recoil nuclear emissions from laser fusion targets intended for modern ignition experiments," Plasma Phys. Control. Fusion, 2018, doi: 10.1088/1361-6587/aac739.

[9] "Maize Husk Ash as a Renewable Source for the Production of Value Added Silica Gel and Its Application," Chem. Mater. Res., 2021, doi: 10.7176/cmr/13-3-01.

[10] H. Azechi, N. Miyanaga, R. O. Stapf, K. Itoga, H. Nakaishi, M. Yamanaka, H. Shiraga, R. Tsuji, S. Ido, K. Nishihara, Y. Izawa, T. Yamanaka, and C. Yamanaka, "Experimental determination of fuel density-radius product of inertial confinement fusion targets using secondary nuclear fusion reactions," Appl. Phys. Lett., 1986, doi: 10.1063/1.97093.

CHAPTER 6

ANALYSIS OF NEUTRON INTERACTIONS

Dr. Veerabhadrappa Jagadeesha, Assistant Professor
Department of Physics, Presidency University, Bangalore, India
Email Id-jagadeeshaangadi@presidencyuniversity.in

ABSTRACT:

A possible method for achieving controlled nuclear fusion is inertial confinement fusion (ICF), which involves compressing and heating a target that contains fusion fuel using high-energy laser or particle beams. The concepts, difficulties, and developments in the area of inertial confinement fusion are the main topics of this work. The inquiry looks on the several procedures and parts that go into ICF, such as target design, laser or particle beam systems, compression methods, and ignition circumstances. To comprehend the viability and development of inertial confinement fusion, important factors like fuel pellet compression, energy balance, and fusion reaction dynamics are examined.

KEYWORDS:

Inertial confinement fusion (ICF), Nuclear fusion, Fusion fuel, High-energy laser, Particle beams, Target design.

INTRODUCTION

The nature of neutron chain reactions is dependent on how neutrons from fission interact with materials since, on average, only one of the two or more neutrons produced by each fission must survive to produce a future fission in order to continue a chain reaction. The behavior of neutrons in nuclear reactors is mostly determined by their kinetic energy, as well as how they move across space and interact with nuclei. The idea of the cross section, or the cross-sectional area of a nucleus as it appears to an approaching neutron, lies at the heart of neutron interactions.The fundamental scientific facts that underpin the characteristics of chain reactions include such cross sections, their reliance on the neutron's kinetic energy, and the relative odds that a collision will lead to scattering, capture, or fission[1]–[3].

Neutron Cross Sections

The neutral particle is the neutron. A neutron's path is unaffected by the electric field produced by a positively charged nucleus or the electrons around it. Neutrons thus go in straight lines and only veer off course when they actually collide with a nucleus to be dispersed or absorbed. Thus, a neutron normally experiences many scattering collisions before being absorbed, which is when its identity is lost. Space looks to a neutron moving through a solid to be quite empty.Since an atom's radius is typically of the order of 108 cm and its nucleus is only of the order of 1012 cm, a

single dense layer of atoms would only block about (1012) 2 / (108) 2 = 108 of the cross-sectional area perpendicular to a neutron's flight path, which is a very small portion. In order to do this, neutrons often pass through millions of layers of atoms before colliding with nuclei. Nearly all neutrons would be anticipated to travel through thin target materialslike a sheet of paperwithout colliding.

Microscopic and Macroscopic Cross Sections

We consider a beam of neutrons moving in the x direction to look at how neutrons interact with nuclei. We define I 14 n000v as the beam intensity if the beam has n000 neutrons per cm3 that are all moving at a speed of v in the direction of the x axis. Neutrons/cm^2 /s are used to express the beam's intensity when the speed is expressed in cm/s. Assume that a neutron will either be absorbed or dispersed in a different direction if it collides with a nucleus. Then, only neutrons still moving in the x direction will have not yet collided. As a result, the uncollared beam's intensity decreases as it moves farther into the substance.

Let Ix be the intensity of the beam at x cm of material penetration. The proportion of neutrons colliding will be equal to the portion of the 1-cm^2 area perpendicular to the beam direction that is shaded by nuclei after travelling an extra infinitesimal distance dx. The shadowing of one nucleus by another may be disregarded if dx is modest and the nuclei are distributed at random. This assumption is false only when neutrons are going through a single crystal, which is an uncommon occurrence. Assuming that the material has N nuclei per cm^3, there will be N dx per cm^2 in the infinitesimal thickness.

Transport in a stochastic field

Magnetic islands may occur at surfaces when magnetic disturbances with a field component across the equilibrium flux surfaces are resonant with the local q value, changing the topology of the system. In a sense, these islands short-circuit transportation. A density gradient cannot be sustained in a large area if the field is stochastic and field lines may roam across adjacent islands if they overlap Rochester and Rosenbluth computed the diffusive motion of particles as a consequence of using a random phase approximation, supposing that the perturbation amplitudes are much higher than the stochasticity threshold[4].

The particles flow down the field line diffusively for durations longer than the collision time, i.e., being the parallel collisional diffusion. The particles will travel radially with 1/2 D t s yielding 0 for a long period if the field lines diffuse across the equilibrium surfaces with diffusion Dm; there is no cross-field diffusion because of diffusive motion along the field line.

A second effect, brought on by the gyro radius, however, causes the particle to move to a different field line during a contact. When a field is stochastic, neighbouring field lines often diverge exponentially from one another, with the distance between lines being given by the formula 0 hz d d e, where z is the distance along the line and h is the Kolmogorov entropy. The particle will then be transported away from the original line at a time interval, with and the wavelength across the unperturbed field determining the decorrelation distance of the initial field.

Turbulent Transport

Fusion devices must inevitably be in an inhomogeneous condition in order to contain hot, dense plasmas and prevent boundary damage from excessive heat. In addition to being unstable to a variety of linear instabilities with diverse wavelengths and complicated frequencies, such magnetically confined high temperature plasmas often non-linearly self-organize into states that are more advantageous from an energy standpoint.

A disruption occurs when a large scale MHD instability becomes highly unstable and may destroy a tokamak plasma by tossing it against the wall. Tokamak transport is often anomalous, which indicates that the transport rate is much greater than predicted by theories based on Coulomb collisions, even in the absence of large scale MHD instabilities. Small scale collective instabilities, which are often fueled by gradients in temperature, density, and other factors, are what lead to this anomalous transport. Due to non-linear causes, these micro instabilities saturate at low amplitude. As a result of varying electric fields, particles E B float radially in an unpredictable way. Plasmas leave a tokamak's interior in this manner.

Large scale gyrokinetic models are now able to replicate these tokamak microturbulence features. For instance, is an output from a shaping-capable Gyrokinetic Tokamak Simulation (GTS) code simulation of ion temperature gradient (ITG) driven turbulence. According to density fluctuation contours in the presence of self-generated zonal flows, the average turbulence eddy size is close to several ion gyroradii across the magnetic field, and the fluctuation is almost parallel to the magnetic field with a parallel wavelength of the order of the connection length.A tokamak plasma's microturbulence is made up of several modes or eddies that interact with one another nonlinearly. The growth of the free energy source contained in n, i, or eT is what causes the small-scale linear instabilities, also known as micro instabilities.This free energy should be available for waves to tap in order to make collective waves unstable.

Non-linear gyrokinetic equations for tokamak turbulence

We introduce the fundamentals of the non-linear gyrokinetic equation in preparation for more in-depth considerations of micro instabilities and turbulence induced transport in the next sections. The direct simulation of actual-size fusion plasmas in realistic geometry using simple non-linear plasma equations (like the Kalmanovich or Vlasov equations) is still far beyond the computational capability of even the foreseeable future, despite the enormous increase in computing power in recent years. Thus, to make the fundamental dynamical equations simpler, simplified equations have been used. In this part, we go through the essential steps in the derivations of the non-linear gyrokinetic equations, which are now extensively employed in a variety of turbulence studies in magnetically confined plasmas, from the most basic, the Vlasov equation. We concentrate on collision less plasmas in this talk.

The wavelengths and correlation lengths of such fluctuations are much smaller than the size of the device or the scale length of the magnetic field inhomogeneity, while the timescales of collective electromagnetic fluctuations of interest are much longer than the period of a charged particle's cyclotron motion (gyromotion) for turbulence and transport issues in magnetically confined plasmas. In these conditions, the specifics of the charged particle's gyration motion are

not of physical interest, hence it is preferable to design a more condensed set of dynamical equations while maintaining the ability to capture the key characteristics of the low frequency phenomena that are relevant to practical applications. One may obtain the gyrokinetic equation, which characterizes the spatio-temporal evolution of the gyrocenter distribution function and is independent of the gyro phase, by decoupling the gyromotion. This equation is specified over a five-dimensional phase space (R, v,). By using a time step that is larger than the gyroperiod and fewer dynamical variables while modelling highly magnetized plasmas, one may therefore significantly reduce the amount of computer time required. We see that in the gyrokinetic method, the magnitude of the perpendicular velocity enters as a parameter in terms of an adiabatic invariant (2 v / 2 B), and the gyrophase is an ignorable coordinate. This is an adiabatic invariant's leading term, meaning it doesn't vary for each particle.

Different channels of turbulence transport

The wavelengths and correlation lengths of such fluctuations are much smaller than the size of the device or the scale length of the magnetic field inhomogeneity, while the timescales of collective electromagnetic fluctuations of interest are much longer than the period of a charged particle's cyclotron motion (gyromotion) for turbulence and transport issues in magnetically confined plasmas. In these conditions, the specifics of the charged particle's gyration motion are not of physical interest, hence it is preferable to design a more condensed set of dynamical equations while maintaining the ability to capture the key characteristics of the low frequency phenomena that are relevant to practical applications. One may obtain the gyrokinetic equation, which characterizes the spatio-temporal evolution of the gyrocentre distribution function and is independent of the gyrophase, by decoupling the gyromotion. This equation is specified over a five-dimensional phase space (R, v,). By using a time step that is larger than the gyroperiod and fewer dynamical variables while modelling highly magnetized plasmas, one may therefore significantly reduce the amount of computer time required. We see that in the gyrokinetic method, the magnitude of the perpendicular velocity enters as a parameter in terms of an adiabatic invariant (2 v / 2 B), and the gyrophase is an ignorable coordinate. This is an adiabatic invariant's leading term, meaning it doesn't vary for each particle[5]–[7].

Ion thermal transport

Compared to other transport routes, ion thermal transport is now well understood. Atypical levels of ion thermal transport that are significantly higher than those predicted by neoclassical collisional transport theory have been seen in auxiliary heated plasmas. The most likely explanation for the anomalous ion thermal transport is ion temperature gradient induced turbulence.

In tokamak experiments, the linear threshold of ITG instability is also of great practical importance. This is due to the fact that very unstable ITG modes may generate substantial quantities of radial ion heat flow, which lowers the local ion temperature gradient. This leads to ion temperature profiles that do not appreciably differ from the onset condition when combined with a competing effect brought on by ion heat deposition for example, through neutral beam injection (NBI) or ion cyclotron resonance heating (ICRH). Several gyrokinetic codes may be

used to correctly determine this onset state. You may find a parametrization of many dependencies in for example. Theoretically, "the onset condition" is further altered by the burst behaviors of a driven system towards marginality and the E B zonal fluxes For basic examples, theoretical predictions from several gyrokinetic codes start to agree, both numerically and in terms of the underlying non-linear physics principles. The zonal flow-induced upshift of the ITG onset condition is a notable example.

One of the unsolved mysteries of ion thermal transport is the scaling of the plasma current confinement, as stated. From zonal flow features that rely on the q value, it is feasible to derive the q dependency of the transport. Geodesic acoustic modes (GAMs) can only exist in a high-q area because of their Landau damping. Therefore, only motionless zonal flows will last in a low-q area. GAMs are not particularly good in reducing turbulence because of their very high frequency oscillations. Therefore, in the low-q area, where static zonal flow is dominant, we anticipate less turbulence. The ion heat flux from ITG turbulence is smaller for the situation with lower q, as the stationary zonal flows predominate, as shown by a recent non-linear gyrofluid simulation. A separate gyrokinetic simulation supports this. However, it still has to be shown how this process relates to experiments.

Electron thermal transport

Since many years ago, it has been well known that anomalous electron thermal transport has been present in all operating modes of tokamaks and spherical tori. There is proof that tokamak electron temperature profiles are rigid. This is a possibility that has been suggested by perturbative transport experiments, such as the propagation of heat pulses, and the need for an inward heat squeeze factor in the transport analysis of auxiliary heated plasmas. The trapped electron mode (TEM), the ITG mode with trapped electrons, the electron temperature gradient (ETG) mode, and magnetic flutter-driven transport are a few theoretical contenders for electron thermal transport.

Starting with the TEM, it may generate an experimentally relevant electron thermal diffusivity when very turbulent. It's intriguing to notice that DTEM-based non-linear theory may yield an electron thermal diffusivity scaling of e that is quite similar to the Neo-Alcator scaling that has been extensively seen in several ohmically heated tokamak plasmas. The ASDEX-Upgrade ECH experiment provides a TEM-supporting finding. The transport exhibits a threshold behaviour that is consistent with the prediction of the TEM theory. Additionally, as functions of the electron temperature gradient, the experimentally observed heat flow and the estimated TEM linear growth rate exhibit a comparable pattern On the other hand, it is uncommon to find evidence of TEM-like changes in measurements[8].

Momentum transport

The importance of plasma rotation in magnetic confinement is now well acknowledged. Rotation may be produced by microturbulence through Reynolds stress, which in turn can minimize turbulence and transport Instabilities caused by MHD, such as resistive wall modes, may be stabilized, but they can also be dampened by non-axisymmetric magnetic fields.Additionally, energetic particles interact with the radial electric field. Thus, it is crucial to comprehend

momentum conveyance. We specifically want to know whether ITER will have enough wave and neutral beam power to create enough rotation to reduce turbulence and transport and stabilize resistive wall modes in order for ITER to operate successfully.

Nearly all tokamaks have shown intrinsic toroidal rotation in the absence of an external torque input from neutral beams. The behavior of L-mode plasmas is still complicated and intimately related to fluxes in the scrape-off layer On the other hand, the Rice scaling of Hmode plasmas shows straightforward empirical tendencies. In H-mode plasmas, toroidal rotation rises with more stored energy and decreases with plasma current. It rotates in the co-current direction. These findings seem to support the idea that rotation starts near the transition's edge and moves inside from there. Additionally, certain experimental results cannot be explained by diffusion and a pinch alone[9], [10].

CONCLUSION

ICF, or inertial confinement fusion, has a lot of potential as a future energy source. ICF seeks to create controlled nuclear fusion by compressing and heating a fusion fuel target with high-energy laser or particle beams. The field of inertial confinement fusion has advanced thanks to improvements in target design, compression methods, and ignition circumstances. Fuel pellet compression is a crucial part of ICF because it establishes the high temperature and pressure requirements for fusion reactions to take place. Energy balance, when the energy generated by fusion reactions surpasses the energy intake, is difficult to achieve and sustain in ICF.

REFERENCES

[1] P. H. Sadewo and P. I. Wahyono, “Safety Analysis Of Neutron Interaction With Material Practicum Module For The Kartini Internet Reactor Laboratory,” J. Teknol. Reakt. Nukl. TRI DASA MEGA, 2020, doi: 10.17146/tdm.2020.22.3.6017.

[2] A. N. Ivanov, R. Höllwieser, N. I. Troitskaya, M. Wellenzohn, and Y. A. Berdnikov, “Precision analysis of pseudoscalar interactions in neutron beta decays,” Nucl. Phys. B, 2020, doi: 10.1016/j.nuclphysb.2019.114891.

[3] C. M. Lund, G. Famulari, L. Montgomery, and J. Kildea, “A microdosimetric analysis of the interactions of mono-energetic neutrons with human tissue,” Phys. Medica, 2020, doi: 10.1016/j.ejmp.2020.04.001.

[4] J. L. Autran and D. Munteanu, “Electronics reliability assessment of future power fusion machines: Neutron interaction analysis in bulk silicon,” Microelectron. Reliab., 2021, doi: 10.1016/j.microrel.2021.114223.

[5] S. Qian, V. K. Sharma, and L. A. Clifton, “Understanding the Structure and Dynamics of Complex Biomembrane Interactions by Neutron Scattering Techniques,” Langmuir, 2020, doi: 10.1021/acs.langmuir.0c02516.

[6] B. L. Sjöberg and H. Mommsen, “Interaction and the end of the Late Bronze Age as displayed through neutron activation analysis of Late Helladic sherds: a case study on Asine in the Argolid, Greece,” Archaeol. Anthropol. Sci., 2021, doi: 10.1007/s12520-021-01356-7.

[7] W. Kockelmann and E. Godfrey, “Neutron diffraction,” in Spectroscopy, Diffraction and Tomography in Art and Heritage Science, 2021. doi: 10.1016/B978-0-12-818860-6.00006-4.

[8] R.-T. Chiang, “Analysis of Radiation Interactions and Biological Effects for Boron Neutron Capture Therapy,” ASEAN J. Sci. Technol. Dev., 2018, doi: 10.29037/ajstd.535.

[9] L. Gajdos, M. P. Blakeley, A. Kumar, M. Wimmerová, M. Haertlein, V. T. Forsyth, A. Imberty, and J. M. Devos, “Visualization of hydrogen atoms in a perdeuterated lectin-fucose complex reveals key details of protein-carbohydrate interactions,” Structure, 2021, doi: 10.1016/j.str.2021.03.003.

[10] S. A. Abdullah, M. Z. Sahdan, N. Nayan, Z. Embong, C. R. C. Hak, and F. Adriyanto, “Neutron beam interaction with rutile TiO2 single crystal (1 1 1): Raman and XPS study on Ti3+-oxygen vacancy formation,” Mater. Lett., 2020, doi: 10.1016/j.matlet.2019.127143.

CHAPTER 7

GLOBAL ENERGY CONFINEMENT SCALING STUDIES

Dr. Usman Pasha, Associate Professor
Department of Physics, Presidency University, Bangalore, India
Email Id-mahaboobpasha@presidencyuniversity.in

ABSTRACT:

For comprehending and forecasting the behaviors of energy confinement in fusion plasmas, global energy confinement scaling studies are crucial. The primary goal of this work is to better understand the empirical scaling laws that link plasma properties to global energy confinement time, a crucial measure for assessing the effectiveness of fusion devices. The paper examines experimental and theoretical methodologies, including data analysis from multiple fusion devices, statistical modelling, and theoretical insights, used to analyses global energy confinement scaling. Analysis of important variables, including device size, temperature, magnetic field, and plasma density, reveals the fundamental physics driving energy confinement. The research also looks at the effects of global energy confinement scaling on the creation of sustained fusion reactions as well as reactor design and optimization.

KEYWORDS:

Global Energy, Confinement Scaling, Fusion Plasmas, Empirical Scaling Laws, Energy Confinement Time, Plasma Parameters, Fusion Devices.

INTRODUCTION

Studies on global confinement scaling help to provide a broad overview of how the plasma energy confinement behaves when the discharge parameters are independently changed. In order to gain insight into and test the viability of theories thought to be responsible for local energy transport, scaling have been developed that quantitatively describe how the energy confinement time E and L-mode to H-mode threshold power vary as other parameters change across a wide range of plasma conditions and energy states. The characteristics that get the greatest attention are those that can be changed externally, such as heating power, toroidal magnetic field, density, and so-called engineering parameters like plasma current. Other, physics-based characteristics that rely on how the plasma reacts to external control, such as the plasma beta, collisional, and normalized gyroradius, are more difficult to set.The term "laws" is often used incorrectly to describe global scaling. They cannot be compared to the basic rules of physics in any way.As derived representations of the behavior of the data, each scaling expression contains a great deal of ambiguity in its quantitative formulation, as will be demonstrated.

The global scaling expressions (GSEs) may be derived using simple methods like conventional least squares regression or more complex methods like maximum likelihood, Bayesian, and error-in-variables. As can be shown, the various methods result in statements with distinct quantitative properties. It is risky to use these expressions for extrapolations because the GSEs are descriptive and are not based on fundamental physics, especially if the extrapolations go far beyond the range of independent parameters being studied and without understanding the systematic and random uncertainties inherent in the expressions and their predictions[1]–[3].

In certain cases, equilibrium reconstructions based on magnetic measurements may provide accurate estimates of the overall thermal plasma energy stored as well as any rapid ion energy component produced by auxiliary heating techniques such neutral beams, radiofrequency waves, etc.Direct measurements of the thermal ion and electron energy content may be used to determine and separate these components in more detail. The temperature and density of the electrons and ions may be measured to do this. Direct measurements of the electron temperature and density are possible. Currently, measurements of these profiles for the primary plasma impurity (such as carbon) and subsequent adjustments resulting from collisions between the impurity and primary ion species provide coverage of the principal plasma species ion temperature and density.

The capacity to directly monitor the temperature and density of the primary ion species is currently being developed. The thermal ion density is lower than that of the electrons because low-Z and high-Z impurities are often seen in plasmas.Lasma profiles often peak in the plasma's core and decline as radial distance increases towards the plasma boundary. Temperatures and densities in low-confinement, or L-mode, plasmas are typically very low at the plasma separatrix. Temperature pedestals up to several hundred eV and density pedestals up to several 1019 m-3 inside (within) a few centimetres of the plasma separatrix are characteristics of high-confinement, or Hmode, plasmas. Strong pressure gradients created by these pedestals at the plasma edge have the potential to periodically destabilise edge localised modes and cause instability pushed close to the plasma edge, which would temporarily reduce the edge pressure gradient and confine the plasma. Deterioration of confinement in that area might result from other, more fundamental localised instabilities such sawtooth and ripping modes.

Energy Confinement Scaling: Dimensional parameters

Ohmic and L-mode plasma confinement trends

The first foundation for creating energy confinement time scalings came from ohmic plasmas from a variety of investigations The Alcator (or INTOR) scaling is 2 1/2 E e n a q, where e n is the line averaged plasma density, an is the plasma minor radius, and q is the inverse cylindrical rotational transform. At lower densities, it was shown that the confinement duration in ohmic plasmas depends on plasma density, size, and q. This scaling was changed by Pfeiffer and Waltz using 2 E e n aR, and with the inclusion of a q1/2 factor, it came to be known as "neo-Alcator" scaling. In this linear (with density) ohmic confinement (LOC) regime, the confinement period was independent of both the plasma current and the toroidal field. While the confinement

duration did exhibit a reliance on plasma current at greater densities (saturated ohmic confinement, or SOC regime), it did not demonstrate a further rise with density.

H-mode confinement trends and scaling

The L-mode is the only confinement state found in plasmas, and it seems to provide the minimum energy for a given set of engineering parameters when there isn't much MHD activity. There are further confinement states, called ITBs or internal transport barriers, or ETBs or edge transport barriers, where the areas of decreased transport that cause high pressure gradients also occur at or inside the plasma edge.

An example of an ETB plasma is the H-mode. In trials with closed divertor operation (restricted neutral transfer from the divertor to the main chamber regions), the H-mode was first seen and originally published on ASDEX.

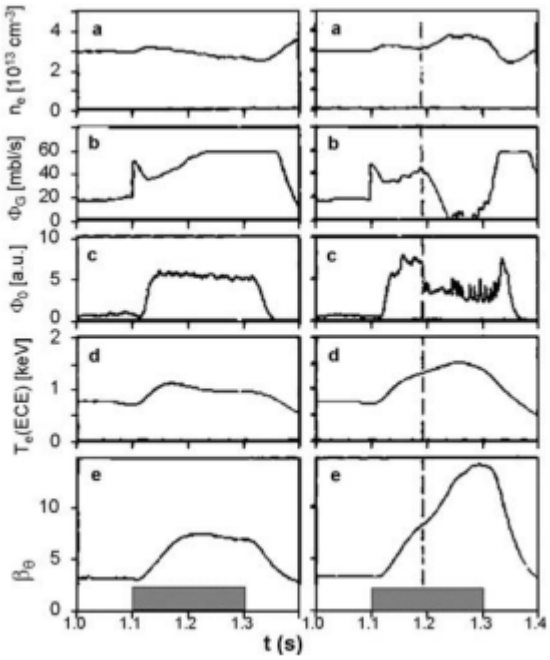

Figure 1: Represents the Time dependence of various plasma parameters.

The H-mode was caused by a spontaneous change in the plasma's confinement state from the L-mode to another state were, under comparable engineering conditions, the energy confinement might be up to two times greater. The development of pedestals in the edge electron temperature and density profiles, reflecting the development of an edge transport barrier, as well as a sharp decrease in the D-mode emjissivitya sign of recycling at the plasma edgeas well as an increase in the plasma density's rate of growth were all observed during the transition to the H-mode. Comparison of the temporal development of an early ASDEX discharge in L-mode (left column) and H-mode (right column).

An attempt to put up an H-mode confinement database similar to the one for the L-mode database was made beginning in 1988-1989 in order to assess the confinement trends more

statistically and completely.For around two years, representatives from ASDEX, D-III, JET, JFT-2M, PBX-M, and PDX met often to define the database's components and make sure that the definitions of the data given by each experiment were consistent.

This database goes one step farther than the L-mode database by defining and accepting both the thermal plasma confinement time and the total confinement time (plasma + fast ion content). The initial H-mode confinement database had 3466 observations in total.

The researchers went one step further by formulating a set of selection criteria that might narrow the scope of the investigation to a certain subset of discharges. The selection criteria excluded from analysis discharges that had high radiated power or rapid ion fractions, were too transient, or exhibited excessive MHD activity due to either high beta or low q. Following the application of these criteria, a total of 1239 observations made up the subset that would be examined. For this "standard" H-mode data set, the first multiple linear regression result showed a scaling, for total energy confinement duration[4]–[6].

Two more roughly comparable statistical techniques, a Bayesian approach and maximum-likelihood, have also been used. Both of these techniques employ expressions that describe the probability density for the observed data and take into account both the data and the mistakes, despite their divergent approaches to making probabilistic conclusions. The value of the independent variables is assumed to originate from a normal distribution with a known standard deviation in applications of both approaches for the confinement investigations. In maximum likelihood, the parametric scaling results from the best fit to the probability distributions.

Numerous meticulously prepared experiments were conducted to study the confinement change with these parameters due to the significance of the physics variable scalings in reflecting the underlying physics theories influencing confinement.One dimensionless parameter was changed in these tests, while the others were kept as constant as feasible during their whole profile. An great recent analysis of these tests and their findings.

L-H threshold scaling

High performance, and hence the performance targets, in current and future devices depend on operation in H-mode. Based on the certainty that such a regime can be achieved, the design and operation scenarios of these devices must be devised. Controlled experiments have been carried out to investigate regimes in which the H-mode is accessible, using a methodology comparable to that for the global confinement scaling. These device-specific studies have been coupled with a statistical approach to understand what variables are crucial for obtaining the H-mode. Most of this research have relied on empirical data, making it difficult to fully comprehend the mechanics behind the L-H transition.

When a certain threshold power is exceeded, the H-mode is attained. Similar to energy confinement, this threshold power is influenced by plasma characteristics in both overt and subtle ways. It is true that the transition takes place near the plasma border, creating pedestals for temperature and density.

The following are the main characteristics of the threshold dependences from early investigations. Compared to single null setups where the drift is in the other direction or in an unbalanced double null configuration, the threshold power is lower for single null plasmas when the ion B drift is in the direction of the dominating X-point. Lower power thresholds are also a result of efficient wall conditioning, a divertor layout that improves neutral retention in the divertor zone, and a lower neutral density in the main plasma chamber. Based on single parameter scans over a variety of devices, it is discovered that the threshold power is almost linearly dependent on plasma density (above a certain density) and toroidal field. Finally, it was discovered that the power threshold for hydrogen plasmas was almost two times higher than for deuterium plasmas.

Implications relative to theoretical models

It might be challenging to link the findings of global scaling analysis to intricate physics theories. One reason is that theoretical foundations are often presented in terms of local characteristics that are difficult to translate into global variables. Furthermore, rather than at the global level, these theories are often validated at a lower level (for instance, local turbulence and transport features).

Therefore, it is better to make comparisons to particular theories at the local level; this is handled in a different chapter.Nevertheless, it is possible to tie the global scalings to broad classes of theories; this has been covered in some detail in the section on dimensionless scalings. For instance, it was commonly discovered that L-mode plasmas were more Bohm-like when the scalings based on engineering factors were transformed to those based on physics variables[7]–[9].

The simplest solution for the steady state transport may be found in these equations, which are simply made up of the diagonal elements of the transport matrix. While not included in this collection, further terms, such as those proportional to pinches, may be found using perturbation methods However, the majority of the components in these transport relations may be observed or estimated in order to solve the equations above. Measurements are made of density, temperature, rotation patterns, and their temporal development. Additionally, the radiated power is gauged. Once the source of the particles is identified, the convective radial velocity, abbreviated vr, may be derived using the particle balance equation. This component is then carried over to the momentum and heat transfer equations. Although this calculation mainly depends on models, source and loss terms owing to convection, ionisation, and charge exchange are computed, as well as the source terms.

Neutral beam models

The most efficient and well-understood auxiliary heating technique for magnetically confined plasmas has been neutral beam heating. It has been employed in a variety of equipment, from little to enormous tokamaks to stellarators, and it is effective in raising plasma temperatures required for fusion energy generation.

This technique of heating involves injecting high energy neutral particles into the plasma, generally with energies of >>Te. If the plasma is thick enough to reduce "shine-through" losses,

the fast neutrals are ionized by collisions with, principally, the electrons. The magnetic field traps the fast ions, but they may escape through charge exchange, bad orbits (fast ions striking material surfaces as a result of large gyro- and/or banana orbits), static or varying inhomogeneities in the magnetic field (such as ripple, MHD modes, respectively), or bad orbits. When rapid ions collide with electrons and other ions, they slow down and lose energy, functioning as a heating, torque, and particle source for the thermal plasma[10], [11].

This Monte Carlo method provides excellent agreement with measurements for MHD quiescent plasmas, including global measurements (e.g., calculated versus measured neutron flux) and indirect or direct measurements of the fast ion profiles from neutral particle analysers or from the fast ion diagnostic (FIDA), as appropriate. Agreement to within 15% should be regarded as good given the uncertainties in the local plasma/impurity composition and the neutral density, both of which might impair rapid ion confinement. There may be large discrepancies between classical calculations and observation due to the existence of MHD activity, most notably Alfvén eigenmodes (AEs), which are driven unstable by free energy in the fast ion distribution and which non-linearly link to and affect the fast ion distribution. Applying an ad hoc rapid ion diffusivity with a spatially constant magnitude of 0.5 m2 /s may usually restore agreement. However, in other circumstances, a considerably more complex anomalous diffusivity that depends on energy and is geographically and/or temporally variable must be utilised. In one such case, the disagreement with neutrons and FIDA on DIII-D must be resolved by an anomalous diffusivity with a very high core value . Even when these amplitudes are increased by a factor of five, this degree of rapid ion transport much surpasses that determined from observed AE mode amplitudes, derived from Even though these instances are usually rare, it is nevertheless critical to comprehend the physics behind the ad hoc adjustments and take into account any unintended consequences brought on by the rapid ions. The hypothesised stochastic heating of thermal ions owing to compressional AEs made unstable by the perpendicular component of the beam ion distribution is one example of the latter[12], [13].

CONCLUSION

Studies on global energy confinement scaling are essential for understanding and forecasting how energy confinement behaves in fusion plasmas. The link between plasma properties and global energy confinement timea crucial performance indicator for fusion devicescan be better understood thanks to empirical scaling rules.Researchers work to understand the fundamental physics regulating global energy confinement scaling by examining experimental data from diverse fusion devices and using statistical modelling and theoretical ideas. To pinpoint the variables affecting energy confinement, variables such plasma density, temperature, magnetic field, and gadget size are thoroughly investigated.

REFERENCES

[1] G. Verdoolaege et al., “The updated ITPA global H-mode confinement database: Description and analysis,” Nucl. Fusion, 2021, doi: 10.1088/1741-4326/abdb91.

[2] M. Wakatani et al., “Plasma confinement and transport,” Nucl. Fusion, 1999, doi: 10.1088/0029-5515/39/12/302.

[3] G. Fuchert et al., “Global energy confinement in the initial limiter configuration of Wendelstein 7-X,” Nucl. Fusion, 2018, doi: 10.1088/1741-4326/aad78b.

[4] G. Fuchert et al., “Increasing the density in Wendelstein 7-X: Benefits and limitations,” Nucl. Fusion, 2020, doi: 10.1088/1741-4326/ab6d40.

[5] S. M. Kaye, J. W. Connor, and C. M. Roach, “Thermal confinement and transport in spherical tokamaks: A review,” Plasma Physics and Controlled Fusion. 2021. doi: 10.1088/1361-6587/ac2b38.

[6] S. Baschetti et al., “A κ−ε model for plasma anomalous transport in tokamaks: closure via the scaling of the global confinement,” Nucl. Mater. Energy, 2019, doi: 10.1016/j.nme.2019.02.032.

[7] M. Wakatani, “Chapter 2: Plasma confinement and transport ITER Physics Expert Groups on Confinement and Transport and Confinement Modelling and Database *,” Nucl. Fusion, 1999.

[8] A. A. Mavrin, “Effect of impurity radiation and helium particle confinement on tokamak-reactor plasma performance,” Plasma Phys. Control. Fusion, 2020, doi: 10.1088/1361-6587/abab5d.

[9] J. M. Polson, “Free Energy of a Folded Semiflexible Polymer Confined to a Nanochannel of Various Geometries,” Macromolecules, 2018, doi: 10.1021/acs.macromol.8b01148.

[10] T. Rafiq et al., “Microtearing instabilities and electron thermal transport in low and high collisionality NSTX discharges,” Phys. Plasmas, 2021, doi: 10.1063/5.0029120.

[11] K. Tanaka et al., “Isotope effects on transport in LHD,” Plasma Phys. Control. Fusion, 2021, doi: 10.1088/1361-6587/abffb6.

[12] A. E. Hubbard et al., “Edge energy transport barrier and turbulence in the I-mode regime on alcator C-mod,” Phys. Plasmas, 2011, doi: 10.1063/1.3582135.

[13] I. physics expert Groups et al., “Chapter 2□: Plasma confinement and transport,” Nucl. Fusion, 1999.

CHAPTER 8

DETERMINATION OF TURBULENCE MEASUREMENT

Dr. Pradeep Bhaskar, Assistant Professor
Department of Engineering Physics, Presidency University, Bangalore, India
Email Id- pradeepbhaskar@presidencyuniversity.in

ABSTRACT:

Understanding and describing turbulent flows is essential in a variety of disciplines, including fluid dynamics, atmospheric science, and engineering. The methods and approaches used for turbulence measurement and analysis are the main subject of this work. The study examines experimental and computational methods for calculating turbulence intensity, turbulence spectra, and turbulent energy dissipation rates. The merits and disadvantages of important measuring methods including hot-wire anemometry, laser Doppler velocimetry, and particle image velocimetry are explored. The paper also looks at how turbulence measurement is used to simulate turbulent flow, regulate turbulence, and analyses turbulent transport processes.

KEYWORDS:

Turbulence Measurement, Turbulent Flows, Turbulence Intensity, Turbulence Spectra, Turbulent Energy, Experimental Techniques.

INTRODUCTION

The domain of precise turbulence measurements is perhaps the most crucial and weakest link in our knowledge of turbulent transport.Since turbulence is thought to be the fundamental source of anomalous transport and is notoriously difficult to quantify in the harsh environment of tokamak plasma interiors, precise measurements are the best way to evaluate theories. In this part, we provide a description of the methods used to quantify turbulence in the tokamak plasma core as well as the outcomes[1], [2].

Measurement Techniques

In order to detect density, temperature, potential, disrupted magnetic fields, and even flows, material probes may be inserted into the scrape-off layer (SOL) and the confinement zone's border of tokamaks. These probes must be swiftly immersed and withdrawn from high power plasmas in order to avoid overheating. However, it is feasible to quantify the characteristics of edge and SOL plasma turbulence in a surprising amount of detail, including intriguing characteristics like correlations between fluctuating quantities and the poloidal variation of fluctuation amplitudes.Hot plasma fluctuations need more indirect measuring methods. Far-infrared or microwave beams are introduced into plasmas and either dispersed or reflected off of the surrounding turbulence. Doppler backscattering, a novel technology that combines elements

of each of these, has been created. The turbulence always changes the emerging light's frequency, and in certain situations, both spatial and wavenumber information about the turbulence may be inferred.In addition to using electromagnetic waves to probe plasmas, particle beams have also been successfully used to assess turbulence. Single-charged heavy ion beams may be accelerated to energies in the MeV range and can pass through the magnetic fields of tokamaks of a reasonable size. They may get doubly ionised as they go through the plasma and then depart on closer orbits while carrying data about the local density and electric potential. More often, the 100 keV neutral deuterium beams used to heat plasma are collisionally excited as they pass through the plasma and generate D radiation proportionate to the varying local plasma density.

It is possible to improve several well-known temperature measuring methods to capture changing ion and electron temperatures. Charge transfer from neutral deuterium atoms with a mass of around 100 keV to, for instance, totally stripped carbon ions is the foundation of charge exchange recombination spectroscopy. Very high throughput observations of the light spectrum released when captured electrons drop to lower excitation states may be used to calculate the variation in the temperature of the carbon ions. Due to photon statistics at long wavelengths, high throughput optics cannot be used in an analogous way to improve the time resolution of electron temperature measurements of electron cyclotron emission. Instead, correlation techniques that focus on slightly different frequencies are used.

Electromagnetic Wave Reflectometry

Electromagnetic waves may be reflected off of surfaces when the wave is shut off rather than scattered off of turbulent plasma. Ordinary waves are reflected at the point in the plasma where the electron plasma frequency rises to equal the wave frequency, pe, and extraordinary waves are reflected at the point in the plasma where the right-hand cut-off rises to the wave frequency, ce, where ce is the electron cyclotron frequency. With exceptional waves, it is conceivable to launch from the low-field side of the plasma and investigate its high-field side.

The typical setup is to propagate waves directly to the cut-off layer and measure the radiation that is directly reflected. It can be shown that the normal WKB integral, kdl, with an extra component of p, gives the phase difference between the incoming and outgoing waves in a straightforward, non-turbulent scenario. This component appears when the WKB approximation falters close to the cut-off, as shown by the symbol k. Thus, in the hypothetical instance of a perpendicular surface travelling back and forth in front of the beam, one may monitor the turbulent velocity of the cut-off layer by observing the fluctuation in the phase difference. Since the cut-off layer itself is where the majority of the variance in k(l) originates, this measurement ought to be quite localized.

Reflectometry is a reasonably simple method; however, it might be difficult to understand the results. It is true that in the tokamak turbulence regime, where 1 / () n n k L, the turbulent cut-off surface forms angles of order one radian with respect to the equilibrium cut-off surface, and the situation resembles shining a torch on moving, crumpled tin foil, as opposed to the idealised case of a flat surface moving back and forth in front of the beam Except for extremely low turbulence levels, the profoundly non-linear inversion issue has not yet shown to be solvable.

Beam Emission Spectroscopy

In order to perform beam emission spectroscopy, uses high current neutral deuterium atomic beams with energies between 100 keV. If not for the fact that many tokamaks are outfitted with very potent beams of this kind for the purpose of heating plasma, this would not be a technology that could be used in a practical manner. Conveniently, these beams' energy must be selected in such a way that a sizeable portion heats the plasma core and is thus accessible for plasma diagnostics.

Neutral ion collisions with neutral atoms may excite them as they move through the plasma. The radiative decay of these excited states, which includes the emission of D light (3 2 transition, 656.1 nm), provides a relatively well localized assessment of the changing plasma density since the lifetime of these excited states is in the region of a few nanoseconds. In order to maximize spatial resolution perpendicular to B, detectors are set up to look tangential to the magnetic field where intense beam neutrals intersect the plasma. Filters are employed to only allow D light that has been correctly Doppler shifted for emission by energetic beam neutrals. The most effective method currently in use uses a 30-detector array to provide imaging capacity across a 30 cm2 region at MHz sample rates. Shot after shot, the image array is moved over the plasma. With this method, fluctuation amplitudes, k spectra across a moderate range, and flow rates may be measured as markers for plasma fluxes, including flows that the turbulence itself[3].

DISCUSSION

Correlated Electron Cyclotron Emission

With the exception of the extreme edge, tokamaks often have optically thick electron cyclotron emission (ECE) at the second harmonic, which should allow for precise determination of the local electron temperature. In fact, the optical depth is often great enough that the spatial resolution of an ECE fluctuation diagnostic depends more on the size of the beam point on the plasma than it does on the depth from which the emission originates. In high beta, high density plasmas, electron cyclotron emission may also be suppressed, yet a large operational window is often accessible.

One could be tempted to believe that precise measurements of variable electron temperature might be provided by high sensitivity detectors for ECE emission. Interestingly, the inherent noise level for long-wavelength photons is such that this is impossible.This issue can recently be solved by correlating the signals from two ECE measurements made at slightly different frequency. To circumvent the inherent statistical difficulty, they must be spread apart by a distance greater than the detection bandwidth of each channel, while yet being sufficiently near together to ensure good correlation of any variations in the plasma. Although this method has also not been widely used, it offers a crucial foundational test for comprehension of plasma turbulence.

Equilibrium and Macroscopic Stability

Particles are propelled into circular orbits perpendicular to a homogeneous magnetic field, but motion along the field lines is unaffected. The drifts and the mirror force are caused by

inhomogeneities un the magnetic field B. We have two options for reducing contact between a thermonuclear grade plasma and the walls when its temperature is in the 107 K range: either restrict field lines to closed surfaces or increase B along field lines prior to wall contact in order to reflect a sufficient number of energetic particles. The magnetic fields will be uneven in both scenarios, and we also need to be concerned about losses from particle drift[4], [5].

The tokamak line, which will also be continued by the ITER experiment, has been by far the most successful in its approach to fusion reactor values of pressure, temperature, and energy confinement time. This has been true over the course of more than fifty years of fusion-motivated plasma research. Therefore, this arrangement is the main emphasis of this book's explanation of fusion physics and technology. However, the tokamak serves as a model for all confinement systems that include closed magnetic surfaces that generate topological tori.

For the purpose of describing the equilibrium and dynamics of magnetically confined plasmas, a hierarchy of plasma models has been used. The fastest large-scale instabilities are described by ideal MHD, as well as macroscopic equilibrium. This model, however, severely limits the range of stable plasma equilibria, even though it results in perturbations growing more slowly. Finite electrical resistivity, which is only significant in thin ("resonant") layers, can also significantly limit the range of stable plasma equilibria. Although these models tend to anticipate very tiny characteristic dimensions of these resonant layers when taking into consideration realistic values of the plasma resistivity, this means that two-fluid (drift-) effects and limited Larmor radii may have an impact on the actual local dynamics. Last but not least, rapid particles that are connected to plasma heating may have a range of effects on plasma stability. Their motion is often independent of the background plasma's motion (which is characterized by a fluid), which may average out the perturbation but also enable resonant exchanges because parallel velocity or drift speeds can be equivalent to the propagation speed of intrinsic plasma modes.

As opposed to the latter, which can typically be attributed to discernible instability and categorized in a reproducible manner, disruptions are not a well-defined instability (just as death is not a well-defined illness) and can have a variety of causes, leading to quite different dynamics during the initial phases. In reality, if an instability does not saturate at a small enough amplitude, it may cause a disruption. Therefore, the section on disruptions emphasizes the very practical need to control them as a threat to the integrity of the device: experimental characterization and theoretical understanding primarily serve to estimate and extrapolate the resulting loads and to develop strategies to avoid or mitigate these events.

Extensions to the MHD model

The ideal MHD model is one in which the fundamentals of global stability against large-scale perturbations are well known. No aspect of the conservation of field/plasma energy or momentum is approximate, making the model both beautiful and profoundly consistent. The important dynamics, however, are often completely absent from the MHD image once additional factors like saturation of small-scale instabilities or even dissipative effects on large scale disturbances still in the linear development phase enter the picture.

Reduced MHD and resistive MHD, which refer to the low frequency domain and dissipation by collisional friction between electrons and ions, respectively, are terms related to the MHD model that are often employed. In reduced MHD, the electrostatic potential serves as a stream function, and the plasma velocity perpendicular to the magnetic field is treated as an E B drift. Due to the spatial fluctuation of the magnetic field, the velocity may be adiabatically compressible. The inverse variation with respect to the main radius is the predominant component of this in a torus. Due to the scale difference in frequency, treating the velocity as a drift eliminates the fast magnetosonic (compressible Alfvén) wave from the dynamics. To Ohm's Law, resistance (the transfer of momentum from electrons to ions as a result of frictional drag) is added.

The fundamental physical image that supports MHD is still there in these models: Any instabilities are caused by the current gradient in Alfvén dynamics, which also includes the current and E B velocity. The parallel flow and parallel pressure gradients are involved in sound wave dynamics (including the spread of plasma along magnetic field lines), and any instabilities are fueled by the parallel flow velocity gradient. Pressure and E B velocity play a role in exchange dynamics, and the pressure gradient is what causes any instabilities. These forms of motion are theoretically distinct within MHD, despite the fact that parallel dynamics may limit the effects of instabilities caused by perpendicular dynamics.

lfvén dynamics because a vortex's turnover motion, which represents the E B velocity, bends the field lines. When the cost of bending the field lines outweighs the release of free energy during interchange motion, instability results. But only the current and the electric field are involved in the Alfvén motion, which is connected to the magnetic and E B flow disturbances through Ampere's Law and the Lorentz force balance, respectively. There is no direct energy coupling of parallel currents to pressure gradients in MHD because Alfvén motion is not coupled to the pressure gradient in Ohm's Law. Similar considerations apply to the kink instability, a current-driven instability, as well as dissipative-dependent dynamics like field line reconnection and the tearing instability, where resistivity is both the only dissipative mechanism available and the only effect not found in pure ideal MHD.

The circumstances in which these limitations apply are essentially the same as the circumstances in which one may derive MHD from a more comprehensive model without making the one-fluid assumptions. The Braginskii equations are often the more general model in the purely fluid physical picture.

For each species, whose velocities and pressures are now handled independently, these rules consist of a set of dissipative conservation laws for particles, momentum, and thermal energy. Dissipation, which results from collisions between and within species, is handled generically. When treating the parallel heat flux as a dynamical variable, adjustments may be necessary to give the temperature/heat-flux pair characteristics comparable to those of the density/velocity pair. This comes into play, in particular, when drive-by temperature gradient special effects are taken into account and the collisional dissipation effects do not totally dominate the relationship between heat flux and temperature gradient. However, the concept of a collection of distinct fluids—one for each particle speciescoupled by Maxwell's equations—under sufficiently non-relativistic circumstances to permit the neglect of the displacement current (hence, directly non-

neutral plasma effects)is sufficiently clear to be used as a starting point. Making the bare minimum number of assumptions required to arrive at the MHD equations allows one to deduce the MHD model from inside this system[6], [7].

The remaining forces are the sum of the Lorentz forces, the total pressure force, and the inertia.The last method is the well-known j B effect, which separates a highly conductive plasma from a neutral fluid. Only when the main velocity or the electric field are separately removed by subtraction, which then becomes the process for deriving the MHD model from inside the two-fluid equations, are currents and pressure gradients, respectively, kept. The process is described in full below, beginning with a simple, isothermal two-fluid model.

The distinction between pressure or fluid dynamics and Alfvén dynamics is no longer a part of the set of assumptions for the two-fluid model.However, depending on the variables and the size of the instability taken into account, it is still possible to achieve this separation in the results (for example, small amplitude instabilities in a tokamak may be selected based on the toroidal mode number, due to axisymmetric; the perpendicular wavenumber has a component within the flux surface arising from the finiteness of the poloidal component of the magnetic field; in general, this results in a drift of the eigenmode[8]–[10].

CONCLUSION

Techniques for measuring turbulence are essential for understanding and describing turbulent flows in a variety of contexts. Researchers may learn a lot about the dynamics of turbulent flows by measuring turbulence parameters such turbulence intensity, turbulence spectra, and turbulent energy dissipation rates.The direct measurement of turbulence parameters in physical investigations is made possible by experimental methods including hot-wire anemometry, laser Doppler velocimetry, and particle image velocimetry. In addition to experimental observations, computational tools, such as numerical simulations and data analysis strategies, provide a better knowledge of turbulent flows.

REFERENCES

[1] A. F. Nerushev and R. V. Ivangorodsky, “Determination of turbulence zones in the upper troposphere based on satellite measurements,” *Sovrem. Probl. Distantsionnogo Zo. Zemli iz Kosmosa*, 2019, doi: 10.21046/2070-7401-2019-16-1-205-215.

[2] S. Lou, M. Chen, G. Ma, S. Liu, G. Zhong, and H. Zhang, “Modelling of stem-scale turbulence and sediment suspension in vegetated flow,” *J. Hydraul. Res.*, 2021, doi: 10.1080/00221686.2020.1780491.

[3] P. Clark Di Leoni, A. Mazzino, and L. Biferale, “Synchronization to Big Data: Nudging the Navier-Stokes Equations for Data Assimilation of Turbulent Flows,” *Phys. Rev. X*, 2020, doi: 10.1103/PhysRevX.10.011023.

[4] J. Prytherch and M. J. Yelland, “Wind, Convection and Fetch Dependence of Gas Transfer Velocity in an Arctic Sea-Ice Lead Determined From Eddy Covariance CO2 Flux Measurements,” *Global Biogeochem. Cycles*, 2021, doi: 10.1029/2020GB006633.

[5] L. Wang, M. A. Geller, and D. C. Fritts, "Direct numerical simulation guidance for thorpe analysis to obtain quantitatively reliable turbulence parameters," *J. Atmos. Ocean. Technol.*, 2019, doi: 10.1175/JTECH-D-18-0225.1.

[6] J. H. Pu, "Velocity profile and turbulence structure measurement corrections for sediment transport-induced water-worked bed," *Fluids*, 2021, doi: 10.3390/fluids6020086.

[7] F. K. Owen and A. K. Owen, "Measurement and assessment of wind tunnel flow quality," *Progress in Aerospace Sciences*. 2008. doi: 10.1016/j.paerosci.2008.04.002.

[8] V. A. Banakh, I. N. Smalikho, and A. V. Falits, "Estimation of the height of the turbulent mixing layer from data of Doppler lidar measurements using conical scanning by a probe beam," *Atmos. Meas. Tech.*, 2021, doi: 10.5194/amt-14-1511-2021.

[9] K. G. Klein, G. G. Howes, and J. M. TenBarge, "Diagnosing collisionless energy transfer using field–particle correlations: Gyrokinetic turbulence," *J. Plasma Phys.*, 2017, doi: 10.1017/S0022377817000563.

[10] A. M. Helmi, "Assessment of CFD turbulence models for free surface flow simulation and 1-d modelling for water level calculations over a broad-crested weir floodway," *Water SA*, 2019, doi: 10.17159/wsa/2019.v45.i3.6739.

CHAPTER 9

AN OVERVIEW OF THE DISRUPTIVE INSTABILITIES

Dr. Puthanveetil Deepthi, Associate Professor
Department of Engineering Physics, Presidency University, Bangalore, India
Email Id- deepthi.pr@presidencyuniversity.in

ABSTRACT:

Understanding and describing turbulent flows is essential in a variety of disciplines, including fluid dynamics, atmospheric science, and engineering. The methods and approaches used for turbulence measurement and analysis are the main subject of this work. The study examines experimental and computational methods for calculating turbulence intensity, turbulence spectra, and turbulent energy dissipation rates. The merits and disadvantages of important measuring methods including hot-wire anemometry, laser Doppler velocimetry, and particle image velocimetry are explored.

KEYWORDS:

Turbulence Measurement, Turbulent Flows, Turbulence Intensity, Turbulence Spectra, Turbulent Energy.

INTRODUCTION

In the current tokamaks, a complicated feedback mechanism generates and controls a plasma discharge during its entire length. Its duration, which ranges from a few seconds to hours, is determined by the energy supply system powering the plasma toroidal current.A tokamak discharge is also restricted to a large but constrained area of the multidimensional operating space. Any effort to cross these lines causes a disruption, a serious plasma instability that ends the discharge.

These limits have been investigated during many years of tokamak operation, and some of them are now rather well recognized. For instance, it is generally known that MHD instabilities place a limit on the ranges of achievable plasma density, current, and pressure, and that any effort to elevate these parameters over the stable value results in a disruption.Away from the density, current, and pressure limitations, unstable current and pressure profiles may also develop; in fact, the stability boundaries are intricate functions of the plasma parameter profiles[1]–[3].

The plasma resistivity rises and the plasma current is ohmically dissipated. Since the ionised particles are very hot, the plasma serves as a storehouse for both thermal and magnetic energy. It also carries a significant toroidal current. When there is a disruption, energy confinement is lost, which results in heavy heat loads and mechanical stresses on the machine's parts. As a result,

interference not only prevents the discharge from occurring or reduces the operating area, but also poses a threat to the tokamak's structural integrity. On all significant tokamaks, techniques for anticipating, preventing, and minimising their effects are being developed.

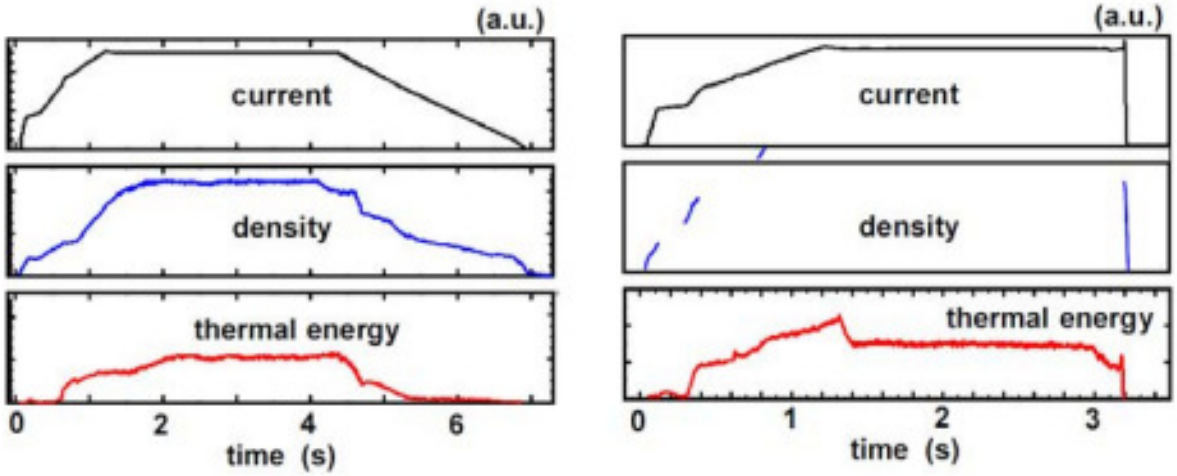

Figure 1: Represent the discharge on the left the plasma current.

Phases of disruptions

i. Thermal Quench

The progressive degradation of confinement caused by the magnetic field's ergodization may be followed by an abrupt loss of the thermal energy that was still there. Thermal quench is the name of this quick phase. The limiter and divertor surfaces are where the plasma thermal energy is deposited, mostly via conduction, and the duration of this deposition is highly influenced by the machine size. In tiny tokamaks, it is on the order of tens of microseconds, while in JET, it is just a few milliseconds.

The progressive degradation of confinement caused by the magnetic field's ergodization may be followed by an abrupt loss of the thermal energy that was still there. Thermal quench is the name of this quick phase.

The limiter and divertor surfaces are where the plasma thermal energy is deposited, mostly via conduction, and the duration of this deposition is highly influenced by the machine size. Small tokamaks have a time scale of tens of microseconds, while JET has a time scale of a few milliseconds.

Without substantial plasma energy loss, the cooling of the plasma core occurs first. The electron temperature profile as a whole fall, the energy barrier inside the closed flux surface area breaks, and the energy is lost to the divertor plates in the second phase. A comparable degradation of the profile is shown in the electron temperature and SXR observations, which is consistent with the cold bubble model's prediction.

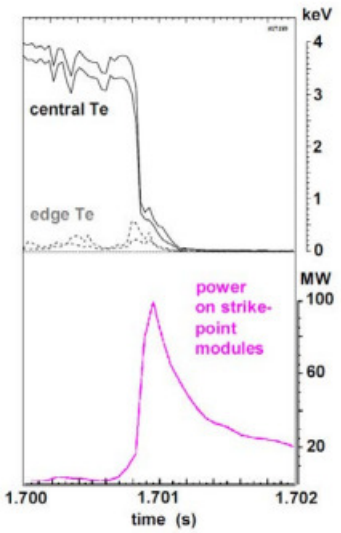

Figure 1: Represents the Sudden and fast decay of the electron temperature.

DISCUSSION

Heat pulse

The limiter and divertor plates receive the majority of the thermal energy lost by the plasma during the thermal quench via the SOL. If the heat pulse on the plasma-facing components causes the ablation of surface material or if impurities are already present in the plasma, a sizeable portion of it may also be radiated during this phase. The majority of the magnetic energy is recombined and radiated by the whole plasma during the current quench, although conduction and convection are projected to deposit energy locally where the plasma meets the wall[4]–[6].The surface temperature of the wall may be inferred from thermographic data, such as the one nd the deposited power flux can be calculated. Additionally, they demonstrate that the SOL clearly expands during the thermal quench, dispersing the thermal load across a significant area within the footprint of the pre-disruptive impact spots.

The rise in surface temperature wT is determined by the quantity of deposited energy (th E), the length of the surface on which the heat is deposited (S), and the duration of the heat pulse (hp), in addition to the thermal characteristics of the wall material. The substance confronting the plasma will then either evaporate or melt during a disruption depending on the temperature that is attained on the surface. Conduction parallel and perpendicular to the open magnetic surface of the SOL, affected by turbulence and stochasticity, and flux limit through the sheet at the plasma-wall interface are some of the physical factors that determine the broadening of the SOL and the timescale of the heat pulse duration. However, a reliable physics model for the quantitative assessment of the primary processes influencing the widening of the SOL is still lacking, and it is unclear to forecast the thermal impact of disruptions in future bigger machines. However, as the thermal energy density would be higher in a bigger machine, it is envisaged that local melting and erosion of the surfaces crossing the extended SOL will occur.

Such occurrences are often brought on by the abrupt shift in plasma current that occurs during a disruption. This current-induced current in the vessel attracts the plasma to the passive parts that are magnetically more firmly linked. This effect can be recognised and clearly seen for a plasma that is positionally stable and has a roughly circular cross-section, but it will only move the equilibrium position. However, it may be the catalyst for an unstable displacement event in an extended plasma. Evidently, placing the plasma at the neutral point has a major positive impact on its capacity to be controlled.

Runaway generation

Such occurrences are often brought on by the abrupt shift in plasma current that occurs during a disruption. This current-induced current in the vessel attracts the plasma to the passive parts that are magnetically more firmly linked. This effect can be recognised and clearly seen for a plasma that is positionally stable and has a roughly circular cross-section, but it will only move the equilibrium position. However, it may be the catalyst for an unstable displacement event in an extended plasma. Evidently, placing the plasma at the neutral point has a major positive impact on its capacity to be controlled.

$$F_{e,e} = \frac{e^4 n_e \ln \Lambda}{4\pi\varepsilon_0^2 m_e \mathrm{v}_e^2}$$

Mitigation Methods

Because they take place in well-known areas of the parameter space, disruptions may often be avoided. Additionally, they are often preceded by confinement deterioration and the emergence of MHD modes, which may be seen and exploited to forecast and mitigate them.Injecting impurity atoms into the plasma may all be used to lessen the disruption effects discussed in the preceding chapter. Cryogenic or solid pellet injection was first used to start a plasma shutdown with impurity injection. However, due to a number of drawbacks, including the solid pellets' inadequate ablation and a propensity to act as a seed for runaway electrons, this technology was abandoned in favor of enormous gas injection.

Before magnetic instabilities may trigger the thermal quench, the injected impurity gas must dissipate the majority of the plasma's thermal energy in order to decrease the localized heat deposition during the disruption's thermal quench.Following the lowering of the induced toroidal, poloidal, and eddy currents in the plasma structure, the forces are reduced. The techniques of injecting impurities may use one of two ways, depending on the plasma's vertical stability properties.

Eddy currents produced by the plasma current quench exert the most mechanical stresses in tokamaks with vertically stable plasmas. The present quench should grow gradually in this situation. This helps prevent runaway electrons from occurring. In this situation, low-Z impurities are appropriate for injection because they chill the plasma more gradually and radiate less. On the other hand, in vertically unstable plasmas, it is necessary to minimize the toroidal and poloidal (halo) currents that are generated in the machine's mechanical structures. This is possible if the current quench is anticipated before the vertical displacement begins. the effect of

increasing the quantity of injected contaminants. The halo current and the passive stabilizing vessel structures' currents eventually decrease, lowering the vessel's total vertical force[7]–[9].

Plasma Diagnostics

The capacity to regulate a high temperature plasmapossibly the most complex thing ever made by humanswhich has unique features is essential for the development of peaceful fusion power. Over the course of many years of fusion research, a new field of study known as plasma diagnostics has emerged. This discipline requires expertise in nearly all branches of physics, from electromagnetism to nuclear physics, as well as the most recent advancements in engineering and technology materials, electronics, and mathematical methods of data treatment.

In the past, work on controlled fusion began with pulsed systems, and as a result, the techniques for measuring plasma parameters were first created for brief and dense plasmas. Special experimental procedures must be developed for diagnosing magnetically confined hot plasmas.The diagnostic set is the component of a plasma device that requires the highest scientific expertise. Many years of research operations resulted in the resolution of certain scientific problems as well as the emergence of new ones. New responsibilities frequently call for substantial adjustment.

Mathematical modelling of the anticipated plasma characteristics, which predicts the plasma's location and form as well as its temperature and density profile, is the initial stage in the creation of a diagnostic. For the very first shot, it is vital to establish the starting diagnostic set. The starting diagnostic set's content is only tangentially affected by the machine's quirks. 66Sometimes just one approach can be used to satisfy the measuring criteria. Additionally, a duplicate of procedures is required for the critical parameter measurements to be reliable. For core, edge, and divertor plasmas, it is sometimes necessary to use unique procedures. MNOver fifty different diagnostic techniques have been created in the recent years. Each of them has unique peculiarities. There aren't many techniques that can directly measure plasma properties, thus it's critical to understand the difference between measurements and interpretations. The technically easiest solution is often the most difficult to comprehend. Local measurements are usually preferred over averaged ones since they may be interpreted more easily.

Deuterium, or hydrogen-2, cross sections exhibit a similar behavior, however the scattering cross section is much bigger than the absorption cross section.Other nuclei, like hydrogen, exhibit elastic scattering cross sections, which are comparable to straightforward collisions between billiard balls when kinetic energy is conserved. Because the neutron scatters off the nucleus' surface rather than penetrating its inside to create a complex nucleus, these cross sections are known as prospective scattering cross sections. Energy does not affect the cross sections of potential scattering unless at extremely low or high energies. Their size is inversely correlated with the cross-sectional area of the nucleus, where R=1.25 1013A1/3 cm is the radius of the nucleus expressed in terms of atomic weight. However, in order to better comprehend neutron cross sections, it is necessary to look at processes that happen when compound nuclei are formed.

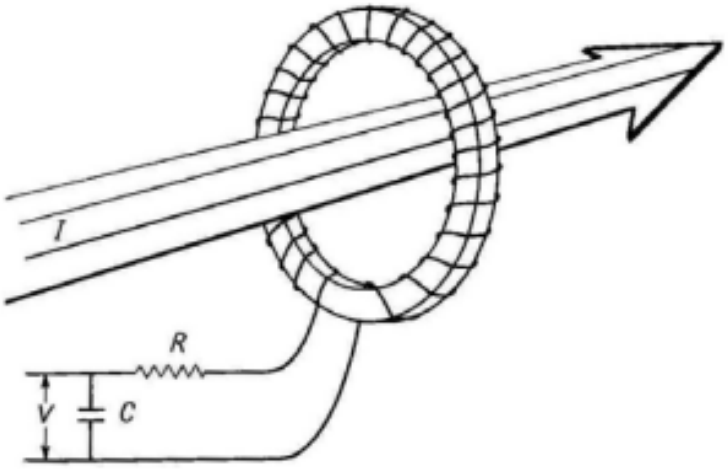

Figure 2: Represents the Scheme of plasma current measurements.

Installing two ring loops on the inner and outer borders of the equatorial plane is adequate. For an appropriate evaluation of the ohmic power for a non-circular plasma, it is important to know the voltage distribution in the poloidal direction along the contour enveloping the plasma column. Additionally, a high number of loops are required for the accurate reconstruction of the form of the edge magnetic surface. Naturally, all of these factors point to a stationary or substitutionary plasma discharge condition. This perfect circumstance seldom occurs in reality, and several modifications must be made when interpreting flux data for resistivity. It is crucial to consider the inductive terms in the loop voltage, such as (/) p L dI dt and (/) p I dL dt, where L is the plasma inductance, in the case of time-varying parameters. For discharges with beam or wave current production as well as discharges where runaway electrons are a major factor, further adjustments are required[10]–[12].

CONCLUSION

Techniques for measuring turbulence are essential for understanding and describing turbulent flows in a variety of contexts. Researchers may learn a lot about the dynamics of turbulent flows by measuring turbulence parameters such turbulence intensity, turbulence spectra, and turbulent energy dissipation rates. The direct measurement of turbulence parameters in physical investigations is made possible by experimental methods including hot-wire anemometry, laser Doppler velocimetry, and particle image velocimetry. In addition to experimental observations, computational tools, such as numerical simulations and data analysis strategies, provide a better knowledge of turbulent flows.

REFERENCES

[1] B. B. Kadomtsev, “Disruptive Instability In Tokamaks.,” Sov J Plasma Phys, 1975.

[2] J. Kates-Harbeck, A. Svyatkovskiy, and W. Tang, “Predicting disruptive instabilities in controlled fusion plasmas through deep learning,” Nature, 2019, doi: 10.1038/s41586-019-1116-4.

[3] F. Turco, T. C. Luce, W. Solomon, G. Jackson, G. A. Navratil, and J. M. Hanson, "The causes of the disruptive tearing instabilities of the ITER Baseline Scenario in DIII-D," Nucl. Fusion, 2018, doi: 10.1088/1741-4326/aadbb5.

[4] W. Mau, M. E. Hasselmo, and D. J. Cai, "The brain in motion: How ensemble fluidity drives memory-updating and flexibility," Elife, 2020, doi: 10.7554/eLife.63550.

[5] I. H. Hutchinson, "Magnetic probe investigation of the disruptive instability in tokamak LT-3," Phys. Rev. Lett., 1976, doi: 10.1103/PhysRevLett.37.338.

[6] K. Itoh, S. Inoue, and S. Yoshikawa, "Nonlinear Magnetohydrodynamic Instability and Disruptive Instability," J. Phys. Soc. Japan, 1976, doi: 10.1143/JPSJ.40.1757.

[7] V. G. Merezhkin, "Structure Of The Magnetic-Field Perturbations In The Disruptive Instability In The T-6 Tokamak.," Sov J Plasma Phys, 1978.

[8] N. R. Sauthoff, S. Von Goeler, and W. Stodiek, "A study of disruptive instabilities in the PLT tokamak using X-ray techniques," Nucl. Fusion, 1978, doi: 10.1088/0029-5515/18/10/012.

[9] A. Vannucci and S. C. McCool, "Disruptive instabilities in the TEXT-U Tokamak," Nucl. Fusion, 1997, doi: 10.1088/0029-5515/37/9/I04.

[10] E. J. Strait et al., "Progress in disruption prevention for ITER," Nucl. Fusion, 2019, doi: 10.1088/1741-4326/ab15de.

[11] S. Filiz Karabag, "An Unprecedented Global Crisis! The Global, Regional, National, Political, Economic and Commercial Impact of the Coronavirus Pandemic," J. Appl. Econ. Bus. Res. JAEBR, 2020.

[12] A. K. Chattopadhyay, A. Anand, C. V. S. Rao, and S. Joisa, "Analysis of disruptive instabilities in Aditya tokamak discharges," Indian J. Pure Appl. Phys., 2006.

CHAPTER 10

ANALYSIS OF ELECTRICAL PROBES

Dr. Sivasankara Reddy Nanja Reddy, Assistant Professor
Department of Engineering Physics, Presidency University, Bangalore, India
Email Id- sivasankarareddy@presidencyuniversity.in

ABSTRACT:

Electrical probes are often used to test the electrical characteristics and qualities of materials, equipment, and systems in a variety of scientific and engineering fields. Understanding the fundamentals, usage, and developments of electrical probe methods is the main goal of this research. The inquiry examines several electrical probe types, such as capacitance, impedance, current, and voltage probes. In order to comprehend their capabilities and limits, important factors including probe design, calibration, and measuring procedures are examined. In addition, the research looks at how electrical probes are used in industries including electronics, materials science, biotechnology, and electrical power systems.

KEYWORDS:

Electrical probes, Voltage probes, Current probes, Impedance probes, Capacitance probes, Probe design.

INTRODUCTION

Lasmas are crucial to and often even control central plasma activities. The growing attention paid to the experimental investigation of the edge and scrape-off layer plasma reflects this awareness. Aspects of the interaction between the plasma and the surface that cause impurity generation, impurity transport, and core plasma contamination are of special importance.Measurements of the local plasma properties are crucial for understanding the plasma edge and managing the edge conditionsOne of the first methods used in plasma diagnostics is electrical probe measurements. This diagnostic method is still the simplest and most precise approach to detect the local plasma characteristics in plasmas where probes may survive.Even if only the edge plasma is often accessible, the future of electrical probe application is promising due to its significance. Additionally, only electrical probes allow for a complete evaluation of local particle fluxes and electrostatic turbulence-driven transport[1]–[3].

Passive neutral particle analysis

component and for researching the behavior of ions created by radio frequency (RF) heating and neutral beam heating. The significance of CX diagnoses in these trials should not be understated. The H/D/T ratio of the associated atom fluxes measured outside the plasma may be used to describe the plasma fuel isotope composition, which is another direct measurement offered by

CX diagnostics. One of the primary objectives of fusion plasma diagnostics nowadays is the determination of the plasma's H/D/T isotope composition. These metrics have at least two goals in mind. Deuterium and tritium are the primary fuel components in burning plasmas, therefore one strategy is to manage the D/T fuel composition of the plasmas to get the best regime of ignition and fusion burning. For the best burning regime to be achieved, the ideal D/T density ratio must be present. When it comes to fusion reactors, the lack of D/T ratio optimization results in a reduction in efficiency, which raises the cost of power generated in the reactor. From this perspective, one of the most crucial variables to be monitored and regulated in any fusion reactor is the D/T ratio inside the plasma.

Studying energy confinement scaling in plasmas with various hydrogen isotope compositions (H/D/T) is another goal. It has been shown via transport study on tokamaks that the plasma energy confinement time E is isotope-dependent. On ASDEX, this impact was first thoroughly investigated. Deuterium plasmas have been demonstrated to have substantially greater plasma energy confinement than hydrogen plasmas, and the scientists expected that a deuterium-tritium plasma would have even better confinement. Transport analysis carried out in D-T experiments on massive plasma machines such as TFT and JET reveals that plasma conditions rely also on the isotope composition. It has been discovered in TFTR that plasma confinement becomes better as tritium density rises. Although this impact was not seen in the instance of JET, it has been discovered that a rise in tritium content lowers the transition threshold to H-mode.

It should be mentioned that the line integrated form of the signal, the restricted plasma transparency for the examined atoms, and the sharp inward drop in source intensity are the fundamental constraints and inherent challenges of interpretation of passive neutral particle analysis. By employing multi-chord measurements, shot-by-shot scanning of the plasma, or a combination of the two methods, radial profiles may be created using the results of CX diagnostics, which are chord integrated, emissivity weighted measures. By using atomic flux modelling, which is now extremely well developed and is based on the solution of the kinetic equations and Monte Carlo simulations, these constraints may be lessened.

At the Ioffe Institute (St. Petersburg, Russian Federation), neutral particle diagnostics using neutral particle analyzers (NPA) has been actively researched since the 1950s. The first NPA in the world, created at the Institute, eloped in other fusion research facilities throughout the globe An energy and mass spectrometer is the NPA. The ionization of neutral particles released by a plasma and subsequent analysis of secondary ions in the electric and magnetic fields form the basis of this device's working mechanism. Ionization happens when a gas cell strips the material or when it passes through a thin carbon foil. The mass-resolved energy spectra of the particles are provided by the electric and magnetic fields. The classic NPA method makes use of parallel electric and magnetic fields (E B), which separate particles in the detector plane according to their mass and energy. Analyzers use micro-channel plates (MCP), scintillator counters (photomultiplier tubes (PMT) with scintillators), channel electron multipliers, and channel electron multipliers.

The interior design of the nucleus is closely related to how the excitation energy affects neutron cross sections. Although the comparison is far from perfect, it is possible to generally

comprehend these effects by contrasting atomic and nuclear structures. A source of external energy may stimulate the electrons around a nucleus to higher levels, which are in different quantum energy states. Similar to how nucleon configurations exist in quantum states, the addition of a neutron and its associated kinetic energy produces a compound nucleus that is in an excited state. One of two things may happen after the production of a compound nucleus: either the neutron is reemitted, restoring the target nucleus to its ground state; this scattering is elastic, despite the fact that a compound nucleus was briefly produced in the process. The target nucleus is transmuted into a new isotope as a consequence of the neutron obtained in this reaction, or alternatively, the compound nucleus may return to its ground state by releasing one or more gamma rays.Higher incoming neutron energies may provide the compound nucleus enough excitation energy to release both a gamma ray and a lower energy neutron, leading to inelastic scattering. At even higher energies, further processes may take place. Of course, the fission reaction is the most significant result of compound nucleus creation in fissile and fertile materials[4]–[6].

DISCUSSION

The accelerator chamber, magnet chamber, and detection chamber are the instrument's three primary components.

a) The input diaphragm,

b) Collimator slit mechanism,

c) auxiliary mobile calibration detector,

d) stripping foil,

e) output diaphragm

The components of the acceleration chamber. The acceleration chamber delivers secondary ion acceleration (up to 100 kV) after stripping.

It is crucial for plasma installations that use a D-T plasma and have a strong neutron background. The light emission diode (LED), laser for alignment, Hall probe, analyzing magnet, analyzing electrostatic condenser, and detector array are the components of the magnet and detector chambers. A+ is the flow of secondary ions, and Ao is the atomic flux released by the plasma In the energy range of 5-740 keV for Ho, 5-370 keV for Do, and 5-250 keV for To, the ISEP NPA offers good H/D/T mass separation (with rejection of surrounding masses 10-3) and high detection efficiency (up to 100% at higher energies).

In this regard, a solution to the aforementioned discrepancy issue might be found by creating new apparatus that records spectra with a spatial precision of one to a few centimetres. One method is to employ a doubly curved crystal (such as a spherical, toroidal, etc.) that offers spatial resolution in the direction opposite the dispersion direction. Another method is to measure the spectra of several chords using various spectrometers. The imaging spectrometer that was just installed on NSTX [4.235] completed the first job.

A spherically bent crystal and a 2-D position sensitive detector [4.243], or new pixellated semiconductor detectors with a very high photon count rate capacity of 1 MHz per pixel, make up the imaging spectrometer installed atop Alcator C-Mod. With a spatial resolution of around 1 cm, the spectrometer captures spectra from the whole height (72 cm) of the extended plasma cross-section.

A surface map of the spatially resolved helium-like argon spectra obtained from the Alcator C-Mod discharge is shown in Figure 4.28. Resonance lines of helium-like argon and lithium-like satellites make up the spectra that are emitted from the core plasma area, but only helium-like lines—w, x, y, and z—with z being the strongest—are present in the spectra that are released from the cooler region. Since the electron density on Alcator C-Mod is ten times greater than that of previous tokamak experiments, one would anticipate that the ion distribution would be near to corona equilibrium, which is how the lines in the outer plasma zone are created. The explanation for why hydrogen-like ions looked to be far away is now being thought upon. Time resolved spectroscopic data are also used to generate profiles of ion temperature and toroidal rotation velocity against time.

L stands for the scattering volume's length, for the angle formed between the probing wave's electric field and the scattering plane, d for solid angle, and for the optical system's transmission. Typically, the angle in experiments is 900. S(k,) is the dynamic form factor, where k and are the differential scattering vector and the frequency of the propagating wave, respectively, and explain the frequency changes brought on by the movements of the electrons. The scattering cross-section has a very low value of 7.94 10-30 m-2. As a result, the amount of scattered photons that the collecting optics will be able to detect will similarly be low. The spectrometer must be built with a good optical setup and appropriate devices to reduce the bremsstrahlung and spectral line radiation that the plasma releases. The supplementary apparatus has the ability to block off intense stray light that results from laser radiation reflecting off the diagnostic windows or vacuum chamber walls. Also required in the tokamak are Brewster angle windows, a series of light baffles, and, if practical, viewing and laser beam dumps at the input and output ports for the laser beam[7], [8].

LIDAR system

The LIDAR (light detection and ranging) methodology is an incoherent Thomson scattering approach that uses the time-of-flight technique to quantify a brief light pulse. By using a high-speed detection system to capture the backscattered light from a sub-nanosecond laser pulse, the necessary spatial resolution is attained. The transit period of the laser pulse through the plasma determines the temporal resolution of a single measurement.

The necessary temporal resolution for periodic measurements is provided by a laser system with a high repetition rate. The line of sight often travels through the plasma core and is in the poloidal cross-section. On JET, the LIDAR diagnostic consists of a Q-switched ruby laser (Eo = 3-5 J per pulse depending on repetition rate, t = 300 ps) and detection subsystem outside the biological shield, optical transmission lines for the laser and the collected light, a common window for input and output at the flange of the standard equatorial port, and the collection

optics inside the port. A 3-fold labyrinth with a reduced cross-section is employed to lower the escaping neutron flux via the blanket penetration. A self-aligning connection absorbs the significant relative motions between the vacuum vessel and cryostat.

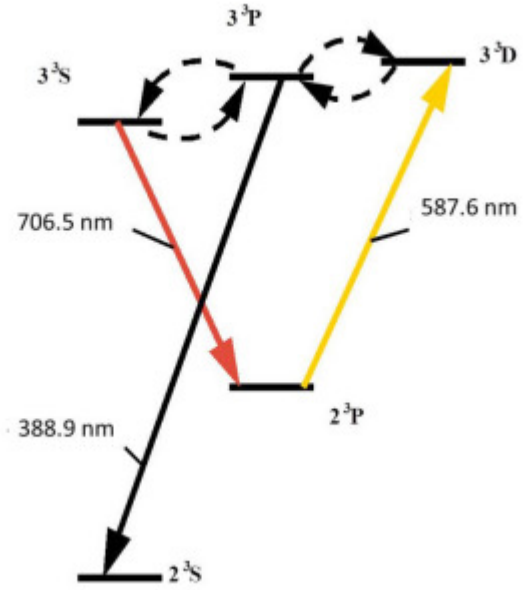

Figure 1: Represents the Spectroscopic scheme of helium atom probing by LIF-technique.

Neutral beams designed for plasma diagnostics have been employed a lot in magnetic fusion studies recently. Even if there are currently a lot of diagnostics based on neutral beam injection, fresh, innovative concepts keep popping up.The diagnosis and the plasma's properties that are being studied dictate the necessary beam parameters. In general, the beam intensity has to be strong enough to provide a reasonable signal-to-noise ratio, particularly for fluctuation investigations that call for a precise temporal resolution. For a decent spatial resolution, the beam size must be small enough. The diagnostic in which the beam is employed also affects the species of the beam and the energy of the particles[9], [10].

Particularly interesting are hydrogen beams with energy of 50–60 keV, which are about at the maximum of the charge exchange cross-section for excitation of the 7-8 transition of C5+ ions. With a minor plasma radius of 0.5–1 m and an average density of around 1020 m-3, this energy also enables adequate beam penetration into the core of the plasma in contemporary plasma physics studies. According to estimates, the spectroscopic detection system can reliably produce signals when an equivalent beam current of at least 1 A is incident on a plasma. The beam power density should be low enough to prevent the plasma from being significantly heated locally at the same time. If the beam current is restricted to several equivalent amps, this criterion is often compatible with the requirement of having enough signal in the detecting system. Many specialized diagnostic neutral beams have been created and are being used in plasma physics studies.

Charge exchange produces diagnostic neutral beams with energy up to 100 keV. A multi-aperture ion optical system generates an ion beam with current of several amps from the surface of the

plasma emitter in the ion source of a diagnostic injector. In a neutralizer gas target, the ion beam that was produced is charge exchanged into atoms. Additionally, effective neutral beam injectors used for plasma heating follow a similar creation strategy. However, in diagnostic injectors, a very tiny angular divergence and focusing of the initial ion beam are necessary for the accomplishment of a high neutral atom flux density in the plasma observation zone. Modulation of the diagnostic beam and great energy stability are often needed in investigations.

CONCLUSION

Electrical probes are adaptable instruments used to measure electrical characteristics and qualities in a variety of engineering and scientific applications. Electrical probes of many kinds, such as voltage probes, current probes, impedance probes, and capacitance probes, each have a special ability to record certain electrical characteristics. For precise and trustworthy electrical measurements, consideration should be given to probe design, calibration, and measuring methods. To get accurate and insightful findings, probe properties like impedance, bandwidth, and sensitivity must be carefully taken into account.

REFERENCES

[1] R. S. Waremra and P. Betaubun, "Analysis of Electrical Properties Using the four point Probe Method," 2018. doi: 10.1051/e3sconf/20187313019.

[2] M. Kim, "Analysis of Electrical Performance on Probe Pin," *J. Softw. Assess. Valuat.*, 2019, doi: 10.29056/jsav.2019.06.13.

[3] A. Chinnappan, J. K. Y. Lee, W. A. D. M. Jayathilaka, and S. Ramakrishna, "Fabrication of MWCNT/Cu nanofibers via electrospinning method and analysis of their electrical conductivity by four-probe method," *Int. J. Hydrogen Energy*, 2018, doi: 10.1016/j.ijhydene.2017.11.028.

[4] C. E. de Almeida Souza Torres, C. G. F. Costa, A. P. Pereira, M. das M. R. de Castro, and V. de Freitas Cunha Lins, "Corrosion failure analysis in a biodiesel plant using electrical resistance probes," *Eng. Fail. Anal.*, 2016, doi: 10.1016/j.engfailanal.2016.05.018.

[5] A. Canales, X. Jia, U. P. Froriep, R. A. Koppes, C. M. Tringides, J. Selvidge, C. Lu, C. Hou, L. Wei, Y. Fink, and P. Anikeeva, "Multifunctional fibers for simultaneous optical, electrical and chemical interrogation of neural circuits in vivo," *Nat. Biotechnol.*, 2015, doi: 10.1038/nbt.3093.

[6] A. Wijaya, B. Eichinger, F. F. Chamasemani, B. Sartory, R. Hammer, V. Maier-Kiener, D. Kiener, M. Mischitz, and R. Brunner, "Multi-method characterization approach to facilitate a strategy to design mechanical and electrical properties of sintered copper," *Mater. Des.*, 2021, doi: 10.1016/j.matdes.2020.109188.

[7] Y. J. Yim and S. J. Park, "Effect of silver-plated expanded graphite addition on thermal and electrical conductivities of epoxy composites in the presence of graphite and copper," *Compos. Part A Appl. Sci. Manuf.*, 2019, doi: 10.1016/j.compositesa.2019.05.021.

[8] S. Huang, H. Kuang, T. Zou, L. Shi, H. Xu, J. Chen, W. Xuan, S. Zhan, Y. Li, H. Jin, S. Dong, X. Wang, H. Zhou, L. G. Occhipinit, J. M. Kim, and J. Luo, "Surface electrical

properties modulation by multimode polarizations inside hybrid perovskite films investigated through contact electrification effect," *Nano Energy*, 2021, doi: 10.1016/j.nanoen.2021.106318.

[9] V. Purwandari, S. Gea, B. Wirjosentono, A. Haryono, I. P. Mahendra, and Y. A. Hutapea, "Electrical and thermal conductivity of cyclic natural rubber/graphene nanocomposite prepared by solution mixing technique," *Indones. J. Chem.*, 2020, doi: 10.22146/IJC.44791.

[10] O. H. Olubowale, S. Biswas, G. Azom, B. L. Prather, S. D. Owoso, K. C. Rinee, K. Marroquin, K. A. Gates, M. B. Chambers, A. Xu, and J. C. Garno, "'may the Force Be with You!' Force-Volume Mapping with Atomic Force Microscopy," *ACS Omega*. 2021. doi: 10.1021/acsomega.1c03829.

CHAPTER 11

ANALYSIS OF NUCLEAR DATA PROCESSING

Dr. Thimmapuram Reddy, Assistant Professor
Department of Engineering Physics, Presidency University, Bangalore, India
Email Id- ranjethkumar@presidencyuniversity.in

ABSTRACT:

Nuclear data processing is essential to the study and use of nuclear data for a variety of purposes, including the design of nuclear reactors, the assessment of nuclear safety, radiation protection, and medicinal applications. Understanding the strategies and tactics used in nuclear data processing is the main goal of this research. The inquiry looks at the procedures that go into compiling, analyzing, and validating nuclear data, such as fission yields, decay data, and cross-sections of nuclear reactions. To provide accurate and trustworthy nuclear data, important factors such data formatting, interpolation, uncertainty propagation, and benchmarking are examined.

KEYWORDS:

Nuclear Data Processing, Nuclear Data, Nuclear Reactions, Cross-sections, Decay Data, Fission Yields.

INTRODUCTION

Nuclear data files that have been evaluatedmore often referred to as evaluationsare the result of the measurement and analytical work that was previously discussed. These files provide data that may be used to recreate all the nuclear data necessary for modelling a nuclear system in the most compact way feasible. The ENDF-n format, in where n is a number indicating the format version, is a common U.S. computer format that has been used abroad[1]–[3].

Photon-induced nuclear reactions

Nuclear reactions brought catalyzed by photons may engage in photo-atomic or photo-nuclear interactions with an atom or a nucleus, respectively. To solve the transport* equation in the energy range up to 20 MeV, only photo-atomic interactions (photoelectric effect, coherent and incoherent scatterings, and generation of e+, e- pairs) are considered. However, photo-nuclear interactions are where secondary neutron sources come from, and they need to be analyzed. Calculations involving photon propagation and secondary neutron sources are mostly done using this data[4].

Charged-particle transport data

Following nuclear or photo-atomic interaction processes, charged particles emerge. These particles include recoiling electrons from the Compton or photoelectric effects, alpha and beta particles in connection to radioactive processes, and electron-positron pairs produced by materializing gamma rays.An "electromagnetic cascade shower"a kind of tree-like propagation of electrons, positrons, and gamma raysis what is caused by these occurrences.The following are the key data:The stopping powers of electrons, positrons, and ions in matter. Bremsstrahlung cross sections. Cross sections of electron/positron scattering in matter. Cross sections of nuclear processes generated by charged particles[5].

Nuclear data uncertainties

Insofar as it is practicable, the goal is to assign an uncertainty to the computed value of a physical quantity. This uncertainty is the outcome of a variety of uncertainties, including uncertainties relating to fundamental physical data, calculation-related uncertainties, technology data uncertainties, etc.For safety, particularly to improve design foundation, it is essential to be aware of these uncertainties. They have an effect on the economy as well. Basic nuclear data uncertainties predominate in the majority of neutronics calculations; thus, it is important to understand them well and acquire techniques that will allow you to assess their impact on the uncertainty associated with the physical quantity of interest.The creation of "sub libraries" 30 to 40 of evaluations in ENDF format is motivated by these computations of uncertainties. These files provide covariance information[6], [7].

Nuclear data uncertainties

Insofar as it is practicable, the goal is to assign an uncertainty to the computed value of a physical quantity.This uncertainty is the outcome of a variety of uncertainties, including uncertainties relating to fundamental physical data, calculation-related uncertainties, technology data uncertainties, etc.For safety, particularly to improve design foundation, it is essential to be aware of these uncertainties.They have an effect on the economy as well.Basic nuclear data uncertainties predominate in the majority of neutronics calculations; thus, it is important to understand them well and acquire techniques that will allow you to assess their impact on the uncertainty associated with the physical quantity of interest.The creation of "sub libraries" 30 to 40 of evaluations in ENDF format is motivated by these computations of uncertainties.These files provide covariance information (information on uncertainty in correlations,

Nuclear data processing

Nuclear data from assessments often has to go through a physical, numerical, and computer processing before it can be used in codes for modelling nuclear systems (transport and depletion codes). The latter is dependent on the kind of data kept in assessments, the type of physical issue being looked into, and the computational strategies used in the employed algorithms. A physical data library (or application library) that may be utilized by a certain modelling code is the process's end result.

Spallation

There are alternative uses for this technology that entail higher-energy nuclear reactions or other kinds of particles. This is the case, for instance, with subcritical accelerator-driven systems (ADS*), which are used to irradiate targets or transmute nuclear waste, as well as with spallation sources, which produce neutrons for use in materials research. These devices blast a target made of a heavy element (tungsten, mercury, lead-bismuth) with a stream of protons that have been accelerated to an energy of around one GeV. The next step is a process known as spallation*, during which some particles, mostly neutrons, are expelled, leaving a smaller nucleus than the starting nucleus. A few of the particles released have enough energy to start a fresh interaction with the nearby nucleus. This series of events generates a large number of neutrons in a thick target, the majority of which will escape the target. This enables the production of powerful neutron fluxes that may be used immediately as a spallation source or to make up for subcriticality in an ADS after slowing down[8].

Nuclear physics models that are directly incorporated into the transport code then compute the cross sections and properties of the released particles at each contact at energies greater than 200 MeV since there are far too many potential reaction pathways to enable the use of libraries. In all situations, experimental measurements of quality that are expected to restrict the physics models describing reactions, theoretical advancements that are likely to enhance these models, and validations by integral measurements are required to increase the quality and reliability of simulation codes.

Spallation modeling

Spallation is often defined as a two-stage process: the first phase is a fast one (a few 10-22s), which entails a series of collisions between the projectile and the nuclear building blocks (nucleons), much like the shocks between billiard balls.An intranuclear cascade is the term used to describe it. Nucleons and peons are among the energetic particles that are ejected as a result of these collisions. The incident energy is dispersed across all of the nuclear building blocks (nucleons) at the conclusion of this process, leaving the nucleus in an excited state. De-excitation is the second process, which happens considerably more slowly. It often occurs when low-energy particles (most commonly neutrons, but sometimes protons, alphas, or even much heavier pieces) are emitted. In the case of heavy nuclei, particle emission also competes with fission into two smaller nuclei. Also released at the conclusion of de-excitation are (gamma) photons.

As a result, modelling often involves coupling two models: an intranuclear cascade model and a de-excitation model. The well-known nucleon-nucleon interaction, potential enclosing nucleons inside the nucleus, and the semi-classical Pauli principal treatment are the primary components of the first one. A statistical model is used to tackle de-excitation, and it evaluates the likelihood of a particle emitting from a set of accessible states as well as the likelihood of a reverse reaction (the particle being captured by the nucleus). Fission barriers and how the two pieces split play a role in the fission scenario. These components may come from more microscopic models or phenomenological parametrizations[9].

Elementary measurements

Without a thorough knowledge of the mechanics behind the spallation response, this goal cannot be achieved. This calls for fundamental, high-quality experimental data that span the whole energy and mass spectrum. Contrary to what happens at lower energies, where the influence of structural effects is more prominent, changes depending on the type of the nucleus or the reaction energy are minimal at the energies of interest. Therefore, with relatively large energy steps, it is conceivable to conduct a simple examination of a few regions of the periodic table of elements.

On the other hand, information on production rates and the properties of all reaction products (neutrons, charged particles, and nuclei) must be gathered if the goal is to effectively regulate the different phases of the mechanism. In actuality, event-by-event measurement of each of these goods would be optimal. Several experiments were conducted as part of European programmed that allowed for the coordination of outcomes. More specifically, the teams from the CEA contributed to the collection of data for measurements of residual nuclei at the GSI accelerator in Germany and neutron production on the SATURNE accelerator, which was shut down today (Fig. 19). Thanks to the reverse kinematics approach, which made it possible to quantify the recoil velocities of all the isotopes produced in a reaction at once, substantial advancements in the creation of residual nuclei could be made. This technique bombards liquid hydrogen with proton beams from heavy ions[10], [11].

The benefit is that since the center of mass virtually identifies with the projectile, the nuclei produced in this way are tightly focused in the forward direction.Thanks to a series of magnets and detectors, this makes it easier to identify reaction products. Measured isotope distributions at the GSI were especially useful in evaluating how nuclear models behaved when competing neutron and charged particle emission with fission. The GSI then conducted a second generation of experiments, still using reverse kinematics, that involve measuring a variety of reaction products at once, such as residues and light particles. These experiments provided access to nuclear properties before de-excitation and helped put distinct constraints on the cascade and de-excitation models.

Integral measurements

After the physics models have been included into the transport codes, it is necessary to test the latter on integral experiments to see how predictable the physical variables that are important for applications are. Then measurements are performed on targets that are a representation of a spallation target, known as "thick targets". For instance, a CERN experiment measuring volatile fission products on a thick lead-bismuth target verified that the new models are capable of reproducing the observed production rates to a large extent. Similar to this, models may reasonably simulate the energy spectrum of neutrons that escape from a thick target. This demonstrates that the predictions of high-energy neutron losses, which are crucial for understanding shielding and radiation protection issues, are adequately accurate.

The first full-scale test of a liquid-metal target like those envisaged for ADS was the lead-bismuth spallation target MEGAPIE, which was successfully irradiated for 4 months by the powerful proton beam of the SINQ source at the Paul Scherrer Institute in Zürich. A number of

specimens have been gathered and are undergoing examination after a time of decay, which will assist provide answers to queries about the residual nuclei produced and, subsequently, the material damage.

The foundationsof the transport equation

neutron propagation in a given medium is a member of a family of transport processes that includes phenomena like light (photon) propagation in stellar matter or the Earth's atmosphere, dynamics of rarefied gases, plasma physics, macromolecular orientation in space, and car traffic. The kinetic theory equations, which should not be confused with nuclear reactor kinetics equations, control these processes. We will discuss the main points of these two writers' presentation regarding the connection between the kinetic theory and the transport theory in the sections that follow since it shows an interest in re-connecting the transport equation with a broader context and understanding its roots. It also illustrates the connection between the stochastic and deterministic formulations of the transport issue by relating them to experimental observations of a relevant physical property.

Examples of kinetic theory equations are the Boltzmann equation and the neutron transport equation. The neutron transport equation is really a particular instance of the Boltzmann equation where a neutron "gas" is diffused in a nuclide "gas." Particles (such as gas molecules or neutrons) in neutron transport systems have mean free pathways that are much longer than the range of the interaction potential between the particles.

The Liouville equation, a more generic partial differential equation related to statistical mechanics, may be used to derive the Boltzmann equation, which is often directly proven. The Hamilton's equations serve as the foundation for this equation. Thus, the change from microscopic equations, which control the motion of each individual particle in a physical system, to the kinetic theory equations, which provide access to "mean" and thus measurably macroscopic values, is accomplished.The field known as Nonequilibrium Statistical Mechanic serves as the theoretical foundation for this shift from the microscopic to the macroscopic scale.

In order to solve the transport equation, the Monte-Carlo probabilistic method explicitly simulates the group of equivalent physical systems that were previously taken into account as part of the ergodic assumption. The simulation is then concluded with a statistical average of all the results produced by each of these simulations, much like a group of measurements that would be obtained and averaged within a strictly experimental framework. This average is a statistical evaluation of the relevant outcome. The microscopic level is maintained because it is possible to store, analyses, and retract the features (positions, energy, events) of the simulated history of each system's particles.

The deterministic technique, it should be noted, a priori provides the (mean) value of the physical quantity of interest at every point in the phase space. Due to a straightforward statistical explanation, this cannot really be the case with a realistic probabilistic simulation: the chance for two simulated particles to traverse the same place in space is almost zero.

Neutronics Fundamental Equations

The density of the neutron population is provided as a function of both time and space via the Boltzmann equation's solution. This equation also holds for photon transport, which is important for calculations involving radiation shielding and material heating in reactor research.When neutrons collide with nuclei, their quantum behaviors are on show, but to neutron physicists, these collisions may be seen as punctual, instantaneous occurrences, and only their effects are of interest. Numerous sorts of reactions may occur depending on the incoming neutron's energy and the nucleus it interacts with: the neutron may be absorbed, scattered, or it may cause nuclear fission. Remember that the microscopic cross section is a quantity that describes each reaction's probability. Neutrons act like classical particles between two collisions, and their location and speed may be used to explain these behaviors.They travel in a straight line when uncharged (as neutral particles), at least over short distances when the gravitational impact may be disregarded[12], [13].

CONCLUSION

Nuclear data processing is an essential stage in the analysis and use of nuclear data for different nuclear research and engineering applications. Accuracy and dependability in nuclear studies and simulations are guaranteed by proper nuclear data processing. Compiling, analyzing, and validating nuclear data, such as nuclear reaction cross-sections, decay data, and fission yields, are all part of nuclear data processing. To guarantee the consistency and quality of processed data, steps including benchmarking, interpolation, uncertainty propagation, and data formatting are crucial.

REFERENCES

[1] A. Alonso, S. Marsal, and A. Julià, “Analytical methods in untargeted metabolomics: State of the art in 2015,” Frontiers in Bioengineering and Biotechnology. 2015. doi: 10.3389/fbioe.2015.00023.

[2] J. Ollion, J. Cochennec, F. Loll, C. Escudé, and T. Boudier, “TANGO: A generic tool for high-throughput 3D image analysis for studying nuclear organization,” Bioinformatics, 2013, doi: 10.1093/bioinformatics/btt276.

[3] J. Stanstrup et al., “The metaRbolomics toolbox in bioconductor and beyond,” Metabolites. 2019. doi: 10.3390/metabo9100200.

[4] L. W. Sumner et al., “Proposed minimum reporting standards for chemical analysis: Chemical Analysis Working Group (CAWG) Metabolomics Standards Initiative (MSI),” Metabolomics, 2007, doi: 10.1007/s11306-007-0082-2.

[5] K. W. Dunn, C. Fu, D. J. Ho, S. Lee, S. Han, P. Salama, and E. J. Delp, “DeepSynth: Three-dimensional nuclear segmentation of biological images using neural networks trained with synthetic data,” Sci. Rep., 2019, doi: 10.1038/s41598-019-54244-5.

[6] M. E. Boutin, T. C. Voss, S. A. Titus, K. Cruz-Gutierrez, S. Michael, and M. Ferrer, “A high-throughput imaging and nuclear segmentation analysis protocol for cleared 3D culture models,” Sci. Rep., 2018, doi: 10.1038/s41598-018-29169-0.

[7] S. Roh, “Big Data Analysis of Public Acceptance of Nuclear Power in Korea,” Nucl. Eng. Technol., 2017, doi: 10.1016/j.net.2016.12.015.

[8] S. Rodríguez-Navarro, T. Fischer, M. J. Luo, O. Antúnez, S. Brettschneider, J. Lechner, J. E. Pérez-Ortín, R. Reed, and E. Hurt, “Sus1, a Functional Component of the SAGA Histone Acetylase Complex and the Nuclear Pore-Associated mRNA Export Machinery,” Cell, 2004, doi: 10.1016/S0092-8674(03)01025-0.

[9] B. Kesler, G. Li, A. Thiemicke, R. Venkat, and G. Neuert, “Automated cell boundary and 3D nuclear segmentation of cells in suspension,” Sci. Rep., 2019, doi: 10.1038/s41598-019-46689-5.

[10] C. Baejen, P. Torkler, S. Gressel, K. Essig, J. Söding, and P. Cramer, “Transcriptome Maps of mRNP Biogenesis Factors Define Pre-mRNA Recognition,” Mol. Cell, 2014, doi: 10.1016/j.molcel.2014.08.005.

[11] D. Franke, M. V. Petoukhov, P. V. Konarev, A. Panjkovich, A. Tuukkanen, H. D. T. Mertens, A. G. Kikhney, N. R. Hajizadeh, J. M. Franklin, C. M. Jeffries, and D. I. Svergun, “ATSAS 2.8: A comprehensive data analysis suite for small-angle scattering from macromolecular solutions,” J. Appl. Crystallogr., 2017, doi: 10.1107/S1600576717007786.

[12] M. Escolà Casas and V. Matamoros, “Analytical challenges and solutions for performing metabolomic analysis of root exudates,” Trends in Environmental Analytical Chemistry. 2021. doi: 10.1016/j.teac.2021.e00130.

[13] K. E. Haslauer, P. Schmitt-Kopplin, and S. S. Heinzmann, “Data processing optimization in untargeted metabolomics of urine using voigt lineshape model non-linear regression analysis,” Metabolites, 2021, doi: 10.3390/metabo11050285.

CHAPTER 12

DETERMINATION OF FISSIONABLE MATERIALS

Dr. Chikkahanumajja Naveen, Assistant Professor
Department of Engineering Physcis, Presidency University, Bangalore, India
Email Id-naveen@presidencyuniversity.in

ABSTRACT

Nuclear fission is the process through which energy is released, and fissionable materials are essential parts of nuclear reactors and nuclear weapons. Understanding the traits, attributes, and uses of fissionable materials is the main goal of this research. The study examines several fissionable substances, such as plutonium-239, uranium-235, and other fissile isotopes. To understand the behaviour and use of fissionable materials, key elements such as nuclear reactions, criticality, neutron interactions, and fuel cycle issues are examined. The study also looks at how fissionable materials are used to build weapons, research reactors, and nuclear power plants. For managing nuclear waste, maintaining safe and effective nuclear operations, and developing nuclear technologies, it is essential to have a solid understanding of fissionable materials.

KEYWORDS:

Fissionable Materials, Uranium-235, Plutonium-239, Fissile Isotopes, Nuclear Fission, Nuclear Reactions

INTRODUCTION

There are two types of fissionable isotopes: fertile and fissile. In a fissile material, incident neutrons of any energy lead to fission. The sole naturally occurring fissile material, uranium235, is shown in fission cross section. The threshold in uranium-238's fission cross section that only neutrons with an incoming energy of a MeV or more may cause uranium-238 to fission, which accounts for 99.3% of natural uranium. However, it is fertile because, after neutron capture, it decays according to fissile plutonium-239. The fission cross section of plutonium-239. In order to become plutonium-240, which is also a fertile isotope, plutonium-239 must acquire one extra neutron; otherwise, it will fission and become plutonium-241, which is fissile. Thorium-232 is another naturally occurring fertile isotope alongside uranium-238. It undergoes radioactive decay to produce the fissile isotope uranium-233 after neutron capture[1]–[3].

Neutron Scattering

The range of neutron energies in a reactor sits halfway between thermal equilibrium and fission. The conflict between scattering and absorption responses is a major determinant. While neutrons close to thermal equilibrium may either acquire or lose energy in their interactions with the

thermal movements of the surrounding medium, neutrons with energies much beyond the thermal range experience energy degradation as a consequence of scattering collisions. Neutron slowing down is the term used to describe the energy deterioration brought on by scattering.The neutron spectrum will be near to thermal equilibrium in a material where the average energy loss per collision and the ratio of scattering to absorption cross section is significant, and is therefore referred to as a soft or thermal spectrum.

In contrast, neutrons are absorbed in a system with tiny ratios of neutron degradation to absorption before there is a noticeable slowing down. The neutron spectrum is then referred to be hard or fast and is closer to the fission spectrum. We initially investigate elastic and then inelastic scattering to better comprehend neutron energy distributions on a quantitative level. Recall that mechanical energy is conserved in elastic scattering, meaning that the total kinetic energies of the target nucleus and the neutron are the same before and after the impact. In an excited, more energetic state known as inelastic scattering, the neutron departs the target nucleus. As a result, the amount of energy deposited to create the excited state causes the total of the neutron and nuclear kinetic energies to be lower than it was before the collision. In nuclear reactors, elastic and inelastic scattering play a significant role. First, we address elastic scattering[4]–[6].

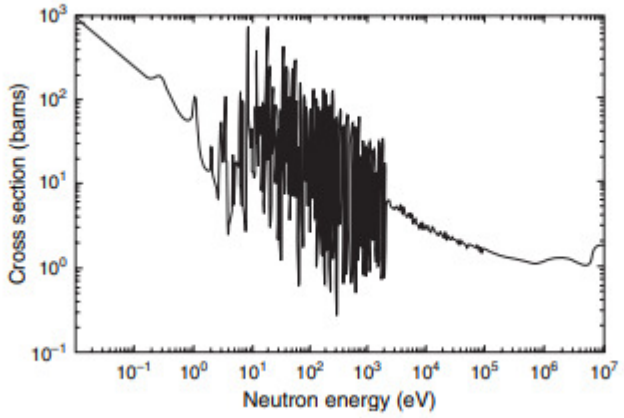

Figure 1: Represents the Microscopic fission cross sections of uranium-235.

Inelastic Scattering

For inelastic scattering, the situation is quite different. Over the whole spectrum of neutron energy, elastic scattering cross sections are important. However, heavy isotopes do not experience the substantial energy losses associated with low atomic weight nuclei, and as a result, their elastic scattering has little impact on reactor physics. In contrast, only neutrons with energies over a threshold that is a property of the target isotope may scatter inelastically, as was previously mentioned. Furthermore, these thresholds are so low that substantial inelastic scattering only happens with materials with a higher atomic weight, like uranium.

Neutrons lose a lot of energy due to inelastic scattering.The energies of inelastically scattered neutrons depend on the distinctive structure of energy levels that distinguishes each nuclide, The target nucleus must be raised to one of these states for the neutron to scatter inelastically, after

which it decays by generating one or more gamma rays. The neutron's energy loss is mostly influenced by the energy level of the state it excites, while the threshold for inelastic scattering is governed by the energy of the target nucleus's lowest excited state.

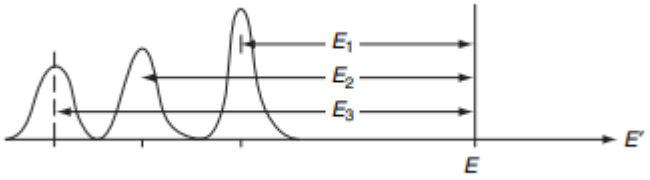

Figure 2: Represents the Inelastically scattered neutrons from energy E to E0.

levels E1, E2, or E3, the neutron would have energy E0 = E E1, E2, or E E3 after the inelastic scatter but as in elastic scattering, conservation of momentum dictates that a neutron deflected via a greater angle would lose more energy than one deflected through a smaller angle. As a result, the peaks are partly masked by energy. The spectrum of scattered neutrons may become highly complicated as the incoming neutron's energy rises if it can trigger a variety of states.

DISCUSSION

Neutron Distributions in Energy

The concept of neutron multiplication, defining it as,

$$k = \frac{\text{number of neutrons in } i\text{th} + 1 \text{ generation}}{\text{number of neutrons in } i\text{th generation}},$$

whereby a generation of neutrons is thought to be created via fission, travel through many scattering collisions, and perish in absorption collisions. The key to studying neutron chain reactions is to understand what controls the size of the multiplication. The fundamental informationthe neutron cross sectionsis extremely energy dependent. As such, this chapter investigates the factors that determine multiplication with a focus on the neutrons' kinetic energy. The two major categories of reactorsthermal and fastare defined by these energy dependencies. The characteristics of nuclear fuel and substances that reduce the neutron spectrum are covered first. With this background, we go on to describe the energy distributions of neutrons in nuclear reactors in greater depth before talking about the averaging of neutron cross sections over energy[7]–[9].

Nuclear Fuel Properties

The energy dependence of the cross sections of fissile and fertile materials over the range of incident neutron energies between the fission spectrum and the Maxwell-Boltzmann distribution of thermal neutronsroughly over the range between 10 MeV and 0.001 eVdetermines much of the physics of nuclear reactors. Remember that fissile nuclides have sizeable fission cross sections across this range, for uranium-235 and plutonium-239, respectively. Contrarily, a fertile material can only fission when incoming neutrons exceed a certain threshold; this threshold is

around 1.0 MeV for uranium-238. Not every neutron taken in by a fissile nucleus will result in fission.There will be some of those that are caught, and that portion also depends on energy. As a consequence, a key factor in calculating a reactor's neutron economy is the quantity of fission neutrons generated for each neutron absorbed:

$$\eta(E) = \frac{\nu\Sigma_f(E)}{\Sigma_a(E)} = \frac{\text{fission neutrons produced}}{\text{neutrons absorbed}},$$

The average value of eta must be much more than one in order to continue a chain reaction since, in a power reactor, neutrons will be lost due to absorption in structural, coolant, and other materials as well as some leakage out of the system.

To prevent the abrupt valley that "E" shows across intermediate energies, reactor designs must concentrate neutrons either in the fast or thermal energy range. Neutrons lose energy in scattering collisions until they attain equilibrium in the thermal neutron range, as is emphasized. As a result, fast reactor cores are designed to have as few components other than fuel as feasible.

They specifically steer clear of low atomic weight substances because elastic scattering in these substances rapidly lowers neutron energy to levels where resonance capture in uranium-238 predominates.However, even if all other components could be removed, a fast reactor powered by natural uranium is still not feasible because the neutrons produced by fission would fall into the intermediate energy range too soon due to the huge inelastic scattering cross section of the 99.3% uranium-238. As a result, fuels enriched to more than 10% are needed for fast reactors.

The scenario is the opposite for thermal reactors. A substantial amount of moderator, or low atomic weight material, must be present in the reactor. Its goal is to slow down neutrons beyond the valley in E, where there aren't many collisions, to the thermal energies, when the fuel's ratio of neutron production to absorption once again exceeds one by a significant amount. Thermal reactors may be constructed with substantially lower enrichments than fast reactors because to optimized moderator to fuel ratios. With various moderators, most notably graphite or heavy water, thermal reactors can even run on naturally occurring uranium.

Neutron Moderators

To avoid resonance capture of neutrons in uranium-238, moderator materials are needed in thermal reactors to lower neutron energy from the fission to the thermal range with as few collisions as feasible. Having a low atomic weight is necessary for a substance to function as a moderator. The slowing decrement, is only then high enough to slow neutrons down to thermal energy with just a small number of collisions. But a good moderator also has to have other qualities. It must have a sufficient macroscopic scattering cross section. Otherwise, despite the fact that a neutron interacting with it would lose a considerable amount of energy, there would be insufficient moderator collisions to significantly alter the neutron spectrum due to competition with other materials.

where the macroscopic scattering cross section is denoted by s 1/4 Ns. Keep in mind that N cannot be allowed to be too low. Gases are therefore removed. For instance, helium has

sufficiently high values of and s to be a useful moderator, but its number density is insufficient to have a major effect on the distribution of neutron energy in a reactor. In contrast, because they do not significantly alter the neutron spectrum, gases like helium may be considered as coolants for fast reactors for the same reason.

the three most frequent moderators' power decline and slowing. The slowing down ratio, or the ratio of a material's slowing down power to its heat absorption cross section, is also included in the table. A material cannot be used as a moderator if the thermal absorption cross section a thermal is large; even though it may be efficient at slowing down neutrons to thermal energy, it will absorb an excessive amount of those same neutrons before they can collide with the fuel and cause fission. Notably, graphite is the material with the slowing down ratio that is by far the highest, followed by ordinary water. It is possible to construct natural uranium-fueled power reactors with D_2O acting as the moderator. The design of naturally uranium-fueled power reactors moderated by graphite is a more challenging task since graphite has worse moderating qualities. Natural uranium cannot be used to power reactors with a light water moderator; some enrichment of the uranium is necessary to make up for the H_2O's greater heat absorption cross section.

Other materials that may act as moderators are ruled out by large heat absorption cross sections. For instance, the power and slowing down decrement of boron-10 are appropriate. But its cross section for heat absorption is around 4000 b. Because of this, boron cannot be employed as a moderator and is instead one of the more popular neutron "poisons" that are used to regulate or stop chain reactions.Since inelastic scattering often plays a significantly smaller role in defining the energy distribution of neutrons in thermal reactors, the discussion above has focused on elastic scattering.

The inelastic scattering cross sections of the lighter weight materials are either zero below a very high energy threshold or absent altogether. There is inelastic scattering over thresholds in the keV to MeV range for both fertile and fissile materials. In thermal reactors, inelastic collisions only slightly increase the rate at which elastic scattering slows down motion. Fast reactors experience a very different scenario because inelastic scattering is given more weight because of the lack of a moderator material. The main sources of unintended energy spectrum deterioration are inelastic scattering of the fuel and elastic scattering with the coolant and structural components.

Neutron Energy Spectra

the conflict between scattering and absorption processes is a major factor in the energy distribution of neutrons. While neutrons in thermal equilibrium have nearly equal chances of gaining or losing energy when interacting with the thermal motions of the nuclei that make up the surrounding medium, neutrons with energies significantly above the thermal range experience energy degradation as a result of scattering collisions. The neutron distribution in energy will be near to thermal equilibrium in a material for which the average energy loss per collision and the ratio of scattering to absorption cross section are both high, and is thus referred to as a soft or thermal spectrum. Neutrons are absorbed before there is a considerable slowing

down in a system with tiny ratios of neutron degradation to absorption, on the other hand. The neutron distribution is thus described as being hard or fast and is located closer to the fission spectrum.

The Power Reactor Core

The composition of a power reactor core is primarily determined by two factors: As fuel is used over the life of the core and throughout the range of needed power levels, criticality must be maintained.Additionally, the design must permit the passage of fission-generated thermal energy from the core without overheating any of its components. The mechanical support of the main structure, the stability and regulation of the chain reaction under a variety of conditions, and many other factors are also taken into account.

However, the building of power reactor cores is most heavily influenced by the interaction between heat transport and the neutron physics covered in the earlier chapters. The main designs of the most popular kinds of power reactors are initially examined in this chapter, along with the relationships between heat transfer and neutronic behaviours. The effect of the reactor lattice structures on the neutronic behaviours, particularly on the estimation of the multiplication, is then presented in greater depth[10]–[12].

CONCLUSION

Fissionable materials are essential elements in nuclear applications because they are crucial to the process of nuclear fission, which releases energy. For nuclear systems to operate safely and effectively, it is essential to understand the traits, qualities, and uses of fissionable materials.Large quantities of energy are released when fissionable substances, such as uranium-235, plutonium-239, and other fissile isotopes, undergo nuclear reactions and maintain a chain reaction to criticality. Neutron interactions, fuel cycle concerns, and other elements that affect the performance and use of fissionable materials all have an impact on their behaviors.

REFERENCES

[1] K. W. Bentley and J. H. Wyatt, “Quantitative determination of fissionable materials in human hair,” Environ. Res., 1980, doi: 10.1016/0013-9351(80)90044-4.

[2] A. Musilek, K. Buchtela, and F. Grass, “Determination of fissionable materials by simultaneous measurement of delayed neutrons and gamma-spectra,” J. Trace Microprobe Tech., 1996.

[3] S. R. Hashemi-Nezhad, I. V. Zhuk, A. S. Potapenko, and M. I. Krivopustov, “Calibration of track detectors for fission rate determination: An experimental and theoretical study,” Nucl. Instruments Methods Phys. Res. Sect. A Accel. Spectrometers, Detect. Assoc. Equip., 2006, doi: 10.1016/j.nima.2006.08.044.

[4] R. T. Kouzes, E. R. Siciliano, J. E. Tanner, and G. A. Warren, “Testing requirements for active interrogation systems,” Nucl. Instruments Methods Phys. Res. Sect. A Accel. Spectrometers, Detect. Assoc. Equip., 2019, doi: 10.1016/j.nima.2018.12.088.

[5] K. Boehnel, “Effect Of Multiplication On The Quantitative Determination Of Spontaneously Fissioning Isotopes By Neutron Correlation Analysis.,” Nucl. Sci. Eng., 1985, doi: 10.13182/nse85-2.

[6] P. De Bièvre, “Isotope dilution mass spectrometry (IDMS),” Tech. Instrum. Anal. Chem., 1994, doi: 10.1016/S0167-9244(08)70150-1.

[7] F. Mokhtari, “Mahmud ahamadinejad’s presidency: What does Iran really want?,” Am. Foreign Policy Interes., 2006, doi: 10.1080/10803920600957051.

[8] E. R. Gonzales, S. R. Garcia, C. Mahan, and W. Hang, “Evaluation of mass spectrometry and radiation detection for the analysis of radionuclides,” J. Radioanal. Nucl. Chem., 2005, doi: 10.1007/s10967-005-0076-3.

[9] G. Om. Ariavie and J. A. Akpob, “Determination of Temperature Distribution in a Nuclear Fuel Element Consisting of a Sphere of Fissionable Material and a Spherical Shell of Aluminum Cladding using Finite Element Method.,” Trans. Mach. Learn. Artif. Intell., 2014, doi: 10.14738/tmlai.26.628.

[10] V. A. Dmitrievskii and I. S. Grigorev, “Determination of critical mass and neutron flux distribution by means of physical models,” Sov. J. At. Energy, 1960, doi: 10.1007/BF01683108.

[11] A. Luca, “Experimental determination of the uranium enrichment ratio,” Rom. Reports Phys., 2008.

[12] H. A. Hassan and J. E. Deese, “Electron distribution function in a plasma generated by fission fragments,” Phys. Fluids, 1976, doi: 10.1063/1.861432.

CHAPTER 13

ANALYSIS OF TURBULENT TRANSPORT

Amit Kumar Sharma, Associate Professor
Department of Electronic Communication Engineering, Teerthanker Mahaveer University, Moradabad, Uttar Pradesh, India
Email id- amit_vashishtha1980@rediffmail.com

ABSTRACT:

From atmospheric dynamics to heat transfer in industrial systems, turbulent transport is essential to many natural and manmade processes. The primary goal of this study is to investigate the fundamental properties of turbulent transport, including its mechanisms, modelling strategies, and applications. The investigation looks at important phenomena like eddy diffusion, turbulent mixing, and how turbulence affects scalar values. The many numerical approaches and experimental approaches used to study turbulent transport are also covered. The findings emphasize the complexity of turbulence and the requirement for precise modelling and prediction techniques in order to comprehend and regulate transport processes in turbulent flows.

KEYWORDS:

Turbulent Transport, Eddy Diffusion, Turbulent Mixing, Scalar Quantities, Numerical Techniques, Experimental Methods.

INTRODUCTION

Fusion devices must necessarily be in an inhomogeneous state in order to contain hot, dense plasmas and prevent boundary damage from excessive heat. These high temperature plasmas that are magnetically boundary are not only subject to a variety of linear instabilities with varying wavelengths and complicated frequencies, but frequently non-linearly self-organize into states that are more favorable from an energy standpoint.A disruption occurs when a large scale MHD instability becomes highly unstable and can terminate a tokamak plasma by tossing it against the wall. Tokamak transport is typically anomalous, which indicates that the transport rate is significantly higher than predicted by theories based on Coulomb collisions, even in the absence of large scale MHD instabilities. Small scale collective instabilities, which are frequently fueled by gradients in temperature, density, and other factors, are what lead to this anomalous transport. Due to non-linear causes, these micro instabilities saturate at low amplitude. As a result of varying electric fields, particles E B float radially in an unpredictable manner. Plasmas leave a tokamak's interior in this manner[1]–[3].

Large scale gyrokinetic simulations are now able to replicate these tokamak microturbulence features. For instance, is an output from a shaping-capable Gyrokinetic Tokamak Simulation (GTS) code simulation of ion temperature gradient (ITG) driven turbulence. According to density fluctuation contours in the presence of self-generated zonal flows, the average

turbulence eddy size is close to several ion gyroradi across the magnetic field, and the fluctuation is almost parallel to the magnetic field with a parallel wavelength of the order of the connection length. A tokamak plasma's microturbulence is made up of several modes or eddies that interact with one another nonlinearly. The expansion of the free energy source contained in n, i, or eT is what causes the small-scale linear instabilities, also known as micro instabilities. This free energy should be available for waves to tap in order to make collective waves unstable.Including reactive mechanisms like poor magnetic curvature and negative compressibility, as well as wave-particle resonance. According to the diversity of the free energy source, accessibility mechanism, and magnetic geometry of a system, micro instabilities can be categorized into several modes. Then, we explore possibilities that are currently thought to be of experimental relevance in both current and future fusion devices in this part after illustrating a few simple instances. We restrict our discussion to el6ectrostatic fluctuations due to severe space constraints.

The collision less drift wave, which is excited by the inverse Landau damping on electrons, and the collisional drift wave, which becomes unstable due to Coulomb collisions of electrons on either electrons or ions, can be classified according to the electron dissipation mechanism. The collision less electron drift instability is frequently referred to as the "universal instability" since it can happen even in the absence of collisions when there is a density gradient, which is a need in magnetically confined plasmas.The linear stability of this unive6rsal instability in a sheared magnetic field has been a topic of the highest theoretical interest since the ion Landau damping when kinetic effects are incorporated in the ion response in has a stabilizing effect until the late 1970s. Although "stability" was the operative word in a sheared slab geometry, it is now thought that collision less drift waves can become unstable in a toroidal geometry, with trapped electron precession-wave resonance serving as a more potent destabilizing mechanism in place of the inverse Landau damping of passing electrons[4], [5].

Non-linear gyrokinetic equations for tokamak turbulence

the fundamentals of the non-linear gyrokinetic equation in preparation for more in-depth considerations of micro instabilities and turbulence driven transport in the next sections. The direct simulation of actual-size fusion plasmas in realistic geometry using simple non-linear plasma equations like the Klimontovich or Vlasov equations is still far beyond the computational capability of even the foreseeable future, despite the enormous increase in computing power in recent years. Thus, to make the fundamental dynamical equations simpler, simplified equations have been used. In this section, we go over the fundamental steps in the derivations of the non-linear gyrokinetic equations, which are now widely employed in a variety of turbulence research in magnetically confined plasmas, from the most basic, the Vlasov equation. Our discussion is focused on collision less plasmas, where E and B are the electric and magnetic fields generated by particle motion and satisfied by Maxwell's equations. This set of equations is capable of describing a variety of occurrences at many different spatiotemporal scales. For example, to examine plasma heating by waves, precise representations of particle dynamics in the presence of high frequency electromagnetic waves are required

The wavelengths and correlation lengths of such fluctuations are much smaller than the size of the device or the scale length of the magnetic field inhomogeneity, while the timescales of

collective electromagnetic fluctuations of interest are much longer than the period of a charged particle's cyclotron motion (gyromotion) for turbulence and transport issues in magnetically confined plasmas. In these conditions, the specifics of the charged particle's gyration motion are not of physical interest, hence it is preferable to develop a more condensed set of dynamical equations while maintaining the ability to capture the key characteristics of the low frequency phenomena that are relevant to practical applications. One can obtain the gyrokinetic equation, which characterizes the spatio-temporal evolution of the gyrocentre distribution function and is independent of the gyrophase, by decoupling the gyromotion. This equation is specified over a five-dimensional phase space (R, v,). By using a time step that is larger than the gyroperiod and fewer dynamical variables while simulating strongly magnetized plasmas, one can therefore significantly reduce the amount of computer time required. We observe that in the gyrokinetic method, the magnitude of the perpendicular velocity enters as a parameter in terms of an adiabatic invariant (2 v / 2 B), and the gyrophase is an ignorable coordinate. An adiabatic invariant with this leading term does not change for each particle.

DISCUSSION

The focus of traditional simulations and formulations has been on tokamak core turbulence, which has relatively small fluctuation amplitudes (the relative density fluctuation amplitude is less than 1%), mild gradients in macroscopic parameters (such as pressure), and characteristic lengths of the order of a fraction of the minor radius.

Three expansion parameters are present in the non-linear gyrokinetic theory: / ci, B, and 0 / / e, f, and T, where ci, B, and t characterize the slow timescale associated with turbulence, weak inhomogeneity of the equilibrium magnetic field, and low relative amplitude of fluctuations, respectively. The traditional gyrokinetic theory makes the assumption that all three parameters are equivalent in formal ordering; however, in particular situations, such as plasmas with transport barriers this assumption needs to be adjusted. The parallel wavelength of the fluctuation is comparable to the connection length of the system, qR, whereas the perpendicular wavelength can be comparable to the gyroradius in the non-linear gyrokinetic ordering. As a result, the ordering matches the sp[6], [7].

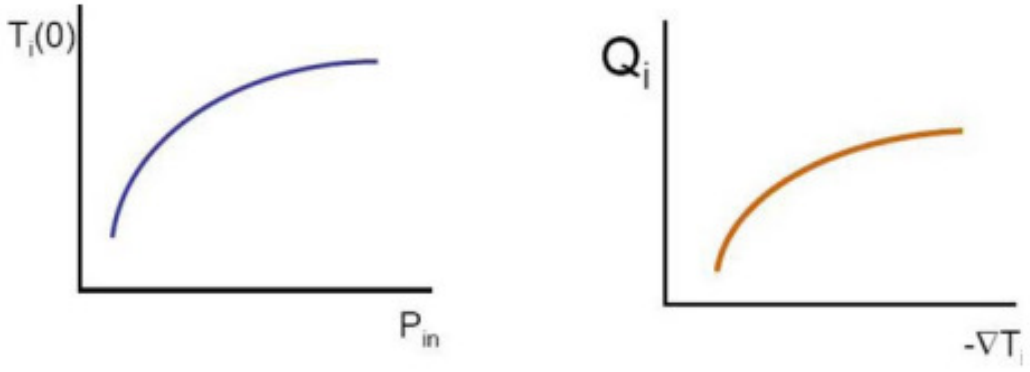

Figure 1: Represents the Ion temperature Ti as a function of heating power Pin, and heat flux Qi.

Different channels of turbulence transport

High ion temperature is one of the main objectives of tokamak fusion research. The center ion temperature is typically plotted by experimentalists as a function of the heating power Theoreticians, on the other hand, like to view the plasma confinement issue in terms of the flux-gradient relation, which is well-known from Fick's law in thermodynamics. For instance, the ion heat flux as a function of temperature gradient.There are numerous sources of free energy for instabilities and transport in confined plasmas. These include the toroidal rotation, density, and radial gradients of ion, electron, and atomic temperature. A generalized flux-gradient-relation can be formally expressed as a matrix. We observe that the gradients of other quantities can also influence the radial flux of each quantity, in addition to the radial gradient of that particular amount. The diffusive term refers to the diagonal term's contribution to the transport matrix. The non-diffusive flux is the phrase used to describe the contributions made by the off-diagonal terms. Some of these are colloquially referred to as the convective flux or the pinch term.

Ion thermal transport

Compared to other transport channels, ion thermal transport is currently better understood. Atypical levels of ion thermal transport that are significantly higher than those predicted by neoclassical collisional transport theory have been seen in auxiliary heated plasmas. The most likely explanation for the anomalous ion thermal transport is ion temperature gradient driven turbulence.

In tokamak experiments, the linear threshold of ITG instability is also of great practical interest. This is due to the fact that very unstable ITG modes can generate substantial amounts of radial ion heat flow, which lowers the local ion temperature gradient. This leads to ion temperature profiles that do not appreciably differ from the onset condition when combined with a competing effect brought on by ion heat deposition (for example, via neutral beam injection (NBI) or ion cyclotron resonance heating (ICRH)). Several gyrokinetic codes can be used to accurately calculate this onset condition. You can find a parametrization of many dependencies for example. Theoretically, "the onset condition" is further altered by the burst behavior of a driven system towards 6 and the E B zonal fluxes For simple examples, theoretical predictions from several gyrokinetic codes start to agree, both numerically and in terms of the underlying non-linear physics mechanisms. The zonal flow-induced upshift of the ITG onset condition is a notable example.

A paradigm shift from the drift wave-turbulence problem to the drift wave-zonal flow system problem has occurred in the tokamak turbulence theory community over the past ten years as a result of the recognition of the significance of zonal flows [2.51]. Zonal flows have been seen in numerous gyrokinetic models and can be found in nature, such as on Jupiter and the Sun. Many theorists think they ought to be present in ITER plasmas as well. A zonal flow is an E B flow that is toroidally symmetric, poloidally symmetric, and radially variable. In Fig. 33 of Ref. [2.51], the interaction between zonal flows and drift wave turbulence is graphically depicted. The collisional friction between trapped and moving ions can be used to dampen zonal fluxes [2.130]. Additionally, zonal flows control turbulence by E B shearing [2.110-2.112].

The zonal flows' critical responsibilities in defining the transport scalings with regard to important dimensionless parameters are then illustrated in a few cases. Since we want to know by how much future larger machines will perform better than the current ones, transport scaling with respect to machine size, or / i a , is crucial. Our predictions changed as our knowledge of ITG turbulence expanded. It appeared that Bohm scaling would be possible based on theoretical predictions of toroidal ITG instabilities in the early 1980s and of their global radial structures in the early 1990s.

Numerous research on zonal flows conducted starting in the middle of the 1990s have shown that the radially extended global ITG eigenmodes are split up into smaller eddies by zonal flows Most people naturally anticipated gyroBohm scaling from the eddy size scaling. A moderate system size can result in non-negligible deviations from gyroBohm scaling, according to more recent evidence from global gyrokinetic simulations This could happen as a result of turbulence entering the linearly stable zone The research on turbulence spreading dates at least to the middle of the 1990s.

One of the unsolved mysteries of ion thermal transport is plasma current scaling of confinement, =rom zonal flow features that depend on the q value, it is possible to derive the q dependence of the transport. Geodesic acoustic modes (GAMs) can only exist in a high-q region because of their Landau damping. Therefore, only motionless zonal flows will last in a low-q area. Because of their relatively high frequency of oscillation, GAMs are not very successful at reducing turbulence Therefore, in the low-q area, where static zonal flow is dominant, we anticipate less turbulence. The ion heat flux from ITG turbulence is lower for the scenario with lower q, since the stationary zonal flows predominate, as demonstrated by a recent non-linear gyrofluid simulation A separate gyrokinetic simulation]6supports this.However, it still has to be shown how this mechanism relates to experiments.

Electron thermal transport

Since many years ago, it has been well known that anomalous electron thermal transport has been present in all operational modes of tokamaks and spherical tori.There is proof that tokamak electron temperature profiles are rigid.This is a possibility that has been suggested by perturbative transport experiments, such as the propagation of heat pulses, and the requirement for an inward heat squeeze factor in the transport analysis of auxiliary heated plasmas. The trapped electron mode (TEM), the ITG mode with trapped electrons, the electron temperature gradient (ETG) mode, and magnetic flutter-driven transport are a few theoretical contenders for electron thermal transport.

Starting with the TEM, it can generate an experimentally relevant electron thermal diffusivity when highly turbulent. It's intriguing to note that DTEM-based non-linear theory [2.140] can yield an electron thermal diffusivity scaling of e that is quite similar to the Neo-Alcator scaling that has been widely seen in numerous ohmically heated tokamak plasmas. The ASDEX-Upgrade ECH experiment provides a TEM-supporting finding. The transport exhibits a threshold behavior that is consistent with the prediction of the TEM theory. Additionally, as functions of the electron temperature gradient, the experimentally measured heat flow and the estimated TEM

linear growth rate exhibit a comparable trend [2.141]. On the other hand, as stated in Section 2.6.2, there is not much evidence of TEM-like variations from measurements[8], [9].

The ETG turbulence is a different contender. Even while low-k fluctuations in some spherical torus plasmas, like NSTX, are thought to be linearly stable, electron transport in these systems is very abnormal. Most of the heating energy from the energetic particles flows to electrons in NSTX neutral beam heated plasmas which is similar to the condition anticipated for ITER. The high E B shearing rate is projected to make low-k variations stable, leaving only high-k ETG modes unstable, according to the linear stability study.

It should be noted that the ion thermal diffusivity decreased to a level consistent with neoclassical theory, qualitatively supporting the stabilization of low-k ITG/TEM modes. NSTX is a great area to seek for ETG-like fluctuations with strong spatial resolution because of its low magnetic field and resulting large electron gyroradius. The existence of density fluctuations in the ETG spectral range is in fact supported by recent developments in experimental measurements utilizing high-k tangential scattering[10], [11].

CONCLUSION

A variety of natural and industrial processes depend on the complicated and widespread phenomena of turbulent movement. This work provided a thorough overview of turbulent transport, illuminating its underlying principles, modelling strategies, and useful applications. The study of important phenomena, including as turbulent mixing and eddy diffusion, has shed light on the complexities of turbulence and how it affects transport systems.

Additionally, the discussion of computational methods and experimental methodologies has brought to light the variety of ways used to research and comprehend turbulent transport.

REFERENCES

[1] G. S. Sidharth and J. R. Ristorcelli, “Lagrangian analysis for turbulent transport in variable-density turbulence,” Phys. Rev. Fluids, 2021, doi: 10.1103/PhysRevFluids.6.023202.

[2] Q. XIE, Z. REN, K. WANG, H. LIN, S. SHANG, and W. XIAO, “A forced ignition probability analysis method using kernel formation analysis with turbulent transport and Lagrangian flame particle tracking,” Chinese J. Aeronaut., 2021, doi: 10.1016/j.cja.2020.08.023.

[3] J. Jiang, T. Wu, H. Li, M. Sun, and B. Zhang, “Analysis of turbulent transport characteristic in hydrogen diffusion flames using direct numerical simulation,” Numer. Heat Transf. Part A Appl., 2020, doi: 10.1080/10407782.2020.1784678.

[4] A. Ishizawa, Y. Kishimoto, T. H. Watanabe, H. Sugama, K. Tanaka, S. Satake, S. Kobayashi, K. Nagasaki, and Y. Nakamura, “Multi-machine analysis of turbulent transport in helical systems via gyrokinetic simulation,” Nucl. Fusion, 2017, doi: 10.1088/1741-4326/aa6603.

[5] R. Coosemans, W. Dekeyser, and M. Baelmans, “Bayesian analysis of turbulent transport coefficients in 2D interchange dominated ExB turbulence involving flow shear,” 2021. doi: 10.1088/1742-6596/1785/1/012001.

[6] F. C. Li, Y. Kawaguchi, and K. Hishida, “Structural analysis of turbulent transport in a heated drag-reducing channel flow with surfactant additives,” Int. J. Heat Mass Transf., 2005, doi: 10.1016/j.ijheatmasstransfer.2004.09.029.

[7] M. Lafouti and M. Ghoranneviss, “MF-DFA Analysis of Turbulent Transport Measured by a Multipurpose Probe,” Chinese Phys. Lett., 2015, doi: 10.1088/0256-307X/32/10/105201.

[8] O. Schilling and N. J. Mueschke, “Analysis of turbulent transport and mixing in transitional Rayleigh-Taylor unstable flow using direct numerical simulation data,” Phys. Fluids, 2010, doi: 10.1063/1.3484247.

[9] D. Chatterjee and S. Chakraborty, “Entropy generation analysis of turbulent transport in laser surface alloying process,” Mater. Sci. Technol., 2006, doi: 10.1179/174328406X83978.

[10] N. Chakraborty, D. Chatterjee, and S. Chakraborty, “A scaling analysis of turbulent transport in laser surface alloying process,” J. Appl. Phys., 2004, doi: 10.1063/1.1790061.

[11] B. S. Lin, C. C. Chang, and C. T. Wang, “Renormalization group analysis for thermal turbulent transport,” Phys. Rev. E - Stat. Nonlinear, Soft Matter Phys., 2001, doi: 10.1103/PhysRevE.63.016304.

CHAPTER 14

DETERMINATIONS OF PARTICLE TRANSPORT

Ajay Kumar Upadhyay, Associate Professor
Department of Electronic Communication Engineering, Teerthanker Mahaveer University, Moradabad, Uttar Pradesh, India
Email id- ajay_kup@gmail.com

ABSTRACT:

Particle transport plays a crucial role in various fields of science and engineering, ranging from environmental studies to industrial processes. Understanding and characterizing the mechanisms of particle transport are essential for predicting and mitigating the effects of particle dispersion, contamination, and deposition. This study aims to investigate the determinants of particle transport through a comprehensive analysis of the underlying processes and factors influencing particle movement. Through a combination of experimental measurements, theoretical modeling, and numerical simulations, this research explores the interactions between particles and their surrounding environment, including fluid flow patterns, particle size, shape, and composition, as well as environmental conditions such as temperature, pressure, and humidity. The findings of this study are expected to contribute to the development of accurate predictive models and efficient strategies for particle transport control in various applications, enabling advancements in environmental protection, industrial processes, and healthcare technologies.

KEYWORDS:

Contamination, Deposition, Determinations, Environmental, Keywords.

INTRODUCTION

The majority of the time, particle transport is also anomalous, however its corresponding diffusion coefficient is frequently lower than that of ion thermal or electron thermal transport. Even though the particle source is merely at the edge, centrally peaked electron density profiles have been seen in numerous experiments. Theoretical studies on an inward convective flux (pinch) of particles have been driven by this. The particle flux can be expressed as followsi.e. as the product of a convective flux proportional to a pinch velocity v pinch and diffusion **(the** first term), a collisional process involving magnetically confined particles may result in an inward squeeze of particles[1].

$$\Gamma = -D\frac{\partial n}{\partial r} + nv_{pinch}$$

Density peaking in certain tokamak cores may be attributed to the Ware squeeze [, although there are several instances that contradict this, including ones in which there isn't an inductive electric field The shape of makes it obvious that eT or eB, or magnetic field inhomogeneity, may

generate an electron particle pinch. The first kind of pinch is known as a thermoelectric pinch, which makes sense, whereas the second type is known as a turbulent equipartition (TEP) pinch which we briefly describe[2], [3].

Momentum transport666

The importance of plasma rotation in magnetic confinement is now well acknowledged. Turbulence and transport may be reduced by E B shear, and in Microturbulence may produce turn rotation by Reynolds stress. Instabilities caused by MHD, such as resistive wall modes, may be stabilized, but they can also be dampened by non-axisymmetric magnetic fields. Additionally, energe6tic particles interact with the radial electric field. Thus, it is crucial to comprehend momentum conveyance. We specifically want to know whether ITER will have enough wave and neutral beam power to create enough rotation to reduce turbulence and transport and stabilise resistive wall modes in order for ITER to operate successfully.

6In the past, it has been predicted and shown that momentum diffusivity is quite near to ion thermal diffusivity. But more recent tokamak tests showed that there may be large deviations from unity in the ratio between these two values. This may imply that the momentum flow has an off-diagonal component, as shown in the careful experimental tests [2.160]. Indeed, modulation experiments have shown that a momentum pinch exists. It's also vital to remember that fluctuation measurements show a connection between plasma rotation and Reynolds stress[4].

Nearly all tokamaks have shown intrinsic toroidal rotation in the absence of an external torque input from neutral beams . The behavior of L-mode plasmas is still complicated and intimately related to fluxes in the scrape-off layer 6. 6On the other hand, Hmode plasmas exhibit straightforward empirical tendencies that are encapsulated by the Rice scaling In H-mode plasmas, toroidal rotation rises with more stored energy and decreases with plasma current. It rotates in the co-current direction. These findings seem to support the idea that rotation starts near the transition's edge and moves inside from there.

Different physical processes, such as wave-particle resonance, may cause a pinch. This section covers the two-part toroidal momentum squeeze induced by curvature. The E B flow is no longer incompressible in a torus, leading to the formation of the turbulent equipartition (TEP) pinch, which is the first component. This is the basic and reliable portion. The thermoelectric pinch, which is mode dependent and responsive to turbulence features, makes up the second component. The particle pinch on a slab with an inhomogeneous B field in the preceding section serves as a good example of the physics of the TEP pinch[5].

An effective squeeze in the observable physical amount n results from mixing the locally preserved, magnetically weighted quantity n / B. What about momentum, then? One may demonstrate that the magnetically weighted angular momentum 2 nu R B/ is convicted by the turbulent E B flow by starting with the angular momentum density conservation and utilizing the E B flow compressibility. By doing a quasi-linear computation, we may get an inward pinch in the observed amount nu as a result of mixing and diffusion of the magnetically weighted quantity 2 nu R B/. 6 The TEP pinch term may be found by dividing the radial gradients of this expression into two halves. If we define the momentum diffusivity with regard to the angular rotation

frequency, the resultant pinch velocity, normalized to the momentum diffusivity, is -4/R. The conservative gyrokinetic equation may also be used to arrive to same conclusions. The symmetry breakdown in this toroidal pinch is caused by the inflating fluct[6]–[8].

A thermodynamic component of the Reynolds stress linked to ion temperature changes is the thermoelectric pinch. It is based on mode properties, namely the phase angle between i, T, and. Additionally, it is sensitive to the gyrofluid approximation, the dispersion relation employed in the derivation, and the near to the marginality. The aforementioned curvature-driven momentum pinch is attributed to terms linked to the Coriolis pinch force by an independent formulation in the rotating frame.

Momentum may be exchanged between particles and waves, in contrast to the particle transport issue where particle number is preserved and the pinch is the sole off-diagonal flow. The last item in Eq. (2.97), residual stress, may result from this =The resting plasma may be accelerated because the residual stress might contribute in a net way after radial integration from the plasma border. As a result, an intrinsic rotation may be produced by the residual stress operating with the proper boundary condition We need a broken symmetry in the turbulence in order to have a limited residual stress. The crucial aspect of residual stress is how E B shear, via an asymmetry in the transfer of wave to particle momentum, transforms poloidal rotation shear into toroidal rotation shear. As stated by numerous writers this asymmetry may be achieved by having a finite E B shear and generic drift acoustic coupling, which will shift the eigenmode in the radial direction and provide a preferred sign of k. A directional imbalance in the acoustic wave populations and in the profile of momentum deposition by ion Landau damping is the fundamental physical process driving the residual stress.

An early theory of the H-mode, which was based on mechanism, was inspired by the discovery of the H-mode in a diverted tokamak It was pronounced when s becomes very high at the edge, either just inside the last closed flux surface of the diverted tokamak plasma or as a result of current rampdown. Numerous linear stability evaluations on different micro instabilities that address impact have been conducted bare taken into consideration in non-linear simulations of flux tube geometry Although the "ballooning representation" is not appropriate for low mode number fluctuations or near min q of reversed shear plasmas, it is strongly connected to th66e quasi-translational lattice symmetry. Due to this, these simulations conclude that reversed magnetic shear (through mechanism) is preferable to low magnetic shear (via mechanism), which should be more prominent for low mode number fluctuations, for transport reduction.

DISCUSSION

Due to a lack of radial overlap (discontinuity) of poloidal harmonics, ber fluctuations notice transport decrease close to min q an independent global gyrokinetic simulation shows that when additional modes are introduced, this effect weakens and transport tunnels through the min q surface. All of the aforementioned impacts related to q profiles were addressed in a research based on global fluid simulations of ITG turbulence however sub-ion-gyroradius-scale high mode number fluctuations were not taken into account. In general, it may be said that an ITB can develop most readily at the minimum q of RS plasmas, particularly when minimum q is close to

a low order rational value because of the rarefaction of rational q surfaces. When the value of min q is close to a low order rational number, ITB creation near min q occurs, but this does not necessarily mean that mechanism (iii) is to blame. In more recent gyrokinetic simulations, zonal flows powered by turbulence were shown to preferentially form close to gaps in the density of rational surfaces that were localized close to min q Analytic theory has also made the observation that low mode number electrostatic convective cells could be crucial in the mean profile flattening localised to the low-q surface as a transition precursor shown in experiment. Internal transport barriers in RS plasmas in DIII-D and type II ERS transitions in TFTR that happen close to min q when its value goes close to 2 might both be caused by these effects. The JET team's nd the ASDEX-Upgrade team's theories that localized velocity is produced by MHD instability and a loss of rapid ions are further theoretical hypotheses that support the critical function of low order rational q surfaces[9]–[11].

On the other hand, recent results from NSTX experiments seem to support the idea that while electron thermal transport barriers are located where the (negative) magnetic shear minimum is, or where the negative magnetic shear is strongest, ions are formed in the region where the E B shearing rate is a minimum. In various tokamaks, notably JET it has previously been noted that an electron barrier appears for negative magnetic shear. The period of internal barrier creation exhibits minimal link with either the value of min q or the value of (the negative) magnetic shear, according to an investigation of the Tore-Supra plasmas, which is a perplexing finding The central q value, q(0), crossing a low order rational value through time corresponds with it. In conclusion, there are several theoretical and experimental discoveries on the function of the q profile in the establishment of transport barriers.

The threshold particle flow for the forward (RS to ERS, or L to H) and the reverse (ERS to RS, or H to L) transitions are defined, respectively, by the local minimum (at a larger density gradient). Consequently, the issue demonstrates hysteresis.However, a recent theoretical advancement suggests that the hysteresis is overpredicted by the above straightforward example. In contrast to DIII-D, several tokamaks claim that the L-H and H-L transitions don't exhibit considerable hysteresis. The information from C-Mod Hmode plasmas is promising.

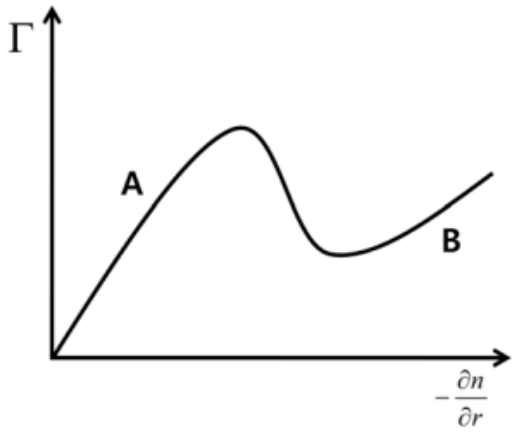

Figure 1: Represents the Particle flux as a function of density gradient.

Light Water Reactors

Ordinary water is used as a coolant and moderator in boiling water reactors (BWRs) and pressurized water reactors (PWRs). Both of these light water reactor (LWR) types make use of square lattice cells, a. In the fuel is uranium.Zirconium-clad dioxide pellets that serve as structural reinforcement and prevent fission products from leaking into the coolant. A 2:1 ratio between the fuel and the moderator is close to being ideal for maximizing k1 in water-moderated systems. The water's neutron slowing down characteristics, which are stated are what determine the ideal volume ratio. Due to hydrogen's low mass and wide scattering cross section, water has the highest slowing power of any moderator.

But of the moderators mentioned, water also has the biggest heat absorption cross section, which is reflected in the lowest value of the slowing down ratio. Despite the fact that water is great at slowing down neutrons, increasing heat absorption in the moderator caus6es an unacceptably significant drop in k1 if higher water to fuel volume ratios is used in reactor lattices. LWR designs with moderator to fuel volume ratios that are far lower than those seen in heavy water or graphite-moderated reactors are made possible by water's combination of having the biggest slowing down power but the lowest slowing down ratio of any of the moderators.

PWRs and BWRs have the most compact lattices of all the thermal reactors due to these smaller ratios and the fact that water acts as both a moderator and a coolant, compared to heavy water reactors or graphite-moderated systems of equivalent power, the moderator to fuel volume ratio results in better power densities and lower reactor sizes. However, obtaining criticality with natural uranium fuel in a LWR is impossible because to the huge heat absorption cross section of water.Water-moderated reactors must use slightly enriched fuel, often between 2% and 5%, to get around this problem.

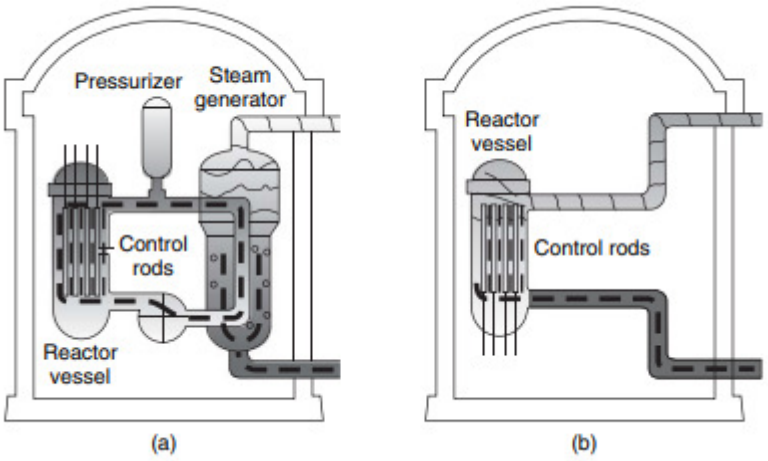

Figure 2: Represent the Light water-cooled reactors.

In PWRs, the core is housed in a vessel that is pressurized to 1520 bar (about 2200 psi) in order to prevent coolant from boiling at operational temperatures of around 316 C (about 600 F). , water that leaves the core is pumped back to the core intake after passing through heat

exchangers known as steam generators. The steam generator's secondary side runs at a lower pressure, causing feed water to scald as it enters and produce steam for the turbine. For BWRs, coolant temperatures are comparable. However, they run at less intense pressures of 690 bar (about 1000 psi), which permits boiling to occur in the coolant channels, BWRs do not need steam generators since the feed water enters the reactor vessel directly and the steam produced there goes directly to the turbine.

REFERENCES

[1] E. J. Davies and R. Nepstad, "In situ characterisation of complex suspended particulates surrounding an active submarine tailings placement site in a Norwegian fjord," *Reg. Stud. Mar. Sci.*, 2017, doi: 10.1016/j.rsma.2017.09.008.

[2] K.w. Gentle, O. Gehre, and K. Krieger, "Determination of particle transport coefficients in ASDEX by gas modulation," *Nucl. Fusion*, 1992, doi: 10.1088/0029-5515/32/2/I03.

[3] H. Takenaga, K. Nagashima, A. Sakasai, T. Oikawa, and T. Fujita, "Determination of particle transport coefficients in reversed shear plasma of JT-60U," *Plasma Phys. Control. Fusion*, 1998, doi: 10.1088/0741-3335/40/2/002.

[4] S. Perri, G. Zimbardo, F. Effenberger, and H. Fichtner, "Parameter estimation of superdiffusive motion of energetic particles upstream of heliospheric shocks," *Astron. Astrophys.*, 2015, doi: 10.1051/0004-6361/201425295.

[5] M. Loula, A. Kaňa, R. Koplík, J. Hanuš, M. Vosmanská, and O. Mestek, "Analysis of Silver Nanoparticles Using Single-Particle Inductively Coupled Plasma–Mass Spectrometry (ICP-MS): Parameters Affecting the Quality of Results," *Anal. Lett.*, 2019, doi: 10.1080/00032719.2018.1459657.

[6] S. Maghami, M. Sadeghi, A. Mehrabani□Zeinabad, and M. Simiari, "Determination of maximum possible contribution of porous particles in gas transport properties of their corresponding mixed matrix membranes," *SPE Polym.*, 2020, doi: 10.1002/pls2.10024.

[7] H. Qian, M. P. Sheetz, and E. L. Elson, "Single particle tracking. Analysis of diffusion and flow in two-dimensional systems," *Biophys. J.*, 1991, doi: 10.1016/S0006-3495(91)82125-7.

[8] D. Azarnykh, S. Litvinov, X. Bian, and N. A. Adams, "Determination of macroscopic transport coefficients of a dissipative particle dynamics solvent," *Phys. Rev. E*, 2016, doi: 10.1103/PhysRevE.93.013302.

[9] C. Robert, H. Dery, L. Ren, D. Van Tuan, E. Courtade, M. Yang, B. Urbaszek, D. Lagarde, K. Watanabe, T. Taniguchi, T. Amand, and X. Marie, "Measurement of Conduction and Valence Bands g -Factors in a Transition Metal Dichalcogenide Monolayer," *Phys. Rev. Lett.*, 2021, doi: 10.1103/PhysRevLett.126.067403.

[10] D. Edelin, P. C. Czujko, C. Castelain, C. Josset, and F. Fayolle, "Experimental determination of the energy optimum for the transport of floating particles in pipes," *Exp. Therm. Fluid Sci.*, 2015, doi: 10.1016/j.expthermflusci.2015.06.018.

[11] S. Cuello-Nuñez, I. Abad-Álvaro, D. Bartczak, M. E. Del Castillo Busto, D. A. Ramsay,

F. Pellegrino, and H. Goenaga-Infante, "The accurate determination of number concentration of inorganic nanoparticles using spICP-MS with the dynamic mass flow approach," *J. Anal. At. Spectrom.*, 2020, doi: 10.1039/c9ja00415g.

CHAPTER 15

DETERMINATION OF HEAVY WATER REACTOR

Pavan Kumar Singh, Assistant Professor
Department of Electronic Communication Engineering, Teerthanker Mahaveer University, Moradabad, Uttar Pradesh, India
Email id- om.pavansingh@gmail.com

ABSTRACT:

The determination of heavy water reactor (HWR) characteristics is essential for understanding and optimizing its performance in nuclear power generation. This study focuses on the comprehensive analysis of HWRs, including their design, operational features, safety considerations, and potential applications. The paper explores the principles behind heavy water moderation, neutron economy, and fuel cycle management in HWRs. Furthermore, it investigates the various types of heavy water reactors, such as pressurized heavy water reactors (PHWRs) and heavy water-moderated boiling water reactors (HWBWRs), discussing their similarities and differences. The evaluation of HWRs encompasses their efficiency, power output, coolant properties, and core configurations. Additionally, safety aspects related to HWRs, including emergency shutdown mechanisms, passive safety systems, and containment strategies, are examined. The environmental impact and advantages of HWRs, such as their potential role in reducing greenhouse gas emissions and their compatibility with non-uranium fuel cycles, are also explored. Finally, emerging technologies and future developments in HWRs are discussed, including advancements in fuel technology, plant design, and operational flexibility. This comprehensive analysis provides valuable insights into the determination of heavy water reactors, facilitating informed decision-making and promoting the efficient and safe utilization of this important nuclear energy technology.

KEYWORDS:

Coolant Properties, Fuel Cycle Management, Heavy Water Moderation, Neutron Economy, Safety Considerations.

INTRODCUTION

The slowing power of heavy water is much lower than that of H2O because of the increased amount of deuterium. D2O, however, has the highest slowing down ratio of any moderator because deuterium's tiny heat absorption cross section. So, in contrast to LWRs, heavy water reactors need huge moderator to fuel volume ratios to enable appropriate neutron slowing. Additionally, because to deuterium's low heat absorption cross section, they may tolerate greater moderator contents.The most prevalent D2O-moderated power plants today are by far CANDU-type pressurized heavy water reactors (PHWRs).

A CANDU core is made up of a large cylindrical tank called a calandria that is positioned on its side and is traversed by a network of horizontal pressure tubes. As shown in Figs. 4.1c and 4.2b, each pressure tube holds a number of fuel assembly segments, also known as bundles, each of which contains 30 to 40 fuel pins. The fuel pins resemble those seen in LWRs. They are made up of pellets of UO2 covered with zirconium. Pumped via the tubes and through steam generators like those seen in PWRs, heavy water, which also acts as cooling, is then returned to the core intake. The reactor's huge moderator to fuel volume ratio is provided by the significant distance between pressure tubes within the D2O-filled calandria. The calandria can function at temperatures and pressures that are close to those of the atmosphere because it is isolated from the pressure tubes. Thus, just the tubes housing the fuel assemblies must be kept under adequate pressure to prevent boiling at working temperatures in the reduced amount of D2O coolant[1]–[3].

Natural uranium may be used to power PHWRs thanks to the moderator features of heavy water, most notably its short thermal absorption cross section. However, without enrichment, the fuel is unable to maintain the burn up levels needed to run the reactor for up to a year without refueling. Instead, while they are running, CANDU reactors get continual refueling: A new fuel bundle is put into one end of the core while a depleted one is taken out of the other by a pair of on-line refueling devices, which isolate one pressure tube at a time. In comparison to batch refueling, this method of operation uses less control poison to keep the reactor in a critical condition. Reactor shutdown is the main purpose of the control rods, which travel via the calandria outside of the pressure tubes.

Graphite-Moderated Reactors

The slower-moving power of graphite is less than that of either light or heavy water due to the larger atomic mass of carbon. But because of its low heat absorption cross section, it has a slowing ratio that falls somewhere between that of light and heavy water. The end result is extremely high moderator to fuel volume ratios in graphite reactor lattices built to maximize k1.Several early power reactor ideas were graphite-moderated, carbon dioxide-cooled systems using natural uranium fuel. The work was more challenging with graphite than with D2O moderator due to the lower values of the slowing down power and ratio. Consequently, natural uranium was substituted in later designs once partly enriched fuel became available. More recently, graphite-moderated power reactors with high operating temperatures have been developed using helium coolant and partly enriched fuel.

Parameters for a high temperature gas-cooled reactor Because the core is made entirely of graphite and ceramics, the helium coolant may reach greater coolant temperatures than it would if there were metal cladding or structures. Heat created in the fuel travels through the graphite moderator before being transported away by the gas coolant in a lattice structure similar to that the fuel is made up of uranium carbide particles that have been compressed in graphite, further boosting the moderator to fuel ratio. The enrichment of the fuel is extremely high. each fuel assembly is made up of a prismatic graphite block with two arrays of holes, one for fuel and the other for coolant. Other axial holes in the prismatic graphite block are occupied by the control

rods.Through a steam or gas turbine, the helium coolant is recirculated before returning to the core. Refuelling for HTGRs is done in batch mode, just as it is for water-cooled reactors[4]–[6].

RBMK Reactors

Thermal reactors where the coolant and moderator are one and the same, or if the coolant is a gas. In the latter scenario, the gas density is so low that its volume's impacts on the calculation of k1 are negligibly tiny. Different liquid coolants from the moderator have been used as the foundation for other power reactors. For instance, designs like CANDU systems may use heavy water moderator and pressurized or boiling light water coolant. The molten salt reactor is less common since it circulates molten fuel, which acts as coolant, through a core made of a fixed graphite moderator structure. There have been other coolant-moderator combinations used, although they were mostly used in prototype reactors. In contrast, the former Soviet Union has made extensive use of the Russian RBMK reactor design for the generation of electricity.

The RBMK is a graphite-moderated, water-cooled reactor. Low power densities and sizes as big as 1000 m3 are required because to the enormous amount of moderator needed. The RBMK has certain characteristics with CANDU reactor designs in that its core is made up of pressure tubes that house fuel assemblies made up of bundles of cylindrical uranium dioxide fuel components covered in zirconium. The graphite moderator, which makes up the majority of the core volume, is passed through via pressure tubes as the water coolant. The RBMK refuels online as the CANDU reactors do by employing devices to isolate one pressure tube at a time. But there are significant variations between the RBMK and CANDU designs. Pressure tubes used in the RBMK design convey light water coolant through the core vertically, boiling as it does so. After the fuel is enriched to around 2%, the tubes and control rods are inserted into the big blocks of graphite moderator.

DISCUSSION

Fast Reactors

In order to prevent neutron slowdown by elastic scattering, fast reactor cores include a minimum amount of low atomic mass material. Fast reactors still need enrichments of at least 10%.Smaller volume ratios of coolant to fuel may be used than in square lattices, hence hexagonal lattice cells like the one in Fig. 4.1b are used. Fast reactors are able to reach greater power densities and hence lower sizes than thermal reactors because to their closely packed lattices.

Fast reactor fuel may be encased in a metal shell or be made of ceramic material. The most popular coolant is liquid metal since it has a heavier atomic weight than other liquids, has good heat transmission capabilities, and can be utilized in low-pressure systems. The most popular designs are fast reactors with sodium cooling (SFRs). SFRs, however, call for the installation of an intermediary heat exchanger between the reactor core and the steam generator; should a steam generator leak occur, the sodium that goes through the reactor would not come into touch with water. This is because sodium reacts severely with water. Some Russian fast reactors have used coolant made of molten lead. Since the gas has no impact on the neutron spectrum due to its low density, gas-cooled fast reactors (GCFRs) provide an alternative to liquid metal-cooled systems.

However, to accomplish sufficient heat transfer, high pressure and significant coolant temperature increases are needed. Fast reactor refuelling happens in batch mode, like the majority of other systems[7]–[9].

Thermal Reactor Lattices

both thermal and rapid reactor lattices. However, cross sections are often bigger in the thermal and intermediate neutron energy ranges than for higher energy neutrons that are primarily of interest in fast reactor physics. These ranges are crucial to understanding thermal reactor physics. Additionally, in fast reactors, the diameters of the coolant and moderator areas are often greater than those of the coolant channels. The combined effect of these two parameters allows the moderator and/or coolant lateral dimensions and fuel pin sizes to measure up to multiple mean free pathways. The magnitudes of the flux in the fuel and moderator areas may vary noticeably under such conditions, with the flux being depressed in the fuel zone across energy ranges where the fuel absorption cross section is high.

Reactor Kinetics

analysis of the time-dependent behavior of neutron chain reactions in detail. We simplify two things in order to emphasize the time variable and do away with the necessity to simultaneously address the neutron energy and geographical variables. First, we assume that both the neutron distribution and related cross sections over energy have been averaged using the methods. Assuming for the time being that neutron leakage from the system is either minimal or can be handled by the nonescape probability assumption previously stated, we postpone the formal discussion of spatial effects until the chapters that follow.

A number of neutron balancing equations and their time-dependent behavior are introduced first. We start by looking at a system known as a nonmultiplexing system, which is devoid of any fissionable components. Then, we add fissionable isotopes and analyses how the resultant multiplying system behaves. We assume that neutron leakage from the systems in both scenarios may be disregarded. Then, in order to investigate the phenomenon of criticality in systems of limited size, we integrate the consequences of leakage.

The assumption that all neutrons are created instantly at the moment of fission is the most notable simplification in these calculations. Since certain fission products decay, a tiny percentage of fission neutrons are actually delayed because they are released. These postponed neutrons have a significant impact on how chain reactions behave. The remaining portion of the chapter focuses on the kinetics of the reactor as a consequence of the combined impacts of quickly generated and delayed fission neutrons. Be aware that the neutron population changes at rapid rates even for very little multiplication deviations from one. These are brought on by the neutron lifetime's modest value, which normally ranges from 108 to 104 s, and appears in the exponentials' denominator. Controlling a nuclear reactor would be exceedingly challenging if all neutrons were created instantly during fission due to the short neutron lifetimes. Fortunately, given certain conditions are satisfied, the existence of delayed neutronswhich have gone unnoticed up until nowsignificantly lowers the rates of change in the neutron populations to more tolerable levels.

Step Reactivity Changes

When an originally critical reactor that has been functioning at steady state is subjected to a step change in reactivity. Solutions t 66 and (5.48) for positive and negative reactivity insertions are shown by the two curves in. The curves initially have a similar appearance to those. Further examination reveals that the curves are more complex, which is due to the inclusion of both prompt and delayed neutrons. The neutron population first experiences a prompt jump in less than a second. The prompt neutron lifetime, here assumed as 14 50 106 s, which is normal for a water-cooled reactor, is what causes the jump to be sudden. Then comes the exponential growth or decline, which seems to be comparable for Because the half-lives of the neutron-emitting fission products are the principal determinant of the neutron population's increase or decay after the prompt jump, the exponential behavior shown happens relatively slowly.

When nt / exp t=T is used to describe the asymptotic behavior, T is the reactor period. The period, which may be positive or negative depending on whether the reactor is super- or subcritical, is likely the most significant variable that can be derived from the kinetics equations. It is the amount of time needed for the reactor power to change by a factor of e.

Prompt Jump Approximation

Using the rod drop and source jerk procedures, it is possible to use the prompt jump that follows modest step changes in reactivity to make experimental evaluations of reactor parameters.This leap is here the flux transients have had their early portion enhanced. It should be noted that after a quick initial increase, the neutron population changes considerably more slowly. Compared to the neutron population, the precursor concentration acts considerably more slowly, hardly altering throughout the time it takes for the neutrons to make their first leap up or down. This behavior results from the lengthy precursor half-lives in comparison to the prompt generation time; the behavior of the precursors described is slow even in response to a quick change in neutron population since the decay constant increasing.

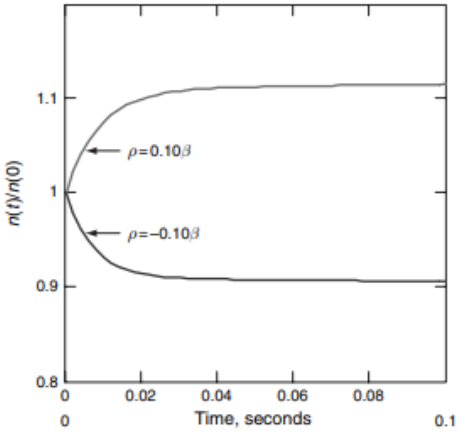

Figure 1: Represents thePrompt jump in neutron populations following reactivity insertions of – 0.10.

Prologue to Reactor Dynamics

The consequences of thermal feedback have not yet been taken into consideration in our analysis of the time-dependent behavior of chain reactions. These procedures are usually referred to as zero-power kinetics for this reason. However, the material densities will alter if the energy produced by fission is sufficient to raise the system's temperature.

Macroscopic cross sections will also alter since they are a function of densities. Resonance cross sections will widen and flatten with rising temperature as a consequence of the Doppler broadening outlined i which will have additional feedback effects in addition to the material density changes. Due to the Maxwell-Boltzmann distribution's temperature dependency in thermal reactors, the spectrum will also harden. The parameters in the kinetics equations will change when these feedback effects are combined. On the reactivity, there is by far the most influence. As a result, reactor design must ensure that the feedback for temperature rises is negative under all operating situations[10]–[12].

For instance, negative feedback has the following effects on the curves If there is negative feedback, the curve will flatten when the neutron population is sufficient to cause a temperature increase, then stabilise and perhaps go down over time. The positive reactivity curve from Figure 5.2 has been redrawn on a logarithmic scale along with a curve for the same reactivity insertion but with the effects of negative temperature feedback added. The straight-line behaviour on the logarithmic plot shows that both curves initially follow the same period. However, when the power increases, the curve with feedback concavely slopes downward and stabilises at the same power. At this time, the original reactivity insertion has been entirely offset by the negative feedback. Reactivity feedback will be thoroughly covered along with its interactions with reactor kinetics and the transient behaviour of power reactors.

REFERENCES

[1] M. E. Argun, M. Akkuş, and H. Ateş, “Investigation of micropollutants removal from landfill leachate in a full-scale advanced treatment plant in Istanbul city, Turkey,” Sci. Total Environ., 2020, doi: 10.1016/j.scitotenv.2020.141423.

[2] A. K. Dureja, D. N. Pawaskar, P. Seshu, S. K. Sinha, and R. K. Sinha, “Experimental determination of thermal contact conductance between pressure and calandria tubes of Indian pressurised heavy water reactors,” Nucl. Eng. Des., 2015, doi: 10.1016/j.nucengdes.2014.11.025.

[3] M. P. Sharma and A. K. Nayak, “Experimental investigation of two phase turbulent mixing rate under bubbly flow regime in simulated subchannels of a natural circulation pressure tube type BWR,” Exp. Therm. Fluid Sci., 2016, doi: 10.1016/j.expthermflusci.2016.03.016.

[4] X. Hou, “Radiochemical analysis of radionuclides difficult to measure for waste characterization in decommissioning of nuclear facilities,” J. Radioanal. Nucl. Chem., 2007, doi: 10.1007/s10967-007-0708-x.

[5] M. P. Sharma and A. K. Nayak, “Determination of turbulent mixing rate for single-phase flow in simulated subchannels of a natural-circulation pressure tube-type BWR,” Nucl. Sci. Eng., 2015, doi: 10.13182/NSE14-102.

[6] M. P. Sharma and A. K. Nayak, “Experimental investigation of void drift in simulated subchannels of a natural-circulation pressure tube-type BWR,” Nucl. Technol., 2017, doi: 10.13182/NT15-127.

[7] C. J. Banks and H. M. Lo, “Assessing the effects of municipal solid waste incinerator bottom ash on the decomposition of biodegradable waste using a completely mixed anaerobic reactor,” Waste Manag. Res., 2003, doi: 10.1177/0734242X0302100306.

[8] R. G. Moore, M. G. Ursenbach, C. J. Laureshen, J. D. M. Belgrave, and S. A. Mehta, “Ramped temperature oxidation analysis of Athabasca Oil Sands bitumen,” J. Can. Pet. Technol., 1999, doi: 10.2118/99-13-40.

[9] M. jalali, M. R. Abdi, and M. M. davati, “Prompt gamma radiation as a new tool to measure reactor power,” Radiat. Phys. Chem., 2013, doi: 10.1016/j.radphyschem.2013.05.033.

[10] V. Bulovič, J. Krtil, F. Sus, Z. Maksimovic, and E. Klosova, “Determination of the balance of the nuclear reactor fuel burn-out process by gamma-spectrometry of fission products III - Determination of the burn-up on the basis of the activity quotients106Ru/137Cs and134Cs/137Cs,” J. Radioanal. Chem., 1983, doi: 10.1007/BF02517663.

[11] S. K. Gupta, N. Goyal, and S. V. Godbole, “Matrix effect studies in the GFAAS determination of magnesium in proposed fuel for Indian advance heavy water reactor (AHWR),” At. Spectrosc., 2011, doi: 10.46770/as.2011.03.005.

[12] S. Chaudhury, C. Agarwal, A. Goswami, A. Mhatre, M. Gathibandhe, and S. C. Dash, “Determination of radioactivity concentration in the primary coolant channel of a Pressurized Heavy Water Reactor,” J. Radioanal. Nucl. Chem., 2010, doi: 10.1007/s10967-010-0610-9.

CHAPTER 16

SPATIAL DIFFUSION OF NEUTRONS

Vishnu Prasad Shrivastava, Assistant Professor
Department of Electronic Communication Engineering, Teerthanker Mahaveer University, Moradabad, Uttar Pradesh, India
Email id- vpshrivastava82@gmail.com

ABSTRACT:

Nuclear reactors, particle accelerators, and materials science are just a few examples of the many scientific and technical applications where neutrons are essential. For these applications to be optimized and run safely and effectively, it is crucial to comprehend the spatial dispersion of neutrons. This research uses experimental and computational methods to look at the spatial dispersion of neutrons in various materials and situations. The neutron flux distribution and diffusion length are used to describe the diffusion behavior. To assess their impact on the diffusion process, factors including neutron energy, scattering cross-section, and material composition are taken into account. The findings may help with the design and improvement of neutron-based systems and materials since they provide important new insights into neutron transport processes.

KEYWORDS:

Neutrons, Spatial Diffusion, Neutron Flux, Diffusion Length, Neutron Energy, Neutron Transport, Optimization.

INTRODUCTION

Nuclear reactors exhibit time-dependent behavior, and in prior chapters, we looked at how the energy spectrum of neutrons affects the multiplication and other reactor characteristics. Other than the discussion of neutron distributions between fuel, coolant, and/or moderator inside lattice cells NB, we have not yet addressed the spatial distributions of neutrons. , we have simply used a no leakage probability to characterize the consequences of the worldwide distribution of neutrons. This probability rises towards a value of one as the reactor core becomes bigger. We study the spatial migration of neutrons in this chapter and the one after it in order to not only derive an explicit expression for the no leakage probability but also to comprehend the connections between reactor size, shape, and criticality as well as to identify the spatial flux distributions within power reactors[1], [2].

We shall take a monoenergetic or one energy group model into consideration while discussing neutron spatial distributions. This indicates that the flux and cross sections of the neutrons have previously been averaged across energy. Similar to this, we presume that when working with reactor lattices, the flux and cross sections have been spatially averaged throughout the lattice

cell. Since the periodicity of the lattice cell pitch does not affect the spatial fluctuations, we are only concerned with the global changes of the neutron distribution.

The simplest method for figuring out neutron spatial distributions is to use the neutron diffusion equation. The diffusion equation and its accompanying boundary conditions. Then, using diffusion theory to solve issues in nonmultiplexing media, we focus only on issues in highly idealized one-dimensional geometries (first, plane, and then spherical geometry), since they provide the most straightforward explanations of the approaches for solving such issues. The behavior of spherical systems with fissionable material but subcritical conditions is next examined[3].

Neutron Distributions in Reactors

selected for its one-dimensional geometry's mathematical simplicity as a criticality method for a spherical system. The spatial distributions of neutrons inside the limited cylindrical cylinders that correspond to the cores of nuclear reactors are the subject of this chapter. The multiplication and the flow distribution from a time-independent solution are obtained by reformulating the diffusion equation in an eigenvalue form to start. The criticality equation and flux distribution for a simple uniform reactor are then discovered, and they are related to the reactor power. In our rough approach, we assume that the cross sections are averaged over energy, enabling an energy-independent treatment, and across the cross-sectional area of the lattice cell. Remember that uniform merely refers to the lattice cells being similar. The neutron nonleakage probability and the consequences of neutron diffusion and slowing down are discussed in further depth in the next section. After treating the cylindrical reactor in its naked form, we look at reactors with reflector areas to boost the neutron economy., first for a single control rod and then for a bank of control rods.

Neutron Leakage

The cross sections and diffusion coefficients that we employ in the diffusion approximation are typically averaged throughout the whole neutron energy spectrum as well as over the compositions of lattice cells as = The diffusion length counts the distance that neutrons cover from conception to decay. However, the diffusion coefficient and cross sections employed in thermal reactor simulations are often those averaged across only the thermal neutron energy spectrum. Such calculations ignore the distance that neutrons diffuse across when they slow to thermal energy when performed incorrectly.

Some systems, especially those with light water moderators, are susceptible to considerable inaccuracy due to such negligence. It is necessary to divide the neutron spectrum into two or more energy groups and create a diffusion equation for each in order to more thoroughly treat the neutron migration during both slowing down and thermal diffusion. However, when it comes to thermal reactors, dividing the flux into just two categoriesfast and thermalis frequently sufficient. This is especially true when taking into account the lattice physics in terms of the four-factor formula, which depicts the same neutron cycle with neutron diffusion added for both fast neutrons as they slow down through the intermediate or resonance regions and for thermal neutrons.

The value of the migration length, which is nonetheless only very weakly dependent on the fuel enrichment, is mostly determined by the core materials and lattice characteristics at this stage, therefore the value of M is essentially set. The feasible core averaged power density, P000, is determined by the core lattice design in conjunction with the maximum to average flux ratio. Following the determination of P and P000, the core volume is calculated using the relationship P 14 VP000. The volume of a cylindrical reactor with a height to diameter ratio of one is V 14 H3=4 and, as a result, H 14 4V= p3 14 4P=P000 p3. A reactor's core volume grows linearly with the needed output P of the reactor at full power, while the core lattice design affects M and the feasible P000. Equation (7.53) shows that the nonleakage probability approaches one, i.e., the leakage probability decreases, as the volume and subsequently H=M grow. In order to achieve the desired value of k1, the fuel enrichmentwhich has very little impact on the migration lengthis changed once a reactor's size and neutron nonleakage probability are established.

the relationship between neutronic and thermal-hydraulic design as well as the thermal and hydraulic characteristics of reactor cores that affect the power densities possible in reactor lattices. The rest of this chapter looks into neutron poisons used to regulate reactivity and how they interact with the spatial flux distributions, starting with reactor reflectors and their impact on multiplication and flux distribution[4], [5].

DISCUSSION

Reflected Reactors

Reflectors get their name from the fact that a portion of the neutrons that leave the core will experience enough scattering collisions in the material that is diffusing the reflector for them to turn around and rejoin the core, or be reflected back into it. Thus, a reflector lowers the percentage of neutrons that leak from the reactor. Schematic representations of cores with axial and radial reflectors are shown in Smaller cores, where there is a high possibility of leakage, are where reflectors have the most effects. The significance of a reflector diminishes, as we'll show.

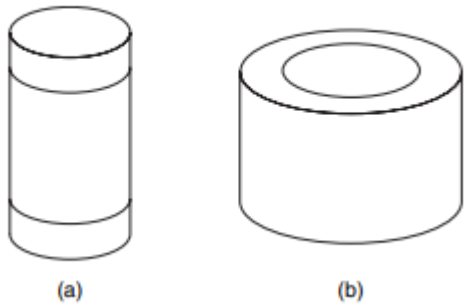

Represents the Reflected reactor cores. (a) Axial reflector, (b) radial reflector.

Reflector Savings and Flux Flattening

In the first, we state B0 z! Bz 14 =H. This is the same as saying that the composition of the core is the same as it would be for a core with a length of H. changing the bucklewhich might be

shown to be less than H. Axial reflector savings are described as z 14 1=2H H0, which is the decrease in the critical reactor's half core height. In the case of a thick reflector, it is about z M _ D=D _.

In Figure 7.5, flux patterns for bare and reflected reactors with unchanged core composition and decreased axial dimension to preserve criticality are compared. With the added complexity of Bessel functions, the treatment of the radial reflector is comparable. Again, for a thick reflector, we would get r M _ D=D _ by applying the thick reflector approximation to the radial reflector savings shown by r 14 R R0.

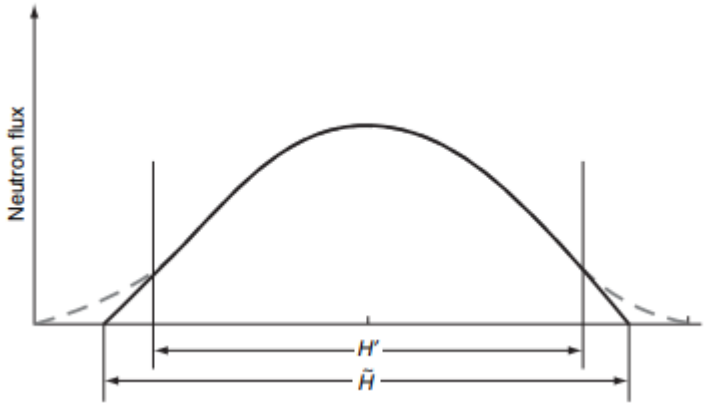

Figure 2: Represents the Axial flux distributions for bare.

reactors that vary the composition while maintaining criticality while keeping the height constant.To sum up, adding a reflector to a reactor enables a reduction in either the volume of the reactor, the value of k1, or a combination of the two. A third consequence is also shown in Figure 7.6. The flux distribution is flattened by the addition of a reflector, which reduces the ratio of peak to average flux. But as the size of the reactormeasured in migratory lengthsincreases, these effects become less important.

It is obvious that as the reflector's size increases, the savings represent a lesser percentage of the core dimension. Similarly, adding a reflector has less of an impact on the multiplication of a big reactor than a small one if the core dimensions are kept constant. With each of the three average fluxes normalized to one, compares the maximum and lowest flux for two reflected reactors with height to migration length ratios of H=M1/4 10 and H=M1/4 50 to a bare reactor. The data clearly shows that as reactor size grows, the reflector's influence on flux flattening decreases[6], [7].

Control Poisons

Neutron absorbers known as control poisons are added on purpose in a reactor core. Control rods, soluble poisons dissolved in liquid coolants, or supposedly burnable poisons permanently ingested into the fuel or other essential components are a few possible manifestations.There are many uses for poisons. For startup, shutdown, and power level adjustments, control rods are inserted or removed to regulate the value of k. By adjusting for fuel exhaustion, a buildup of fission products, temperature variations, or other events that have an impact on the

multiplication, they may also be used to maintain the reactor critical at a fixed power. Control poisons have an impact on a core's multiplication as well as its flux distribution, so we must take both into account.

For the sake of simplicity, we assume that we have a uniform unelected reactor to which we add a control poison before starting our study of control poisons with Eq. (7.3). We also suppose that the poison has negligible impacts on the diffusion coefficient and has no impact on the fission cross section. The absorption cross section will grow as a result, which will be its main consequence. We indicate this increment by using the symbol a!a a. Here, the extra absorption, a, may be localised in the form of one or more control rods or it may be uniform throughout the core, as in the case of the boron absorber added to the coolant of pressurised water reactors. Burnable toxins are often dispersed evenly throughout the core, although this distribution is beyond the purview of the investigation that follows.

Fuel Temperature Coefficient

In low enrichment thermal power reactors, doppler widening of the resonance capture cross sections of the fertile material accounts for the majority of the fuel temperature coefficient, and it also contributes significantly in fast reactors. Thermostatic systems 6As fuel temperature rises, the resonance escape probability decreases, which is the consequence. Since its contribution comes from energies far higher than those at which fuel resonance cross sections exist, "does not exhibit the Doppler effect. When plutonium-239 is present in significant amounts, T and f may undergo relatively small changes since its resonance is just marginally above thermal energy. However, the latter effects are ignored in what follows since they often pale in comparison to the change in the resonance escape probability.

The dependency of neutron cross sections on the relative speed between the neutron and the nucleus is what causes the Doppler effect. Resonance cross sections have abrupt energy peaks, as may be seen, for instance The cross section must be averaged throughout the range of relative speeds brought on by the thermal movements of the fuel atoms, which form the Maxwell-Boltzmann distribution covered for a particular neutron speed. The overall result of this averaging is to look broader and less peaked by gently blurring the resonance in energy. As the fuel temperature increases, the smearing intensifies.

Fast Reactor Temperature Coefficients

Fast reactor temperature coefficients are different from thermal reactor temperature coefficients in a number of ways. First, compared to thermal reactors, fast reactors often have much lower sizes when measured in migration lengths. This is due to both the designs with greater power densities and the reduced neutron cross sections for fast compared to thermal spectrum neutrons. Consequently, the reactivity is more significantly impacted by the leakage factors The Doppler widening of capture resonances accounts for the majority of the negative fuel temperature coefficient in both fast and thermal reactors. But its size is reduced because, as shown by the spectra in Fig. 3.6, only a portion of neutrons in a fast reactor are slowed to the energy range where the significant capture resonances in fertile materials take place.

Fast reactor coolant temperature coefficients are much more challenging to forecast using simple models because they result from the difference between two conflicting influences. The coolant density falls as temperature rises. The removal of coolant atoms hardens the neutron spectrum since the coolant in liquid-cooled fast reactors tends to degrade it to lower energy. Therefore, , the bigger value of "E" at higher neutron energies causes the increased coolant temperature to raise the value of "k1." On the other hand, the migration duration is lengthened by the lower density brought on by a rise in coolant temperature. According to an analysis of an increase in M will likewise result in an increase in neutron leakage, a decrease in the chance of nonescape, and a decrease in reactivity. Which of these impacts is more significant must be determined using computational models that are more complex than those covered in this article[8]–[10].

CONCLUSION

The design and optimization of systems that depend on neutron transport may benefit practically from the information acquired from this research. For instance, comprehending neutron diffusion aids in managing the distribution of power and reactivity inside the core of nuclear reactors. When studying the interactions between neutrons and materials, which may affect the structural integrity and performance of nuclear fuels, shielding materials, and other neutron-sensitive components, materials scientists must consider neutron diffusion behavior.We can increase the security, effectiveness, and functionality of many neutron-based systems by better understanding the spatial dispersion of neutrons. Future studies in this area should concentrate on examining more intricate materials and systems while taking geometry, pressure, and temperature effects on neutron diffusion into account. The development of nuclear science, technology, and materials research will be aided by such developments.

REFERENCES

[1] A. Carreño, A. Vidal-Ferràndiz, D. Ginestar, and G. Verdú, “Modal methods for the neutron diffusion equation using different spatial modes,” Prog. Nucl. Energy, 2019, doi: 10.1016/j.pnucene.2019.03.040.

[2] A. Carreño, A. Vidal-Ferràndiz, D. Ginestar, and G. Verdú, “Spatial modes for the neutron diffusion equation and their computation,” Ann. Nucl. Energy, 2017, doi: 10.1016/j.anucene.2017.08.018.

[3] K. Il Jo, Y. Oh, T. H. Kim, J. Bang, G. Yuan, S. K. Satija, B. J. Sung, and J. Koo, “Position-Dependent Diffusion Dynamics of Entangled Polymer Melts Nanoconfined by Parallel Immiscible Polymer Films,” ACS Macro Lett., 2020, doi: 10.1021/acsmacrolett.0c00608.

[4] N. Maleki Moghaddam, H. Afarideh, and G. Espinosa-Paredes, “Development of a 2D-Multigroup Code (NFDE-2D) based on the neutron spatial-fractional diffusion equation,” Appl. Math. Model., 2015, doi: 10.1016/j.apm.2014.12.036.

[5] E. E. Lewis, “Spatial Diffusion of Neutrons,” in Fundamentals of Nuclear Reactor Physics, 2008. doi: 10.1016/b978-0-12-370631-7.00006-1.

[6] N. Maleki Moghaddam, H. Afarideh, and G. Espinosa-Paredes, “Modifying the neutron diffusion equation using spatial fractional operators and developed diffusion coefficients,” Prog. Nucl. Energy, 2015, doi: 10.1016/j.pnucene.2015.03.002.

[7] J. A. Ferguson, J. Kópházi, and M. D. Eaton, “Virtual element methods for the spatial discretisation of the multigroup neutron diffusion equation on polygonal meshes with applications to nuclear reactor physics,” Ann. Nucl. Energy, 2021, doi: 10.1016/j.anucene.2020.107884.

[8] M. A. Shafii, W. W. Yunanda, D. Fitriyani, and S. Pramuditya, “Neutron flux distribution calculation for various spatial mesh of finite slab geometry using one-dimensional diffusion equation,” 2019. doi: 10.1063/1.5135510.

[9] T. Seydel, M. M. Koza, O. Matsarskaia, A. André, S. Maiti, M. Weber, R. Schweins, S. Prévost, F. Schreiber, and M. Scheele, “A neutron scattering perspective on the structure, softness and dynamics of the ligand shell of PbS nanocrystals in solution,” Chem. Sci., 2020, doi: 10.1039/d0sc02636k.

[10] A. G. Mylonakis, P. Vinai, and C. Demazière, “Numerical solution of two-energy-group neutron noise diffusion problems with fine spatial meshes,” Ann. Nucl. Energy, 2020, doi: 10.1016/j.anucene.2019.107093.